This report was funded by the Bonneville Power Administration (BPA), U.S. Department of Energy, as part of BPA's program to protect, mitigate, and enhance fish and wildlife affected by the development and operation of hydroelectric facilities on the Columbia River and its tributaries. The views in this report are the author's and do not necessarily represent the views of BPA.

For copies of this report, write to:

Bonneville Power Administration
Division of Fish and Wildlife - PJ
P.O. Box 3621
Portland, OR 97208

FY 1989

Annual Report

Mainstem Clearwater River Study: Assessment for Salmonid Spawning, Incubation, and Rearing

by

William P. Conner, Project Leader
Billy D. Arnsberg, Field Crew Supervisor
Nez Perce Tribe Department
of Fisheries Management

Ed Connor, Biologist
C. Mike Prewitt, Manager
EBASCO Environmental

<u>Other Contributors</u>
Markley J. Pishl, Fisheries Technician
Marc A. Whitman, Fisheries Technician

Funded by
Jeff Gislason, Project Officer
U.S. Department of Energy
Bonneville Power Administration
Division of Fish and Wildlife
P.O. Box 3621
Portland, Oregon 97208
Contract No. DE-AI79-87BP37474
Project No. 88-15

Columbia River Basin Fish and Wildlife Program Measure
703(c)(3)

June 1990

ACKNOWLEDGEMENTS

The Nez Perce Tribal Executive Committee authorized this research, which was funded by the Bonneville Power Administration. Paul Kucera, Silas Whitman, and Anita Two Moon of the Nez Perce Tribe Department of Fisheries Management provided valuable technical and administrative guidance throughout 1989. Many dedicated professionals contributed to our study during it's formative stage including: Paul Kucera, David Johnson, John Barthalow, Ted Bjornn, Ken Bovee, Jack Griffith, Tracy Hillman, Tom Payne, Bob Raleigh, and Terry Waddel. Mark Pishl and Marc Whitman, our fishery technicians, subjected themselves to long work days and physically trying weather conditions without complaint. John Knudsen, Scott Wilcox, and Ken Winnick assisted during the collection of hydraulic cross-section data and Lisa Russel summarized and entered these data into data base format. Greg Delwitch, Jeff Hanson, Ed Kim, and Mark Lindgren of the U.S. Army Corps of Engineers coordinated controlled dam flows, which were essential to our study. Numerous employees of the U.S. Geological Survey transferred gaging station data to our project personnel. Bill Miller, Travis Coley, and Ralph Roseberg of the U.S. Fish and Wildlife Service Federal Assistance Office at Dworshak National Fish Hatchery furnished equipment and were always available for questions of a technical nature. Meetings were held for the purposes of peer review and interagency coordination. Attendents and mail correspondents included: Terry Barilla, Bert Bowler, Bob Buggert, Tim Cochanauer, Doug DomPier, Al Espinosa, Kathy Hopper, Ray Latham, John McKern, Hudson Mann, Rob Palmer, Steve Pettit, Carl Ross, and Mark Von Lindern.

TABLE OF CONTENTS

ABSTRACT

This is the second annual progress report for studies conducted by the Nez Perce Tribe to evaluate the potential for increasing fall chinook salmon (*Oncorhvnchus tshawvtscha*) populations and establishing summer chinook salmon spawning in the lower 57.5 km (36 mi) of the mainstem Clearwater River (LMCR) of Idaho. The report presents study methods and preliminary results for the 1988-1989 phase of the study. The overall study plan was designed to quantitatively evaluate the available spawning, incubation and rearing habitat for fall and summer chinook salmon. We also studied steelhead trout (*O. mykiss*) rearing habitat since there is a stable population of these fish in the LMCR's tributaries and their parr are known to rear periodically in the mainstem. Resident fish were studied to assess the potential for habitat overlap with that of anadromous fish. Based on these findings the Nez Perce Tribe could determine chinook salmon habitat conditions for selected stocks under existing flow and temperature regimes and consult with the U.S. Army Corps of Engineers concerning the effects of Dworshak Dam operation on flows and measures to restore or establish stocks identified in this study. Since the LMCR was too large to study in it's entirety we stratified the river based on flow and geomorphology into three segments and chose a total of four study sites within these segments. Study sites were assigned primarily to the areas in the LMCR where spawning gravel was abundant and we documented fall chinook spawning. We considered anadromous fish habitat to be the product of water depth, velocity, temperature, and substrate and cover. These variables were measured at a total of 33 cross-sections within the four study sites. Cross-sectional data were used to run version 4 (IFG4) of a hydraulic model developed by the National Ecological Research Center (NERC) of the United States Fish and Wildlife Service (USFWS). We ran IFG4 for a preliminary evaluation and presentation of water velocity and depth over spawning and rearing substrate used by anadromous salmonids and to predict their values under a range of streamflow conditions. Tentatively, it appears that small changes in river flow can have substantial effects on anadromous fish spawning and rearing habitat. Spawning and rearing conditions for anadromous fish may be best met at low to moderate discharges. Higher discharges may result in depths and velocities which are unsuitable for chinook salmon spawning and salmonid parr rearing. The study design also included a fish observation component to evaluate current utilization of the LMCR by anadromous and resident fish species and a study to determine quantitative habitat preferences of selected species. In November of 1988, we counted 21 redds and five fall chinook carcasses by

helicopter. All redds were in the lower islanded segments of the LMCR. We saw no summer chinook redds during a 1989 flight made in mid-September. We also counted juvenile anadromous and resident fish bi-weekly from August through December, within hydraulic study sites, using snorkels and self contained underwater breathing apparatus (SCUBA). An inadequate sample size of chinook salmon parr were observed to calculate densities of these fish. Wild rainbow/steelhead trout parr and residualized hatchery steelhead smolts were more abundant, but even these fish were not found in high densities. Densities of both residualized smolts and wild parr were highest in summer and declined markedly by winter. Mountain whitefish (Prosopium williamsoni) and largescale suckers (Catostomous macrocheilus) were found in high densities until December when these species were observed in lower numbers. Habitat preference research is ongoing and our data presentation reflects the state of current analysis and is not intended for IFIM application. In general, both wild rainbow/steelhead trout parr and residualized steelhead smolts preferred relatively shallower and slower water than is available across the channel. Mountain whitefish and largescale suckers were more ubiquitous, having been found over a wide range of water velocities and depths. The significance of these habitat preferences will be discussed in the final report of this research.

INTRODUCTION

Hydroelectric development within the Columbia River Basin caused a major depletion of anadromous fish runs. This depletion can be attributed primarily to passage problems and habitat loss. Accordingly, Congress passed the Northwest Power Act. As a result of this action, the Northwest Power Planning Council (NPPC) was formed with representatives from the states of Idaho, Oregon, Washington, and Montana. The primary goal of the NPPC was to develop a power plan around the fishery needs in the Columbia River Basin which would promote a doubling of the anadromous fish runs. To do so, the NPPC coordinated a cooperative effort between tribal, federal, and state resource managers to author the Columbia River Basin Fish and Wildlife Program (1987). Section 700 of this plan deals with the integration of natural and hatchery production to supplement runs in rivers with depressed natural anadromous fish populations or production potential. Such is the case on the lower mainstem Clearwater (LMCR) of Idaho.

The race composition of the LMCR's indigenous chinook salmon (Oncorhynchus tshawytscha) runs was never conclusively documented because the first anadromous fish survey was not conducted until 1938; eleven years after chinook salmon populations were decimated by ineffective fish passage facilities at the Washington Water Power Diversion Dam (Parkhurst 1950). Parkhurst (1950) did note that spawning gravel was abundant in the LMCR and recommended that this mainstem river be restocked. However, most chinook salmon restoration efforts were concentrated in more pristine headwater tributaries of the Clearwater drainage and none tested the production potential of the mainstem river (Connor 1989).

The removal of the Washington Water Power Diversion Dam and construction of Dworshak Dam in 1971 markedly affected the LMCR's potential for natural anadromous fish production. Although fish could pass freely beyond Lewiston after dam removal, the existence and operation of Dworshak Dam eliminated access to North Fork spawning habitat and changed the temperature and flow regime of the LMCR.

As mitigation for losses of fish runs into the North Fork, Dworshak National Fish Hatchery (DNFH) was constructed near the confluence of the North Fork and the LMCR. Dworshak National Fish Hatchery has maintained the North Fork stock of steelhead trout (O. mvkiss) through smolt releases since 1970. Since 1972 estimates of adult returns to the Clearwater have been as high 28,296 fish (Miller et al. 1989). Kooskia National Fish Hatchery (KNFH), located 30 miles upriver of Dworshak on the Middle Fork of Clearwater River began producing spring chinook smolts in 1972. In 1982, DNFH also began a spring chinook production program. Combined spring chinook adult returns to DNFH and KNFH since 1984 have ranged from a low of 423 in 1984 to a high of 2,704 in 1987 (Miller et al. 1989).

Because these smolts are imprinted to hatchery water and naturally producing spring chinook and steelhead generally prefer habitat conditions available in smaller tributaries for redd building, few returning adults of these species utilize the LMCR for spawning. However, some fall chinook salmon spawning has been documented in the LMCR in recent years (Murphy 1989). Enhancing fall chinook spawning conditions and achieving the maximum production potential of the LMCR will require instream flow management and possibly outplanting of selected stocks into the mainstem river for imprinting to the habitat. The success of this strategy will depend largely on the physical condition and seeding level of spawning, incubation, and rearing habitat in the LMCR and the availability of a stock of anadromous salmonid capable of utilizing this habitat.

With these facts in mind, the NPPC amended the Columbia Basin Fish and Wildlife Program to include measure 703(c)(3) which states:

> "Bonneville shall fund and evaluation of the lower mainstem Clearwater River to study existing habitat and temperature regimes for spawning, incubation and rearing for salmon and steelhead. Proposals for outplanting from the Nez Perce low-capital propagation facilities (Section 703(g)(2)) will be based on the evaluation. The Nez Perce Tribe shall consult with the Corps of Engineers concerning the effects of Dworshak Dam operations on the lower mainstem Clearwater River."

In this study we concentrated on the anadromous fish production potential of the LMCR's physical habitat components. The physical habitat components of interest included water depth, velocity, temperature, and substrate. We contended that these components are key to the river's ability to sustain natural, but hatchery supplemented populations of fall and summer chinook salmon. These races of chinook salmon were selected for study because they are escaping to Idaho's spawning habitat in threateningly low numbers (Fish Passage Center 1989, Irving and Bjornn 1980, Horner and Bjornn 1981) and they can spawn in large mainstem rivers (Fulton 1968). We also studied the biological component, or fish populations of the LMCR, to allow for a well founded estimate of the river's current level of seeding. Our study had the following objectives:

1) Quantify the existing anadromous salmonid spawning and rearing habitat in the LMCR and develop capabilities to predict habitat conditions under various Dworshak Dam discharge regimes:

2) Document the use of the LMCR by anadromous and non-anadromous fish;

3) Investigate the incubation, rearing, and outmigration timing of fall and summer chinook salmon;

4) Use the information generated by objectives 1 - 3 to identify potential outplanting stocks of fall and/or summer chinook salmon for restoration or supplementation efforts; and

5) Determine habitat conditions for selected anadromous fish stocks under existing flow and temperature regimes and consult with the U.S. Army Corps of Engineers concerning effects of Dworshak Dam operation on flows and measures to restore stocks identified in this study.

This report is intended to provide the reader with an overall study scope and location orientation and with methods and results from the second year of the study and analysis. Results presented are relatively unrefined and are not considered suitable for use in Instream Flow Incremental Methodology (IFIM) applications or as the basis for conclusions concerning the feasibility of anadromous fish reintroductions. The results are presented to illustrate the state of current data processing and to give the reader insights into existing hydraulic conditions at the study sites.

DESCRIPTION OF THE PROJECT AREA

The LMCR project area begins at the Clearwater Memorial Bridge at Lewiston and extends approximately 60 km (38 mi) upriver to the North Fork Clearwater Confluence (Figure 1). The morphology of the LMCR's channel was influenced by a number of geological events leading to a variety of rock and soil types. During the Precambrian era, most of Idaho, including the Clearwater basin, was covered by a shallow sea (Asherin and Orme 1978). Subsequential folding, faulting and uplifting gave rise to the mountain formations in the basins's headwaters reaches. These mountain ranges were formed primarily of metamorphosed sedimentary rocks of the Belt series and granitic intrusions of the Idaho Batholith (USACE 1975). Volcanic activity filled the lower valleys of the Clearwater basin with basalt flows (Asherin and Orme 1978). This volcanic activity in the lower basin is probably responsible for the basalt and granite composition of the LMCR's channel.

Winters with little snow accumulation and summers that are hot and dry predominate in the lower portions of the Clearwater basin. Precipitation usually occurs in the late fall-winter and spring periods over much of the area (Asherin and Orme 1978). Average precipitation in the Clearwater basin varies from 36 cm (14 inches) at the mouth(Asherin and Orme 1978) to 178 cm (70 inches) near the summit of the Bitterroot Range (USACE 1986). Prevailing winds are generally westerly from the Pacific Ocean which can carry moist air masses over much of the area. Average annual temperature is 10° C (50° F) in the lower Clearwater basin (USACE 1975), however, winter polar air masses sometimes predominate and produce air temperatures as low as -34° C (-29° F)(USACE 1986). Historically, these cold winter periods commonly produced ice build-up in the LMCR (USACE 1986).

It is believed that the establishment of a permanent botanical community in the riparian zone of the LMCR was precluded by the scouring effect of these ice jams (Kroneman and Lawrence 1988). However, annual forbs, grasses, shrubs and vines are currently colonizing the riparian zone as a direct result of hydrological changes in the LMCR (Kroneman and Lawrence 1988). More specifically, the LMCR's winter instream water temperatures were warmed and its annual hydrograph was stabilized by the impoundment of it's largest tributary.

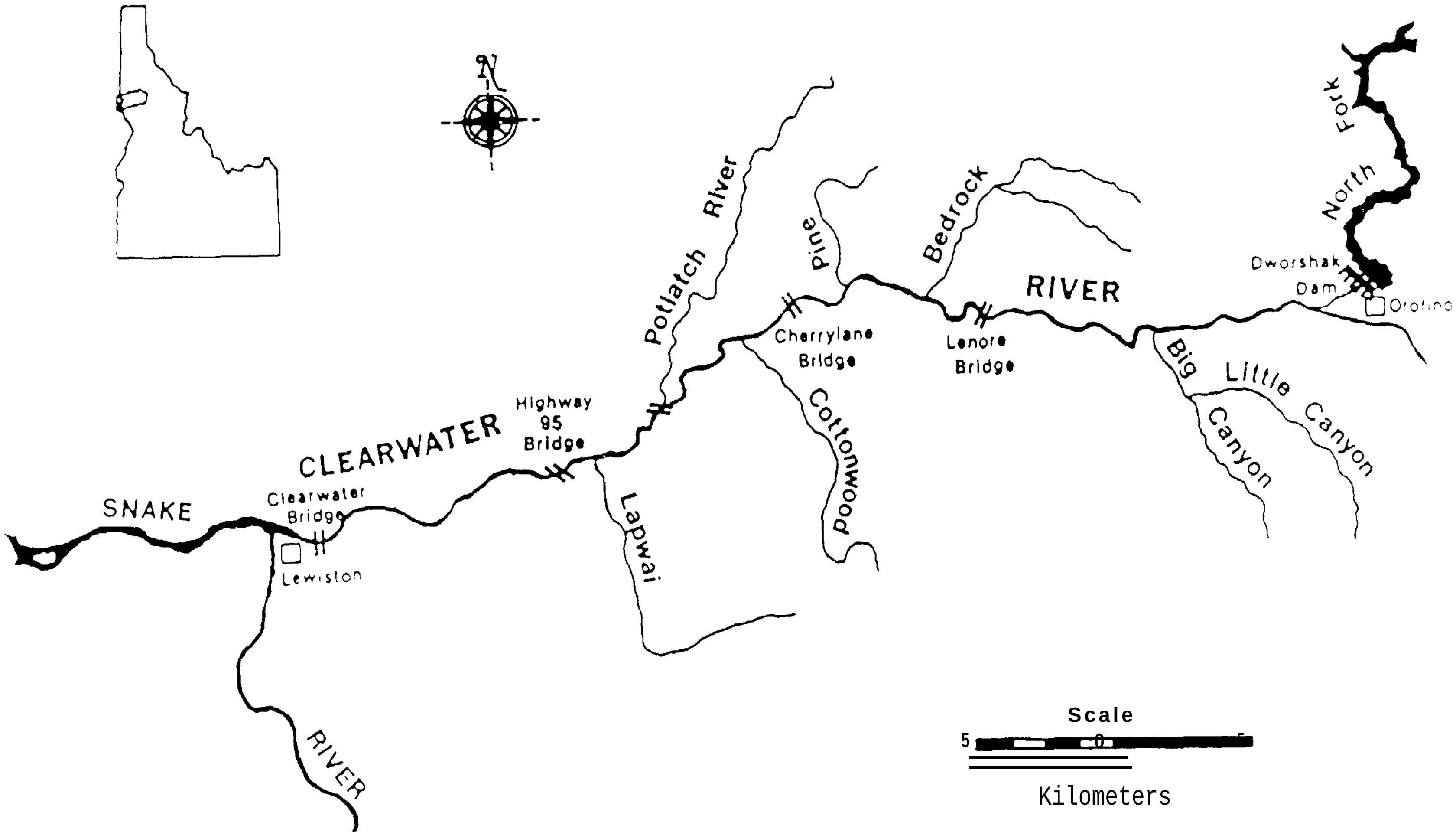

Figure 1. **Lower mainstem Clearwater River (LMCR) project area including Dworshak Dam and major tributaries (modified from Lawrence in Murphy 1989).**

The U.S. Army Corps of Engineers impounded the North Fork Clearwater River by constructing Dworshak Dam in 1971. Dworshak Dam is located on the North Fork 3 km (1.9 mi) up from its confluence with the Clearwater River at river km 61 (mi 38). The dam controls water from a 6,319 km^2 (2,440 mi^2) drainage area (USACE 1986) for flood control, power generation, recreation, water quality, and fish and wildlife uses (USACE 1986).

Dworshak Dam is a straight concrete-gravity structure 218.5 m (717 ft) high with a crest length of 1001.9 m (3,287 ft) and a crest width of 13.4 m (44 ft)(USACE 1986). The dam's power intakes are equipped with multilevel selector gates which allow selection of suitable water temperatures for fish production at Dworshak National Fish Hatchery. Twenty-one temperature sensors located at different elevations along the upstream face of the dam measure water column temperatures (USACE 1986).

North Fork Clearwater discharge contributes 40.8% of the LMCR's average annual flow (Appendix A, Table Al). Pre-impoundment LMCR discharge peaked at about 1,415 cms (50,000 cfs) in May receding to about 113 cms (4,000 CFS) in September. Currently, Dworshak Dam stores North Fork Clearwater River spring run-off and redistributes it throughout historically low flow periods. Post-impoundment average annual maximum discharge is about 990 cms (35,000 cfs) and average annual minimum discharge is approximately 140 cms (4,800 cfs). Average daily dam discharges are regulated to approximate natural mainstem discharge except during August and September when the reservoir is drafted to create approximately 700,000 acre feet of storage for fall flood control. Additional reservoir regulation provides for unforseen power or flood control after January 1 (USACE 1986). Daily discharge fluctuations occur on most days of a given month as a direct result of power production and in some cases as result of flood control and steelhead management requirements.

METHODS

OBJECTIVE 1: Quantify the existing anadromous **salmonid** spawning and rearing habitat in the LMCR and develop capabilities to predict habitat conditions under various Dworshak Dam discharge regimes

We designed and implemented a habitat quantification study to define the relationship between anadromous fish spawning and rearing habitat in the LMCR and instream flow. Spawning and rearing habitat components were determined to be water velocity, depth, substrate composition and cover. We measured these habitat components at cross-sections within sites selected to represent major homogenous river segments or known fall chinook spawning areas. The selected cross-sections were the basis for quantifying the available LMCR habitat.

Water stage and discharge were measured simultaneously at six flow events. Then, water depth, velocity, substrate, and inter-cross section distances were measured at one river discharge and computer simulation was used to predict depth and velocity and wetted substrate over a range of unmeasured flows. In this way, the surface area of suitable substrate and the water velocities and depths over that substrate (and all other channel areas) could be predicted as a function of flow.

We also collected water temperature data to predict instream water temperatures using the United States Fish and Wildlife Services Stream Network Temperature Model (SNTEMP) (Theurer, Voos, and Miller 1984). Basically, SNTEMP predicts the longitudinal response of a rivers water temperature regime to changes in dam discharge. Input, calibration, and validation data must be collected longitudinally along a river at critical points termed hydrology nodes. Collection of these data are ongoing and will be discussed in a later report.

In the following sections we present detailed methods used in river stratification, cross-section placement, data collection, and our hydraulic simulation approach.

River Stratification:

We stratified the LMCR since the river was much too large to study in its entirety. Stratification initially divided the LMCR into segments (the largest representative subdivision) based on flow regime and geomorphologic features. Secondly, study sites within segments were chosen which contained known spawning or typical habitat. Thirdly, cross-sections for hydraulic measurement were assigned to spawning and/or typical habitats within each site.

Bovee (1982) recommends placing a segment boundary wherever a tributary adds 10% more water to mainstem flow (based on average annual discharge). Therefore, we collected average annual discharge data for the LMCR; Big Canyon, Jacks, Bedrock, Cottonwood, and Lapwai Creeks; and Potlatch River (See Figure 1) from the United States Geological Survey (USGS) and literature sources.

Geomorphologic features were also used to segment the river. Abrupt changes in slope, tributaries which contribute significant or disproportionate sediment loads, and sinuosity changes of 25% or more may be considered potential segment boundaries (Bovee 1982). Therefore, we constructed a longitudinal profile of the LMCR using USGS topographic maps, reviewed the literature for documentation of sediment input from tributaries, and measured river sinuosity using aerial photographs.

Study site selection within each segment was based primarily on the presence of known chinook salmon spawning habitat. A spawning gravel survey was made from the North Fork/LMCR confluence to the Clearwater Memorial Bridge using a jet boat, snorkeling, and SCUBA. Substrate conditions were assessed using an index developed by Brusven (1977) with the modifications of Bovee (1982)(Table 1). This technique uses a 3-digit code listing the dominant and subdominant particle size followed by a decimal number to indicate percent of fine material (sand and smaller) in the matrix. On November 30, 1988 from 12 noon to 2:30 P.M. we inspected the LMCR by helicopter for fall chinook spawning activity. We also flew a summer chinook spawning survey on Friday September 8, 1989 from 1:00 P.M. to 3:30 P.M.

Table 1. The Brusven substrate code (as modified by Bovee 1982) used for the lower mainstem Clearwater River (LMCR) spawning gravel survey.

Code	Substrate description
1	Fines (sand and smaller)
2	Small gravel (4-25 mm)
3	Medium gravel (25-50 mm)
4	Large gravel (50-75 mm)
5	Small cobble (75-150 mm)
6	Medium cobble (150-225 mm)
7	Large cobble (225-300 mm)
8	Small boulder (300-600 mm)
9	Large boulder (> 600 mm)

In segments lacking chinook spawning activity we measured sites containing typical habitat. We defined typical habitat using a classification system based on visual analysis of hydraulic characteristics and channel morphology (Table 2). These habitat types were mapped on aerial photographs taken at the river's average annual discharge of approximately 400 cms (14,000 cfs) and their areas were measured with a planimeter.

Table 2. Description of habitat types used to classify and identify the typical hydraulic and morphologic characteristics of the lower mainstem Clearwater River (LMCR).

Habitat types	Description
Run	Smooth hydraulics, low gradient, no channel scour, depth between 2 and 5 meters
Rapid run	Standing waves, higher gradient, no channel scour, depth between 2 and 5 meters
Rapid riffle	Turbulent hydraulics, higher gradient, depth less than 2 meters
Pool	Smooth hydraulics, scoured channel, depth between 5 and 7 meters
Eddy	Swirling hydraulics, scour, depth greater than 7 meters
Side channel	Secondary channel in islanded areas
Intermittent side channel	Secondary channel in islanded areas which dry up periodically

Cross-section Placement:

When assigning the locations of cross-sections, we prioritized spawning habitat. We also assigned cross-sections to typical habitats based on area; the most abundant typical habitats at each site were sampled. In general, if a habitat type contributed less than 10% of the total segment area, it was not sampled, except when this habitat was of special interest (i.e. intermittent side channel capable of stranding rearing juvenile salmon or steelhead trout).

Hydraulic Simulation Approach:

The Instream Flow Incremental Methodology (IFIM), developed by the U.S. Fish and Wildlife Service's National Ecology Research Center (NERC), provides a comprehensive collection of computer models and analytical procedures used to predict changes in hydraulic conditions and corresponding fish habitat characteristics with incremental changes in streamflow (Bovee 1982). PHABSIM, the Physical Habitat Simulation System, is the habitat analysis component of IFIM, and provides the computer based hydraulic and habitat simulation programs required for incremental analysis of habitat-discharge relationships (Milhous 1979).

We employed the IFG4 hydraulic simulation model to predict depths of flow and mean column velocities across each cross-section for discharges ranging from approximately 85 cms (3,000 cfs) to 1,416 cms (50,000 cfs) on the LMCR. IFG4 is a NERC hydraulic simulation program developed for use in instream flow habitat modeling studies. IFG4 is part of the PHABSIM system of computer programs developed and supported by NERC's Instream Flow and Aquatic Systems Group (Milhous et al. 1988), and provides the velocity and depth data required by habitat simulation programs (e.g. HABTAT, HABTAE).

We selected the IFG4 for hydraulic modeling because it is widely accepted for, and applied to, flow-related water resources studies in the United States. IFG4 is generally simpler to use and easier to calibrate than alternative hydraulic simulation programs based on step-backwater techniques, including WSP and HEC-2 (Milhous et al 1984; Milhous et al 1988; Orth and Maughan 1982). Unlike step-backwater models, IFG4 models cross-sections independently from each other, and consequently does not require additional measurements of water surface slopes among cross-sections. In addition, establishing the location of hydraulic controls below modeled cross-sections is not critical in IFG4 as it is with WSP and HEC-2. However, IFG4 requires at least three pairs of stage-discharge measurements, while WSP and HEC-2 require only a single starting water surface elevation and corresponding discharge from which hydraulic calculations at higher flows are based. Acquisition of the multiple stage-discharge measurements required by IFG4 was not difficult in our study because of the time-efficient use of rebar to mark water surface elevations at different discharges, and of a "total station" surveying instrument from which marked elevations were measured.

The IFG4 program is capable of predicting velocities and mean column depths across a cross-section for over 100 discharges in a single IFG4 run (Milhous et al. 1989). In addition to predicting depths and velocities, IFG4 also provides hydraulic geometry calculations including wetted width, mean channel depth, mean channel velocity, wetter perimeter, and hydraulic radius. Additional hydraulic geometry calculations are provided for each cross-section by running REV14 (Review IFG4), a hydraulic review and diagnostics program which is used in conjunction with IFG4 .

Hydraulic simulations using IFG4 are based upon an empirical log-log stage-discharge relationship calculated independently for each cross-section (Bovee and Milhous 1978). As such, it is assumed that an acceptable log-linear relationship can be established at each cross-section. IFG4 hydraulic simulations include the following computation procedures:

1. Streambed elevations are defined at specified distances along each cross-section. Bed elevation data are obtained at specified distance intervals along each cross-section from surveying instrument, level line, or depth measurements. These intervals provide the basis for a common set of "verticals" along the cross-section for which depths and velocities are calculated over a range of simulation discharges. This array of distance (X) and elevation (Y) coordinates is used by IFG4 for all hydraulic calculations. The distance interval between two consecutive X coordinates is referred to as a "cell".

2. An empirical stage-discharge relationship is calculated for each cross-section. This relationship is typically based upon three or more stage-discharge pairs. With IFG4, this relationship is calculated by a least-squares linear regression (Milhous et al. 1984). Since both stage and discharge are logarithmically transformed for this regression, this stage-discharge relationship is expressed as an exponential equation. This equation takes the form:

$$Q = A(WSL - SZF)^B;$$

where Q is the discharge predicted from a given water surface elevation , A and B are regression coefficients unique to a given cross-section, WSL is the given water surface elevation, and SZF is the stage of zero flow. Since water can be retained by downstream hydraulic controls for some cross-sections (e.g. pools) during zero flow conditions, subtracting SZF from water surface elevation provides a net water column depth which can be correlated with discharge.

Alternatively, this regression relationship can be restated as the equation:

$$Stage = x(Q)^y;$$

The range of discharges for which water surface elevations are measured should be the same as that to be modeled, since increased errors are likely when water surface elevations are extrapolated beyond the measured range of flows. This is especially true when discharges are simulated beyond channel banks, or when a cross-section possesses a complex profile.

3. The stage-discharge relationship is then used to predict water surface elevations for unmeasured discharges for which depth and velocity data are desired for habitat modeling purposes. The distribution of depths across the channel are calculated by subtracting measured streambed elevations from the predicted water surface elevation for a given discharge. Hydraulic radius, wetted width, and wetted perimeter are also calculated from the array of X,Y streambed coordinates, and the given water surface elevation.

4. A distribution of velocities along a cross-section are predicted by IFG4 for each simulation discharge, and are based upon a set of velocities measured at the cross-section. Predicted velocity measurements provide a basis for calculating discharge at the cross-section for a given stage elevation. The discharge at which velocities are measured for calibration purposes is referred to as the "velocity calibration discharge". Velocities measured at this discharge are used by IFG4 to calculate the distribution of velocities for all simulation discharges. More than one set of discharges can be used for velocity calibration purposes. Serious problems in hydraulic simulation modeling usually result from multiple velocity calibration measurements, since identifying the exact position of verticals for each set of velocity measurements along a cross-section is very difficult. Because of these difficulties, NERC currently recommends the use of a single velocity calibration set for IFG4 simulations. Consequently, a single discharge velocity calibration procedure, referred to as IFG4-A by NERC, was applied to our study of the LMCR.

Mean water column velocities measured at verticals along a cross-section during the velocity calibration discharge are used by IFG4 to calculate a roughness coefficient for each cell, which is based on the application of Manning's Equation. Manning's Equation, which is normally used to calculate average velocity for a river or stream channel reach, is expressed as:

$$V = 1.49\ R^{(2/3)}\ S^{(1/2)}\ /\ N;$$

where V is mean channel velocity, R is hydraulic radius, S is water energy slope for the channel reach, and N is Manning's roughness coefficient. The coefficient 1.49 is applied to the equation when English measurement units are used. This equation can be rearranged to solve for N:

$$N = 1.49\ R^{(2/3)}\ S^{(1/2)}\ /\ V;$$

Mean column velocity, hydraulic radius, and water surface slope are calculated by IFG4 from measured bed elevation, water surface elevation, and discharge data.

This equation is applied by IFG4 to each cell in a cross-section by restating Manning's Equation as:

$$N_i = 1.49\ D_i^{(2/3)}\ S^{(1/2)}\ /\ V_i;$$

where N_i is the roughness coefficient for the ith cell of a cross-section, V_i is the mean column velocity measured at the cell, and S is the longitudinal water energy slope of the entire cross-section. D_i, the depth of the ith cell, is substituted for hydraulic radius.

IFG4 calculates an N value for each cell from velocity calibration discharge data provided in the IFG4 input data deck. Subsequently, the velocity of a cell can be estimated for any given simulation discharge by rearranging the formula as:

$$V_i = 1.49\ D_i^{(2/3)}\ S^{(1/2)}\ /\ N_i;$$

where D_i is the depth of the cell for each simulation discharge.

5. A mass balance procedure is used by IFG4 to adjust predicted velocities so that the discharge predicted from the velocity set equals the discharge predicted by the stage-discharge relationship. IFG4 calculates a partial discharge for each cell within a cross-section

with the expression:

$$Q_i = W_i D_i V_i;$$

where Q_i is the discharge of the ith cell, which is calculated from the width, depth, and velocity of that cell. The total channel discharge resulting from predicted velocities is estimated by summing the individual cell discharges for the entire cross-section:

$$Q_p = \Sigma Q_i.$$

The discharge, Q,, which is predicted from the resulting set of velocity calculations, is forced to equal the discharge predicted by the stage-discharge relationship by multiplying simulated cell velocities by an adjustment factor. This adjustment factor is referred to as the Velocity Adjustment Factor (VAF), which is calculated by dividing the discharge predicted from the stage-discharge relationship by the discharge predicted from predicted velocities:

$$VAF = Q_{stq} / Q_p;$$

where Q_{stq} is the discharge used in the stage-discharge relationship.

Final velocity estimations are calculated for each cell using the expression:

$$V_{fi} = V_i \times VAF;$$

where V_{fi} is the final velocity estimation for the ith cell.

Accurate hydraulic simulations using IFG4 require that the following assumptions are met:

1. The stage-discharge relationship for each cross-section can be adequately expressed as a log-linear equation. Channels with complex cross-sectional profiles are not well modeled using a log-linear relationship, requiring the use of alternative statistical relationships (e.g. polynomial regression), or alternative hydraulic models (e.g. WSP or other step-backwater models) which provide better estimates of water surface elevations for simulation discharges.

2. A sufficient number of stage-discharge measurements should be obtained to adequately describe the cross-section for the range of discharges to be -modeled.

For this reason, a minimum of three stage-discharge pairs should be measured for each cross-section (Milhous et al 1984).

3. IFG4 is limited to analysis of steady flow conditions in a channel having a stable bed. Because cross-sections are modeled independently of each other, however, discharge does not have to be constant among transect sites within a study reach. Never-the-less, discharge must be constant during velocity calibration measurements.

Simulating hydraulic conditions from cross-section data involved five steps. First, stage-discharge relationships were determined at six discharge events for cross-sectional transect sites located within spawning and typical habitat in the LMCR. Second, velocities and depths were recorded across each transect during a single velocity calibration discharge of approximately 324 cms (11,400 cfs). Third, resulting data was reduced and reviewed for accuracy for input into the IFG4 computer program. Fourth, we used IFG4 to predict changes in hydraulic geometry and habitat characteristics (depth, velocity, wetted width, wetted perimeter, and hydraulic radius) for a range of simulated discharges. Finally, we calibrated the model using standard procedures.

Stage-Discharge Data Acquisition:

Six stage-discharge measurements were obtained at each cross-section in our study. Measurement of six pairs provided for more accurate predictions of water surface elevations for the range of flows expected to be modeled, and facilitated a relatively simple calibration procedure. Water surface elevations were measured at approximately 113, 227, 312, 453, 991, and 1,300 cms (4,000, 8000, 11,000, 16,000, 35,000, and 46,000 cfs). Discharge measurements were obtained from the Peck and Spalding USGS gaging stations located on the LMCR. Discharge values from the Peck station were applied to water surface elevations measured in the North Fork and Big Canyon study sites, while values from the Spalding Station were applied to water surface elevations measured in the Bedrock and Upper Potlatch, and Lower Potlatch study sites.

High discharges exceeding 1700 cms (60,000 cfs) prevented identification of habitat features, including spawning gravels, and placement of transects until mid-summer. To allow this study to be initiated in 1989 instead of 1990, measurement of water surface elevations for use in stage-discharge relationships preceded the establishment of cross-section locations. Water surface elevations (WSE's) were measured at transects located at points where water surface gradient changed with the study site boundaries. These are referred to as WSE transects, to distinguish then from hydraulic measurement cross-sections. Stage-discharge relationships at cross-sections were calculated by interpolating between water surface elevations recorded at WSE transects using the distances between WSE transects adjacent to the hydraulic measurement cross-sections in question.

Water surface elevation measurements were obtained on both banks of the river and islands. Rebar (0.6 m or 2.0 ft in length) were used to identify the location and elevation of the water's edge during the six discharge events measured at each WSE transect. The location and elevation of all water surface elevation rebar were surveyed on a later date. The use of rebar proved to be time and cost effective, as water surface elevations from all six discharge events could be surveyed at the same time.

Discharge readings were obtained at frequent intervals during rebar placement by calling the USGS GOES stations at Peck and Spalding.

Elevations of WSE rebar were surveyed with an electronic recording "total station" theodolite. This study employed a Wild T1000 electronic theodolite and D1000 infrared distance meter. These coupled units provide a direct readout of horizontal and vertical distances from the instrument to each survey point. Most distances were measured from a single optical prism attached to a surveying rod, which was placed on the rebar at WSE transects, and along hydraulic measurement cross-sections. A triple prism was used to measure distances greater than 610 m (2000 ft).

The instrument provided direct readouts of vertical distances, which facilitated rapid detection of surveying errors. All horizontal distances for hydraulic cross-sections and water surface elevation transects were measured using this instrument.

Elevations relative to instrument height were calculated at each survey point by subtracting the height of the plumb pole prism from the vertical elevation reading. When several instrument positions were used within a given study area, all instrument heights referenced the first instrument position. The first instrument position at any study site was assigned an arbitrary elevation so that water surface and instream flow transect elevations for the study site would have a maximum value of 30 to 33 m (100 to 110 ft). All subsequent instrument heights were referenced to the first instrument height by foreshot and backshot calculations, or by referencing a permanent benchmark rebar.

Surveyed positions were assigned Cartesian (X,Y,Z) coordinates based upon horizontal angle and distance measurements obtained from the first total station location at each study reach. Horizontal angles were referenced from a horizontal zero (HZO) line, which was set to an arbitrary landmark (eg. bridge piling, phone pole). The initial instrument position was assigned an x,y value of 0,0. Subsequent x and y coordinates where calculated using the following formulae for conversion of polar to Cartesian coordinates:

$$X = D * \text{sine}(HZ)$$
$$Y = D * \text{cosine}(HZ)$$

where D = horizontal distance to position
and: HZ = horizontal angle from HZO

When more than one instrument location was required to measure water surface elevations or cross-section positions within a study reach, all instrument locations referenced the first instrument position. A computer spreadsheet was used for all surveying calculations. Distances between surveyed positions were calculated using the formula:

Distance = The square root of $(X2-X1)^2 + (Y2-Y1)^2$

where: (X1,Y1) is the first coordinate position

and: (X2,Y2) is the second coordinate position

Longitudinal distances between cross-section sites and corresponding WSE transect rebar were used to calculate water surface elevations at the transect sites for development of stage-discharge relationships. Longitudinal distances and elevation differences between cross-sections were used to provide the water surface slope values required by IFG4.

Velocity Calibration and Substrate Data:

Velocities and depths were measured across the transects at a flow of approximately 324 cms (11,400 cfs) from a boat using the fixed line, fixed point technique (Bovee and Milhous 1978). This measuring system is most desirable when detailed hydraulic simulation models, such as IFG4, are to be used. Anchor points, either metal fence posts or cable attached to trees and rocks, were established on both banks of the river at each cross-section. The hooked equipped end of a spool of beaded 3 mm diameter (1/8 inch) aircraft cable was ferried from one bank to the other, where it was then attached to the anchor point on that bank. On the opposite bank, come-alongs affixed with cable clamps and attached to an anchor point were then used to strech the cable tight. A 14 ft aluminum boat was attached to the cable using a USGS boat measurement apparatus. This apparatus provided for consistent horizontal location on the cable beads, and was equipped with a quick-release safety system.

Velocities and depths were measured at regular intervals, identified by beads, along this cross-section cable. Either 3 or 6 m (10 or 20 ft) measuring intervals were used on each cross section, depending upon width of the river channel. Velocity and depth measurements were obtained using a USGS cable suspension system. This system employed a crosspiece to which the cross-section cable was attached, and a sounding reel and boom to which a 66 or 110 kg (30 or 50 lb) sounding weight was attached. A Marsh-McBirney velocity meter was attached to the sounding weight for velocity measurements. Velocities at each cable bead interval or "cell" were measured at both 2/10ths and 8/10ths depth when total depth exceeded 0.8 m (2.5 ft), and at 6/10ths depth in shallower water (Bovee and Milhous 1978). Substrate and cover (see Tables 1 and 3) were also measured at each interval along the cross-section cable. Substrate and cover codes were recorded by a single individual to maintain consistency among transects and study reaches. A Plexiglass view-tube was used to view substrate and cover in turbulent surface water.

Table 3. Cover coding system used during the collection of cover data in the lower Clearwater River (LMCR).

Code	Cover description
1	No cover
2	Velocity cover
3	Instream overhead cover
4	Bank overhead cover
5	Combination cover

Beyond the waters edge, bank elevations were measured at regular intervals along the transect line with the total station. The water surface elevation rebar, located at many locations throughout each study site, were used to provide benchmark elevations for these overbank measurements. Depths recorded from the boat were converted to transect elevations by measuring the water surface elevation on each bank, and then referencing recorded depths to the mean of both water surface elevations measured.

Data Reduction:

The IFG4 data deck employed for preliminary modelling of LMCR hydraulics was assembled from several data components. These included:

1) Depth, velocity, and substrate measurements obtained during the single velocity calibration discharge measurement;

2) Overbank elevation and substrate measurements obtained by the survey crew;

3) Stage-discharge relationships obtained from rebar placed during six discharge events; and

4) Inter-transect distances and water surface slope calculations obtained from WSE transect and hydraulic measurement cross-section locations.

A microcomputer spreadsheet program was used to combine cross-section distance, depth, velocity, and substrate measurements with overbank elevation and substrate measurements. Measured depths for each transect were converted into bed elevations by subtracting depth measurements from the average of the right and left bank water surface elevation at each cross-section. Transect distance measurements were obtained by adding the cross-section distance measurements to the overbank distance measurements, using the location of the waters' edge on the right bank and left bank as reference points for these distance calculations.

Resulting spreadsheet distance and depth calculations for each transect were converted into individual IFG4 formatted data files using the I4TEXT text file conversion program. This program also required the input of the six stage-discharge data pairs, the water surface slope and elevation at the calibration discharge, and the distance to the next downstream transect in a downstream direction. IFG4 formatted data files for each transect were then combined to produce an IFG4 data deck for each of the three study sites. In the Bedrock and Potlatch study sites, separate data decks were produced for main channel and islanded side channel transects. Separate data decks were required for calibration purposes, since side channel transects conveyed only a portion of the total river discharge at each of the six measured discharges.

Hydraulic Model Calibration:

Calibration of IFG4 data input decks produced for the LMCR involved five steps. The steps are described as follows:

1. The data decks were reviewed for data entry errors. This was accomplished with the CK14 (Check IFG4) data deck review program. Cross-section elevation, distance, velocity, and substrate data displayed in output from this program was compared to field data and subsequent intermediate calculations obtained from spreadsheets. Data entry errors then were corrected.

2. The water surface elevations employed in the stage-discharge relationships applied to each transect were reviewed and evaluated. The REV14 (Review IFG4) hydraulic review program was employed for this purpose. Where necessary, water surface elevations were corrected using known benchmark elevations established at each cross-section. Interpolation of cross-section water surface elevations between WSE rebar sites provided one source of error for some transects. However, this was easily identified and comparing predicted water surface elevations with known water surface elevations situated within the cross-section.

   This source of error, while minimal, was corrected by a adding a constant correction value to each predicted water surface elevation for given cross-section. This constant was calculated by subtracting the predicted water surface elevation at the velocity calibration discharge from a known measured water surface elevation for this same discharge.

3. Discharges, termed partial discharges, were calculated for each individual channel in multiple channel sites. These partial river discharges were required since stage-discharge mesurements in side channels are based

upon partial river discharges, and not river flow. Partial discharges were calculated for each discharge of six water surface elevations measured at side channel cross-sections. Partial discharge calculations were based upon known discharge, bed elevation, and water surface elevation measurements through application of Manning's equation:

$$V = 1.49\ R^{(2/3)}\ S^{(1/2)}\ /\ N.$$

As mentioned previously, V is the mean velocity for the entire channel, R is the hydraulic radius, and S is the longitudinal water energy slope. Partial discharges for individual channels in multiple channel sites can be obtained from velocity calibration measurements conducted at approximately 323 cms (11,400 cfs). Subsequently, these known discharges form a basis for solving Manning's roughness coefficient, N, at each transect using the rearranged equation:

$$N = 1.49\ R^{(2/3)}\ S^{(1/2)}\ /\ V.$$

Again, R is obtained implicitly from bed elevation and water surface elevation data, and was acquired for these calculations from the REV14 hydraulic review program. S was obtained by calculating the water surface slope from water surface elevation measurements obtained from rebar located above and below each cross-section. Channel velocity V was calculated from the equation:

$$V = Q/A;$$

where Q is the discharge calculated for a given side channel, and A is the cross-sectional area calculated known bed elevations and the velocity calibration water surface elevation for that channel. REV14 provides the cross-sectional area value for each water surface elevation.

The variables R, A, and S were calculated for each of the six measured water surface elevations for transects located in side channels. Partial discharge in each side channel was calculated for each specified water surface elevation by assuming that N is constant, by rearranging Manning's equation as:

$$Q = A\ 1.49\ R^{(2/3)}\ S^{(1/2)}\ /\ N;$$

since average channel discharge can be defined as:

$$Q = V*A.$$

If the sum a partial discharges did not equal the total river discharge, a correction factor was multiplied to each partial discharge. This correction factor was defined by:

$$C_q = Q_{obs}/Q_p;$$

where C_q is the correction factor, Q_{obs} is the observed total river discharge obtained from USGS records, and Q_p is the discharge predicted by summing calculated side channel discharges. Resulting partial discharge estimations were then used to define side channel stage-discharge relationships for IFG4 runs.

4. The log-log stage-discharge relationship was evaluated to determine whether the IFG4 hydraulic model was appropriate for each transect. This relationship was evaluated by comparing water surface elevations predicted by the stage-discharge relationship with those actually measured. In addition, a regression goodness-of-fit analysis was used to assess the linearity of each stage-discharge relationship. In addition, VAF verse discharge plots were used to identify potential calibration problems for each transect VAF plots were produced in calibration IFIM runs. Analysis of VAF plots is reviewed in Appendix B.

5. The distribution of velocities was evaluated at each transect for a range of simulation discharges. One source of error in IFG4 hydraulic simulations involves prediction of velocities for cells which are dry during calibration velocity measurements (Milhous et al, 1988). This often results in the calculation of a cell's Manning's roughness coefficient which is either too high or too low for calculating velocities over a complete range of discharges. This is referred to as an "edge roughness" problem, since it usually occurs to cells located adjacent to either bank of the river. This problem can be minimize by constraining cell roughness coefficients to maximum and minimum values. These constraints can be used in IFG4 simulations by specifying NMAX (N maximum) and NMIN (N minimum) values in the input data deck. The need for NMAX and NMIN values was determined after reviewing cell roughness predictions using IFG4 and REV14 data deck runs.

Cross-sections were grouped according to study site in both calibration and production run IFG4 data decks. A second level of grouping was required in islanded sections, since crossections in the same segment experienced different partial discharges for the total river discharge. In this case, cross-sections were included in the same IFG4 data deck if they experienced the same flow regime, i.e. they were located in the same side channel. Because of the hydraulic complexity of islanded study sites, a total of 15 separate data decks were used for 30 cross-sections.

OBJECTIVE 2: Document the use of the LMCR by anadromous and non-anadromous fish

We determined the relative seasonal densities of fishes present in the LMCR. This was accomplished using a proportional sampling strategy to further stratify the hydraulic simulation study sites (also referred to as study sites) into finer habitat types. Direct observation lanes were then assigned into these habitat types. Then we weighted our sampling effort by habitat type and between hydraulic simulation sites by varying the lane lengths. Finally, we sampled the lanes and recorded the number fish observed.

Microhabitat preferences for the fishes observed were documented by measuring the velocities, depths, substrate, and cover at the exact location where fish were counted. Velocity, depth, substrate, and cover frequency data were reduced to microhabitat preference histograms for graphical display. An excellent description of this procedure was given by Bovee (1986) and Crance and Shoemaker (1986). In general, microhabitat data is collected at the location of an undisturbed fish. The relative frequency of observations in predetermined increments is determined for data from each microhabitat parameter. This produces a microhabitat utilization frequency distribution. Depth, velocity, substrate, and cover are also measured at numerous randomly selected locations within the study site and relative frequency is determined for this habitat component. This component is called habitat availability. Microhabitat preference is computed by dividing the relative frequency of fish observed utilizing an increment of the microhabitat parameter by the relative frequency of observation of that increments availability at the study site. Then the data are normalized and a histogram is constructed to graphically display the microhabitat preference of the species. A curve is then fitted over the histogram by eye or statistics, thereby, producing a Suitability Index Curve (SI). These SI curves are then used in IFIM to predict relationships between streamflow and fish habitat. In our study we collected frequency data that represented microhabitat preference without the intermediate step of correcting for availability. This was done by sampling the habitat using a proportional sampling strategy to be described hereafter. However, we did not normalize our histograms and fit them with curves since they are not yet intended for use in IFIM modelling.

In the following sections, we present detailed methods used in direct observation lane assignment, collection of fish density data, density data analysis, collection of fish microhabitat preference data, and microhabitat preference data analysis.

Direct Observation Lane Assignment:

We established direct observation lanes within the study sites by using a modification of the proportional sampling approach (Bain et al. 1982 in Bovee 1986). Proportional sampling requires the division of each study site into finely delineated habitat types. We used a more simplified approach than Bain's because of the large size of the LMCR. Pool and run habitat types (See Table 2) located on bends were further divided into inside and outside units to provide for habitat differences caused by the triangular shape of the channel and runs deeper than 4 m (14 ft) were classified as deep runs.

We determined which habitat types to sample based on area; the most abundant habitats at each site were sampled. If a habitat type contributed less than 10% of the total site area it was not sampled except when this habitat was of special interest (i.e. intermittent side channel capable of stranding fish). Again, we used a planimeter on aerial photographs taken at a flow approximately equal to the rivers average annual discharge of 397 cms (14,000 cfs) to measure habitat area within each site.

Sampling effort was distributed by varying lane length proportionally to habitat type area. The single most abundant habitat of all sites combined was represented with an arbitrarily established distance of 366 m (1200 ft). The lane lengths at all remaining sites were determined by dividing the area of their respective habitat by the area of the most abundant habitat. We then multiplied 366 m by this fraction to determine the length of the lane. This also insured that sampling effort at each site was proportional to site area; larger sites received more sampling effort (measured in terms of lane length) than small sites.

Lane widths were measured to middle of the channel thalweg. Therefore, as discharge increased lane width increased and vice versa.

The actual placement of the lanes was done by superimposing a numbered grid over site photographs and drawing random numbers.

In the field, study lanes were cross sectionally stratified based on water depth into snorkeling and SCUBA corridors (Figure 2). Snorkeling corridors were up to 1.2 m (4.0 ft) deep and SCUBA corridors ranged from 1.2 to 7.6 m (4.0 to 25.0 ft) deep. Dive buoys were used to mark the boundaries of both strata and to provide guidance for the divers. Hand held range finders and survey tapes were used to measure the distance from the shore to each of the four buoys and total channel width.

Collection of Fish Density Data:

We sampled each lane at each study site bi-weekly from July through November and once in December using two divers and two snorkelers. One counting pass was made in each lane per day.

Two snorkelers completely sampled the inshore shallow snorkeling corridor by creeping downriver (Figure 2). The SCUBA team covered the deeper SCUBA corridor by drifting, crawling, and walking a diagonal downriver descent pattern (Figure 2). Prior to the dive we assessed the maximum underwater visibility. We used maximum underwater visibility to establish the observation distance within fish were to be counted. To do so we first multiplied the maximum underwater visibility by a reduction factor of about 0.6. Secondly, we cut a piece of cable twice this calculated length and marked it's midpoint with flagging. During the dive we held the cable taught between divers to insure that spacing was kept constant. The cable also regulated the observation distance within which fish were counted. Each diver counted fish which passed between himself and the ribbon on the cable and within half a cable length to his left or right (Figure 2).

Divers wore up to 30 Kg (66 lbs) of lead and felt soled wading boots to facilitate control during downriver descent. This technique proved executable in water with bottom velocities less than 1.2 m/sec (4.0 ft/sec).

Each study site contained swift water sampling lanes with bottom velocities exceeding 1.2 m/sec (4.0 ft/sec). Other researchers have sampled swift water using a static

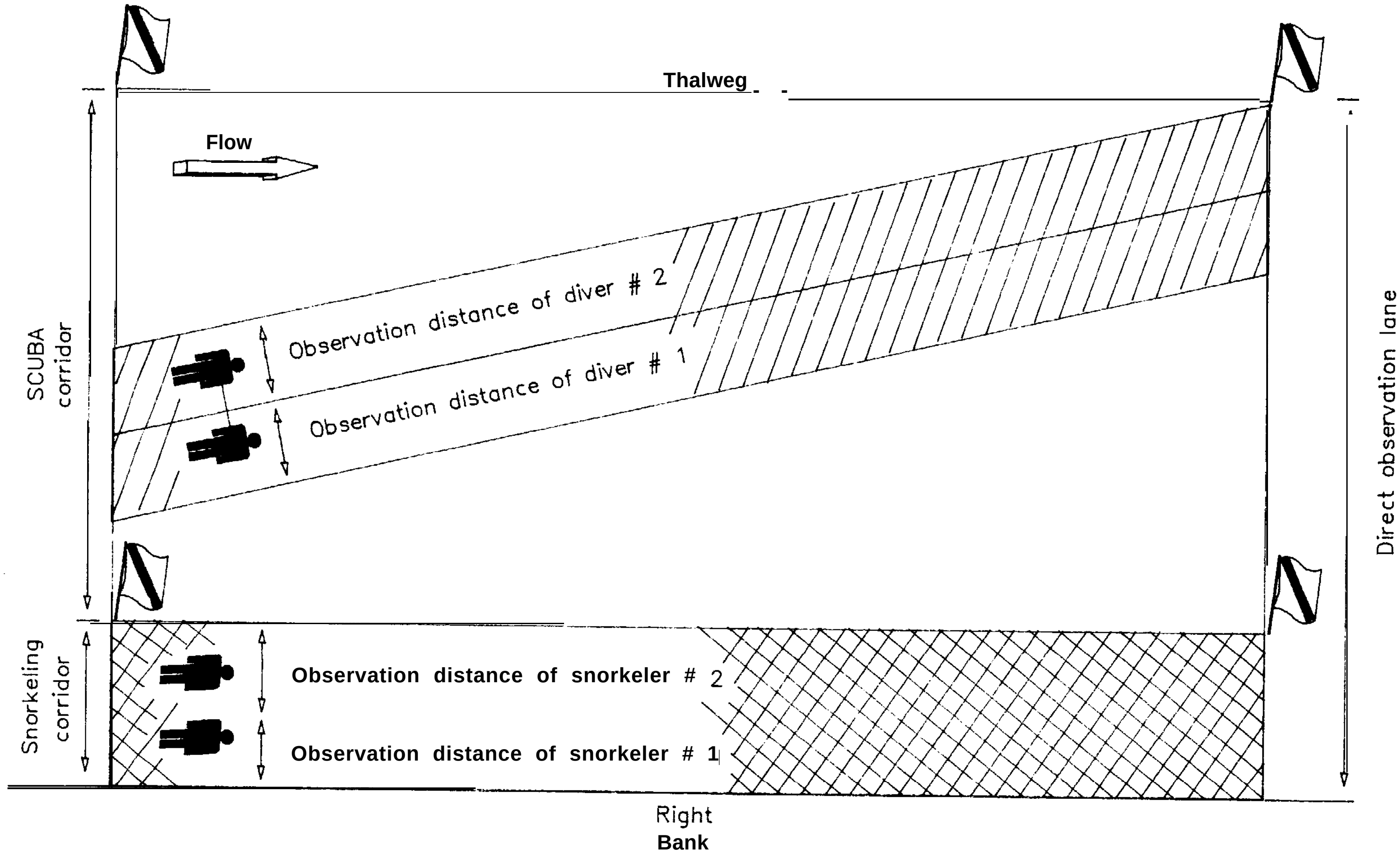

Figure 2. **Direct observation lane divided into the SCUBA sublane, snorkeling sublane and observation area by technique (SCUBA = ▨ and snorkeling = ▩).**

line with drop lines and mountain climbing equipment (Li 1988). However, channel width and water depth commonly exceed 92 and 1.8 m (100 yds and 6 ft), respectively. And more importantly, the use of static lines would threaten the safety of recreational boaters common on the LMCR. Therefore, swift water lanes were sampled using a pass through technique similar to that described by Schill and Griffith (1984). We sampled fast water lanes by dropping two snorkelers off the support boat at the top of the SCUBA corridor. These snorkelers counted fish within a their respective observation distance while floating downriver through the buoy marked boundaries of the corridor.

Density Data Analysis:

Daily fish densities in each snorkeling corridor were calculated by dividing the number of each species observed by snorkeling corridor area. Daily SCUBA corridor densities were calculated by dividing the number of each species observed on SCUBA or pass through by the observation area. Observation area was calculated by multiplying the total observation distance (the sum of both divers observation distances) by the length of the median diagonal that bi-sected the SCUBA corridor (see Figure 2).

Once density estimates were calculated for each species and observation technique, a composite lane weighted mean density was calculated by combining the snorkeling and SCUBA corridor (or pass through) data using the following formula.

$$\frac{(SnSp/m^2 \times Snm^2) + (ScSp/m^2 \times Scm^2)}{Snm^2 + Scm^2}$$

Where: $SnSp/m^2$ = species density in snorkeling corridor

Snm^2 = snorkeling corridor area

$ScSp/m^2$ = species density in the SCUBA observation area

Scm^2 = SCUBA corridor area

composite lane means from upriver sites were summed and averaged by species, size, and season. We also calculated average densities for the same categories using data from lower river sites. Data collected from July through September, October through November, and December were categorized as summer, fall and winter densities, respectively. Age for size groupings of wild rainbow/steelhead was determined with data collected during our tributary study.

The original intent of the this tributary study was to document mainstem rearing of wild steelhead parr produced naturally in the lower tributaries of the LMCR. We planed to differentially mark 1,000 60-200 mm (2-8 in) parr in Lolo Creek, Big Canyon Creek, Cottonwood Creek, and Bedrock Creek. However, late spring runoff reduced our sampling time so we limited our marking efforts to Bedrock Creek.

We electrofished Bedrock creek six times in the last two weeks of June with a battery operated backpack shocker. We measured total length and marked the rainbow/steelhead parr collected. We injected Alcian blue dye into the upper caudal fin with a panjet marker (Hart and Pitcher 1969). Scales were taken on fish midway between the adipose and dorsal fins just above the lateral line. Fish were identified as wild parr or hatchery smolts based on the presence of an adipose clip given to all DNFH steelhead smolts.

Scales of each rainbow/steelhead trout were mounted and pressed on an acetate slide. Clean non-regenerated scales were examined on a microfiche reader at 42X magnification. We recorded the number of annuli measured on each scale.

Collection of Fish Microhabitat Preference Data:

Microhabitat data were collected concurrent with density estimates. The procedure varied by observation technique. When fish were observed by snorkeling, their locations were marked. Fish species, size, nose depth, and association with other fishes were recorded immediately after sighting. After the snorkeling sublane was sampled the observers returned to the marker and measured the water velocity at the nose depth and the highest adjacent velocity within 60 cm (23 in) of the marker. Substrate (See Table 1), cover (see Table 3), total depth, and water temperature were also recorded at the marked site. When fish were observed by SCUBA divers, the same categories of data were recorded. However, all data were collected immediately when the fish was counted. Nose and adjacent velocities were determined using a Price AA current meter and visually counting cup rotations in 40 second intervals. Total depth was measured by dive gauge to 30 cm (12 in).

Fish Microhabitat Preference Data Analysis:

Preliminary microhabitat preference histograms were constructed for each species and age class of fish observed by combining every observation recorded during summer and fall at a range of discharges of approximately 100 to 400 cms (3,500 to 14,000 cfs).

OBJECTIVE 3: Investigate the incubation, rearing, and outmigration timing of fall and summer chinook salmon:

We estimated egg development timing of summer and fall chinook salmon using USGS water temperature data and hatchery chinook salmon egg incubation temperature unit requirements (Connor 1989). Based on this data, we asserted that summer and fall chinook fry would emerge in November and May, respectively. Subsequently, we designed an *in situ* incubation study using summer and fall chinook eggs to verify these predictions. Unfortunately, South Fork Salmon River summer chinook eggs were not available due to the depressed run sizes of these fish. Snake River Fall chinook work commenced on schedule and will be discussed in a later report.

RESULTS AND DISCUSSION

OBJECTIVE 1: Quantify the existing anadromous **salmonid** spawning and rearing habitat in the LMCR and develop capabilities to predict habitat conditions under various Dworshak Dam discharge regimes

River Stratification:

Based on flow regime and channel morphology we divided the LMCR into three segments (Appendix A, Tables Al-A3 and Figures Al-A2). The first segment began directly across from the Potlatch Mill and extends 16.0 km (9.9 mi) upriver to the mouth of Potlatch River. The second segment began at the mouth of the Potlatch River and ends 16.5 km (10.2 mi) upriver at the mouth of Bedrock Creek. The third segment began at the mouth of Bedrock Creek and extends 21.8 km (13.6 mi) upriver to the confluence of the LMCR and North Fork Clearwater River. Notably, we did not study the 1.6 km of Lower Granite Dam influenced backwater from the Clearwater Memorial Bridge to the Potlatch Mill. We also excluded the river reach extending approximately 1.6 km down from the North Fork and LMCR confluence because of the extreme effects Dworshak Dam releases on its hydraulic and morphologic characteristics.

We established study sites within the Potlatch River and Bedrock Creek segments because of the presence of spawning gravel and fall chinook spawning activity (Appendix A, Table A4, and Figures A3-A4). In addition to their value as spawning areas both sites were typical of their respective segment based on habitat type area (Appendix A, Table A5). Since the North Fork segment had supported no detectable chinook spawning activity we selected two study sites containing the dominant rapid riffle/pool sequences of the segment and which were easily accessible by boat (Appendix A, Table A5 and Figure A5).

Cross-section Placement:

The Potlatch River study site was initially divided into lower and upper areas. The lower area represented a very complex islanded reach similar to others within the LMCR below the Potlatch River confluence (Appendix A, Table A6 and Figure A6). Sixteen cross-sections were placed to characterize known spawning and typical habitat. The upper Potlatch area consisted of a simple single islanded reach (Appendix A, Table A7, Figure A6) and was represented by four cross-sections.

The Bedrock Creek study site was represented by 9 cross-sections located above the Cherry Lane Bridge (Appendix A, Table A8, Figure A7). This site was characteristic of the simpler island complexes within the Bedrock Creek segment and had cross-sections located across known fall chinook spawning areas and large areas of suitable spawning gravel. During final cross-section placement within this site we moved the upriver most transect a considerable distance downriver to into identical habitat which was easier to access.

The North Fork segment was composed of rapid riffle and pool sequences and contained two hydraulic simulation study sites. The Big Canyon Creek study site was represented by three cross-sections (Appendix A, Table A9 and Figure A8). Conditions within the North Fork study site were highly uniform and only two cross-sections were preliminarily assigned. The upstream cross-section NF-1 (Appendix A, Table A9, Figure A9), was not measured because of severe hydraulic conditions. Rapid riffle sections of the North Fork site not represented by failure to measure NF-1 were represented by cross-section BGC-2 in the Big Canyon Creek study site (Table A9, Figure A8) of the North Fork segment.

Hydraulic Simulation:

Discharge readings for stage discharge regressions were obtained from the GOES stations and are presented in Appendix B (Table B1). Changes in discharge were noted during some of the days in which rebar were placed, though these changes were relatively small. Slight differences in discharge were observed between the two USGS stations, reflecting tributary inflow over a distance of 39 km (23 miles). Constant release flows from Dworshak Reservoir were maintained in the LMCR by the Army Corps of Engineers for this study. Consequently, steady state flow conditions were assumed to exist during stage-discharge and velocity calibration measurements.

Overall, preliminary runs of IFG4 using stage-discharge and velocity calibration data produced highly acceptable simulations of hydraulic geometry for the LMCR over a wide range of flow (Appendix B, Figures Bl-B30). Analysis of stage-discharge relationships and other output using REV14 and IFG4 indicated that the IFG4 hydraulic simulation model was very appropriate for modelling hydraulic conditions for most cross-sections established on the LMCR. Key to understanding the suitability of the stage-discharge relationship calculated for each transect was the high goodness-of-fit (R-Squared value) and low regression variance observed for the logarithmic stage-discharge relationship calculated at each transect. Accurate hydraulic simulations resulted in many respects from the unusually high number (i.e. six) stage-discharge pairs we obtained at each transect. Also, we did not extrapolate calculated stage-discharge relationships above the maximum or minimum discharges measured. Finally, the the regular cross-sectional shape of most transects contributed to the accuracy of hydraulic simulation.

Only two problems were identified at certain transects during IFG4 calibration runs. First, predicted discharges applied to certain transects located in side channels of islanded study sites resulted in unusually high cell velocities during simulated low flow (less than 6,000 cfs total river discharge) conditions. This problem, which is detectable in our VAF plots (Appendix BO), can be easily remedied by acquiring additional discharge measurements in these side channels during low flow conditions during the summer of 1990. Second, calibration procedures indicated that because several transects had a highly complex cross-section, the stage-discharge relationship calculated for these transects was not predicting discharges at high (greater than 40,000 cfs) and low (less than 6,000 cfs) flow conditions. This problem can be remedied by requiring IFG4 to base simulation calculations for measured water surface elevations, instead of elevations predicted by the stage-discharge relationship, for specified discharges. This procedure is explained in greater detail in Appendix B.

Frequency distributions for velocity, depth, and substrate were presented for: Potlatch River study site intermittent channel and spawning areas; Bedrock Creek study site spawning areas: Big Canyon Creek study site rapid riffles: and Big Canyon Creek and North Fork study site pools. Although a number of flows were modeled with IFG4 during calibration procedures, we presented simulations for low flow (approx. 85 CMS or 3,000 cfs), medium flow (approx. 450 CMS or 16,000 cfs), and high flow (approx. 1300 CMS or 46,000 cfs) conditions. Simulated velocities, depths, and substrate were obtained for each of these discharges from IFG4 production runs.

Hydraulic simulation of of Potlatch River study site intermittent side channel habitat indicated that low to medium flows provided shallow low velocity habitat (Figures 3 and 4). At higher discharges, shallow water became scarce. However, significant areas having low velocities were still observed. The channel bottom in the intermittent channel habitat was composed large gravel and small cobbles (substrate codes 4 and 5), more of which is wetted at moderate flows than at low flows (Figure 5). However, there was little gain in wetted substrate at high modelled flows since the islands forming these side channels are topped over at approximately 566 cms (20,000 cfs).

Depth simulations for Potlatch River study site spawning areas showed considerable change with flow (Figure 6). Shallow water predominated at lower flows and depth increased quickly from medium to high flows. Likewise, simulated velocities increased dramatically from low to medium flows (Figure 7). High flow simulations exhibited a wide range of fast moving water. Substrate in these spawning areas was dominated by small cobbles at all simulated flows (Figure 8). A large increase in wetted substrate was evident between low and medium flows, while there was little change from medium to high flows.

Depth simulations for Bedrock Creek study site spawning habitat elicited a very gradual stair stepping pattern towards deeper water as simulated flow was raised (Figure 9). The same patterns was demonstrated by the response of velocity to flow; increases in flow caused gradual increases in velocity (Figure 10). Spawning substrate in the Bedrock Creek study site was predominantly a mixture of small to medium cobble, which was wetted gradually in even increments as flow increased.

Simulated depths for Big Canyon Creek study site rapid riffle habitat shifted evenly from shallow to deeper water as flow increased (Figure 12). A substantial jump in velocity was detectable with an icrease from low to medium flow, while from medium to high flow a more incremental shift was evident (Figure 13). From low to medium flows large cobble (code 7) emerged as the subdominant particle to medium cobbles (code 6)(Figure 14). More substrate is wetted at high simulated flow, but the particle size pattern remained unchanged.

Pool habitat depth simulations for the Big Canyon Creek study site were complicated becuase of the irregular shape of the channel in measured areas. More depth intervals were accounted for with each increase in flow and the number of counts for each existing interval remained similar (Figure 15). Velocity increased with flow in a stair stepped pattern (Figure 16). Pool substrate was a heterogeneous mixture dominated by small boulders (code 8)(Figure 17). Large cobbles (code 7), which were dry at low flow, were wetted at medium flow .

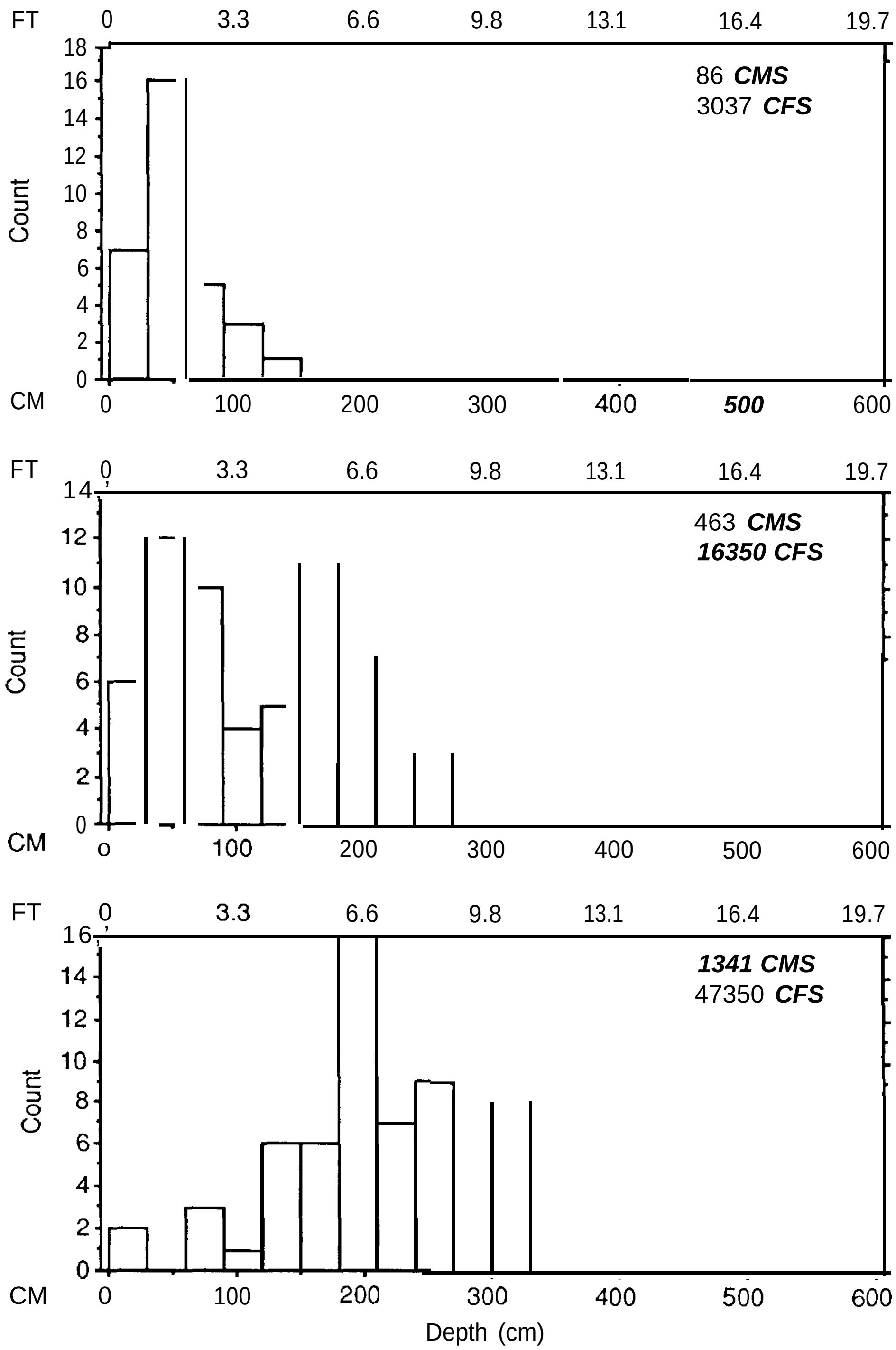

Figure 3. Depth distribution of Potlatch intermittent channel habitat at low, medium, and high flows.

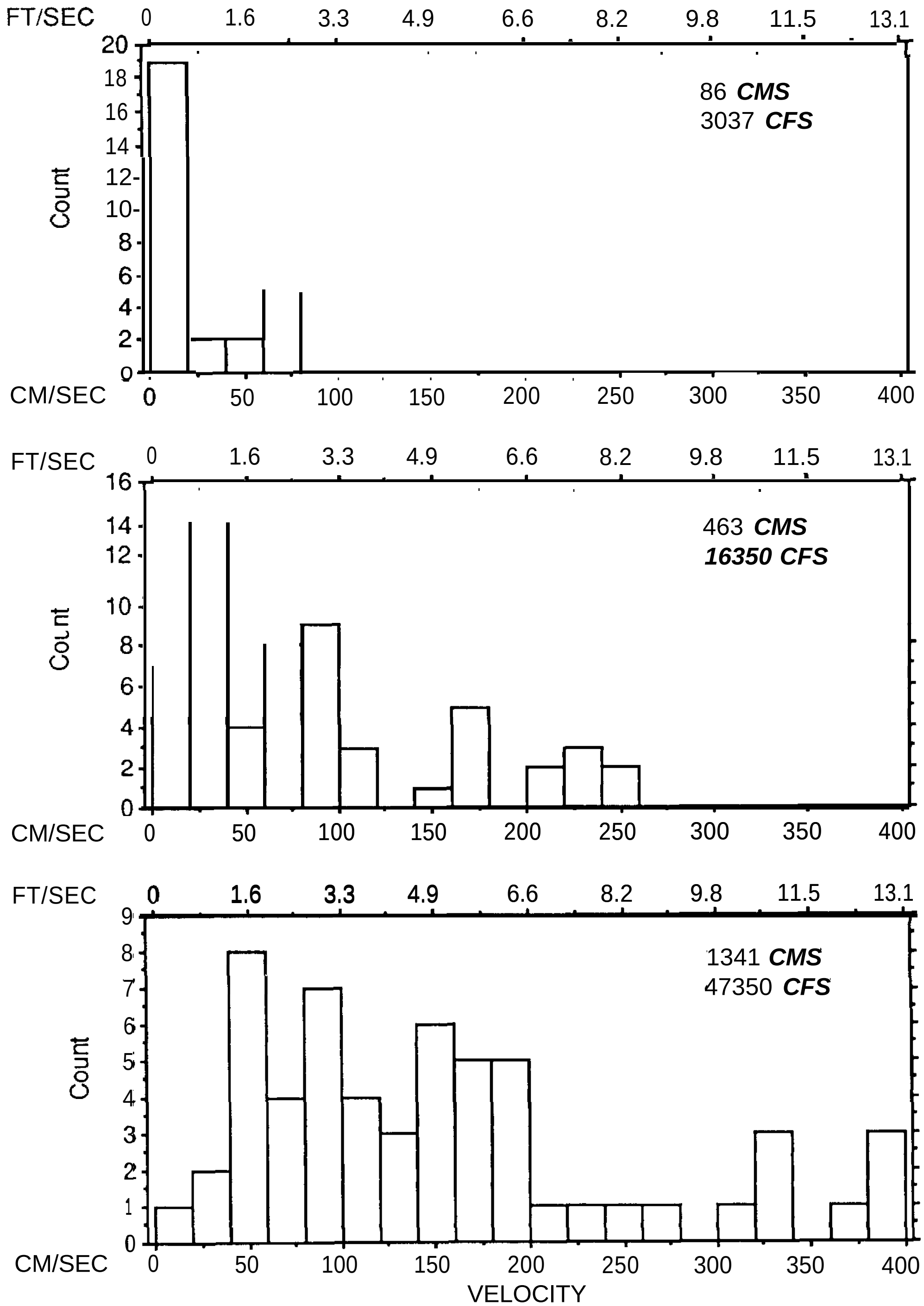

Figure 4. Velocity distribution of Potlatch intermittent channel habitat at low, medium, and high flows.

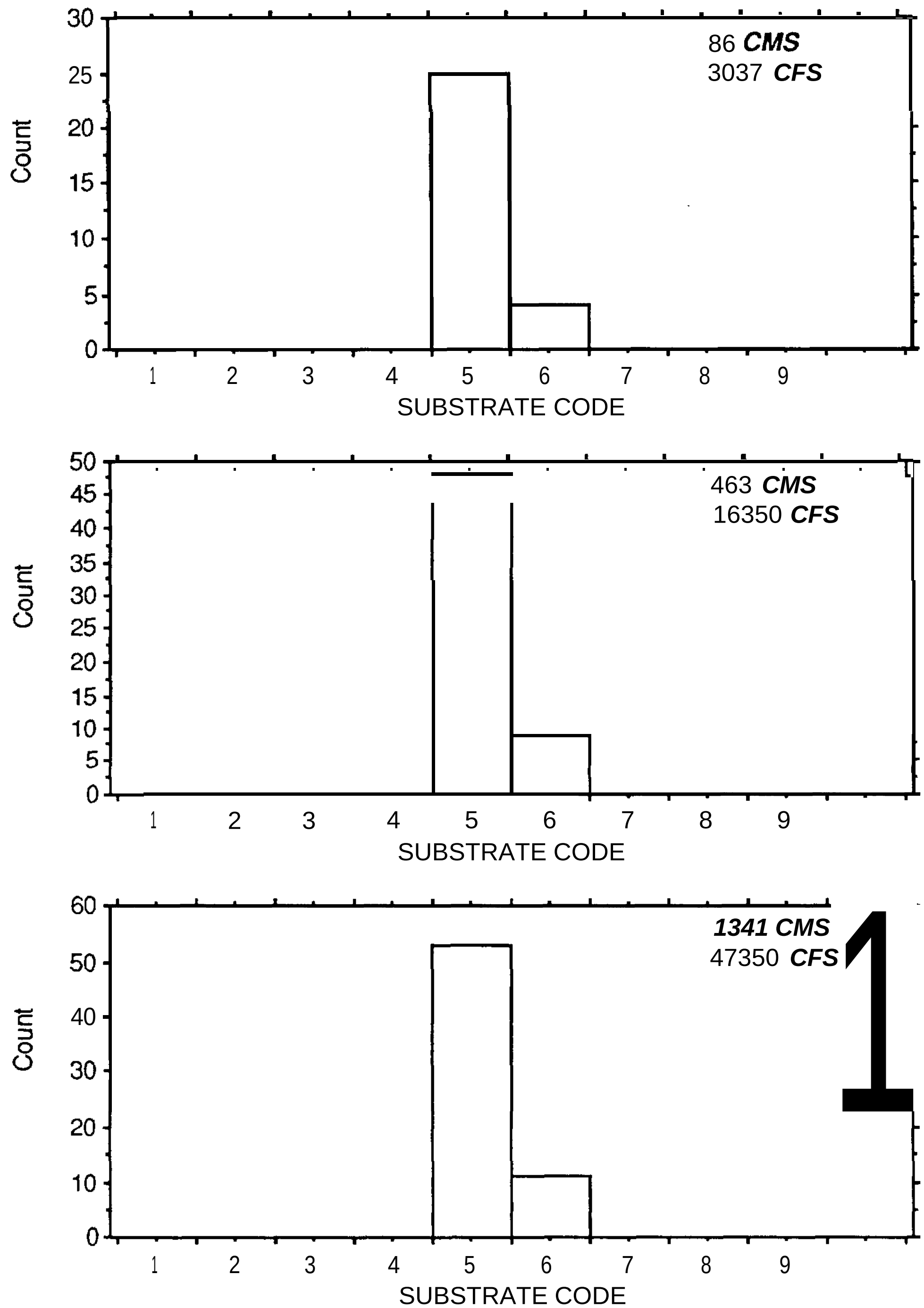

Figure 5. Substrate distribution of Potlatch intermittent channel habitat at low, medium, and high flows.

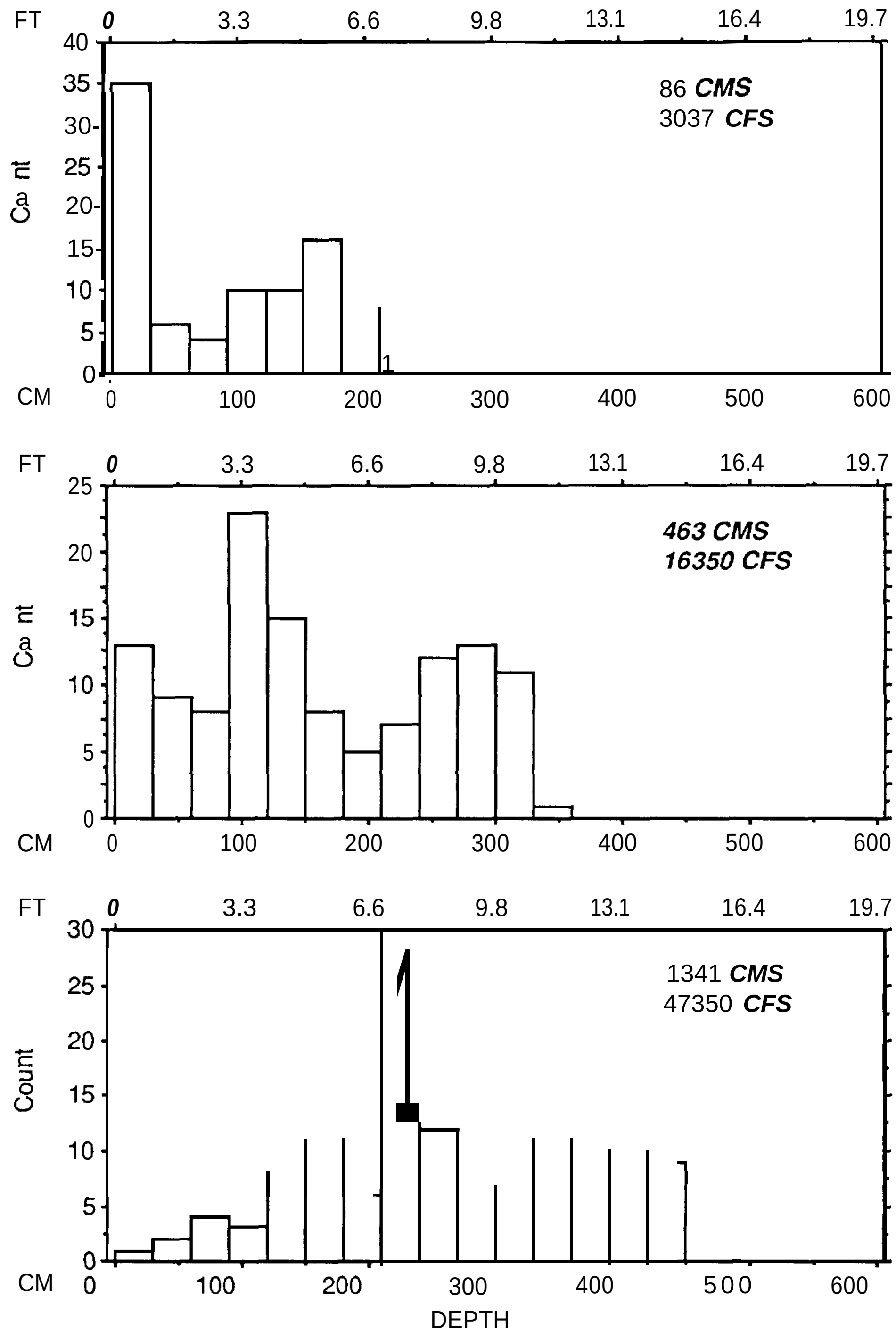

Figure 6. Depth distribution of Potlatch spawning habitat at low, medium, and high flows.

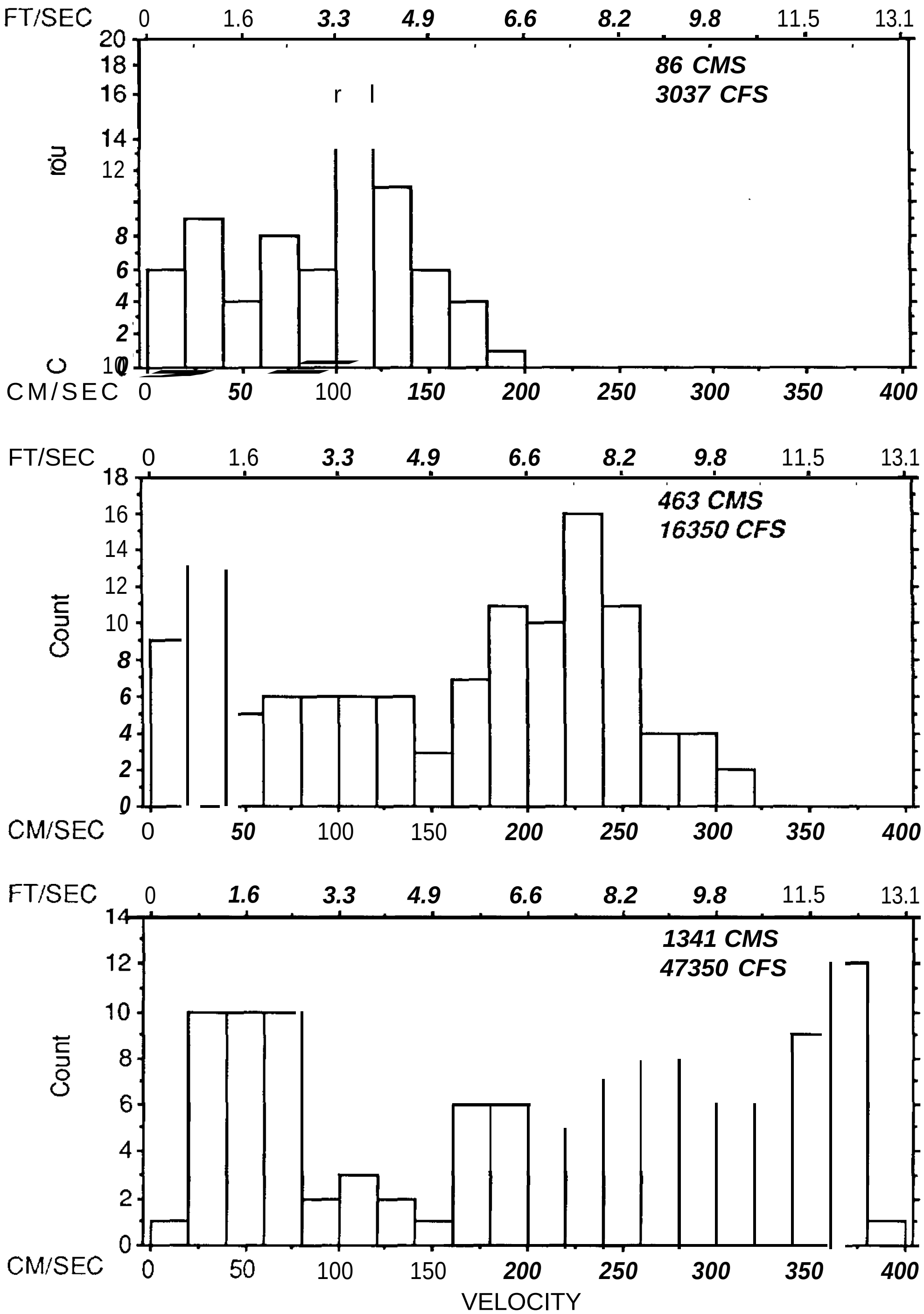

Figure 7. Velocity distribution of Potlatch spawning habitat at low, medium, and high flows.

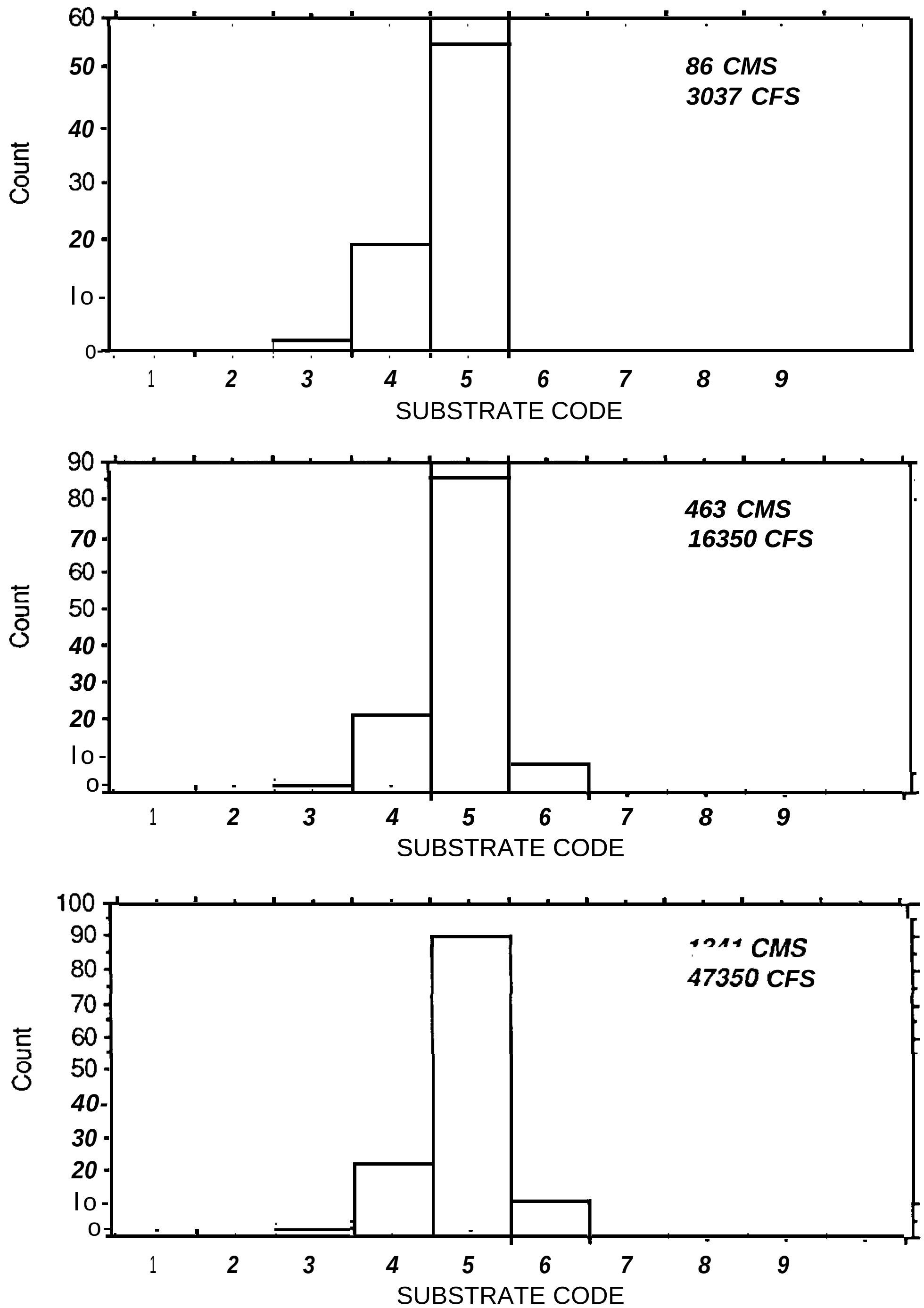

Figure 8. Substrate distribution of Potlatch spawning habitat at low, medium, and high flows.

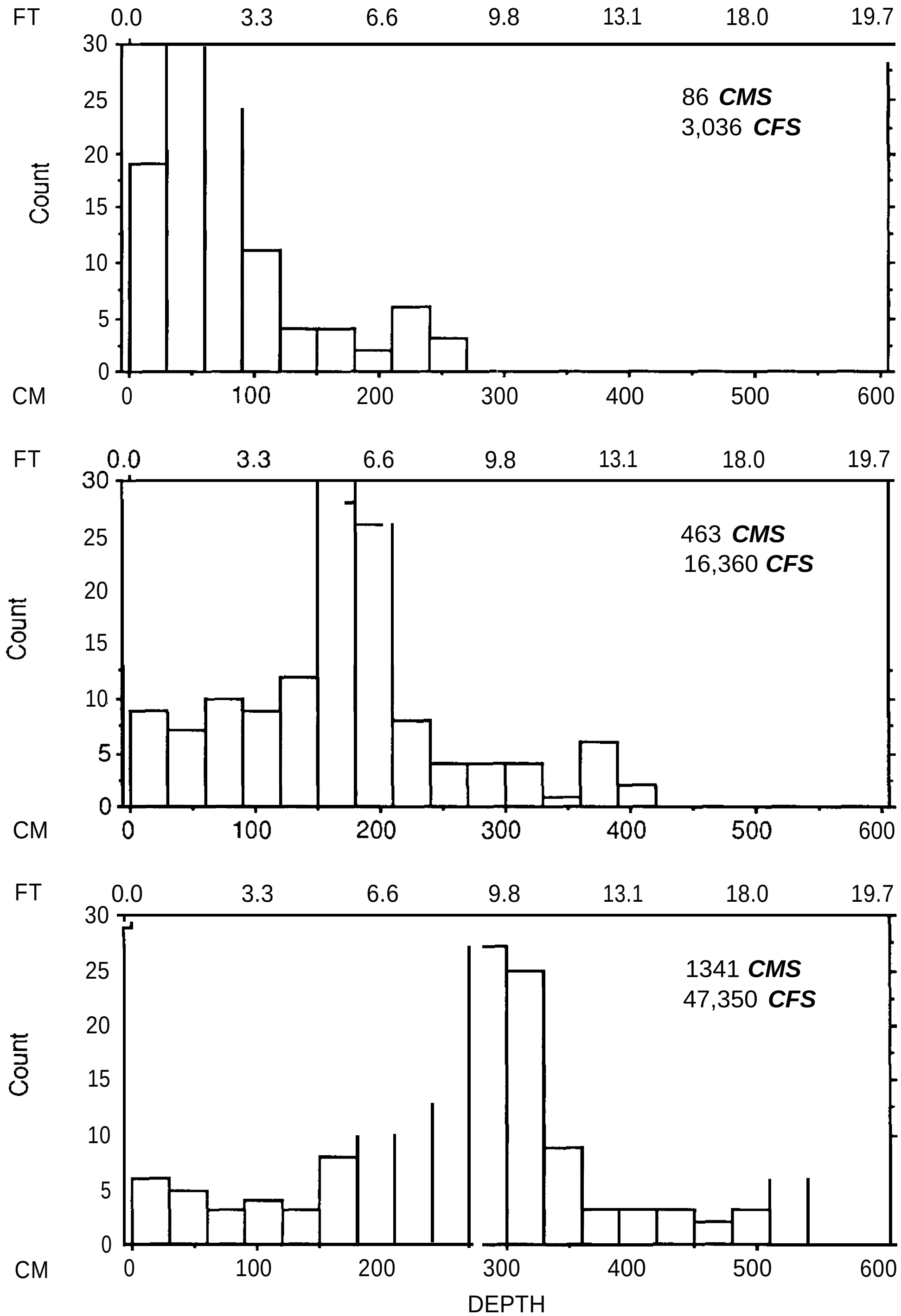

Figure 9. Depth distribution of Bedrock spawning habitat at low, medium, and high flows.

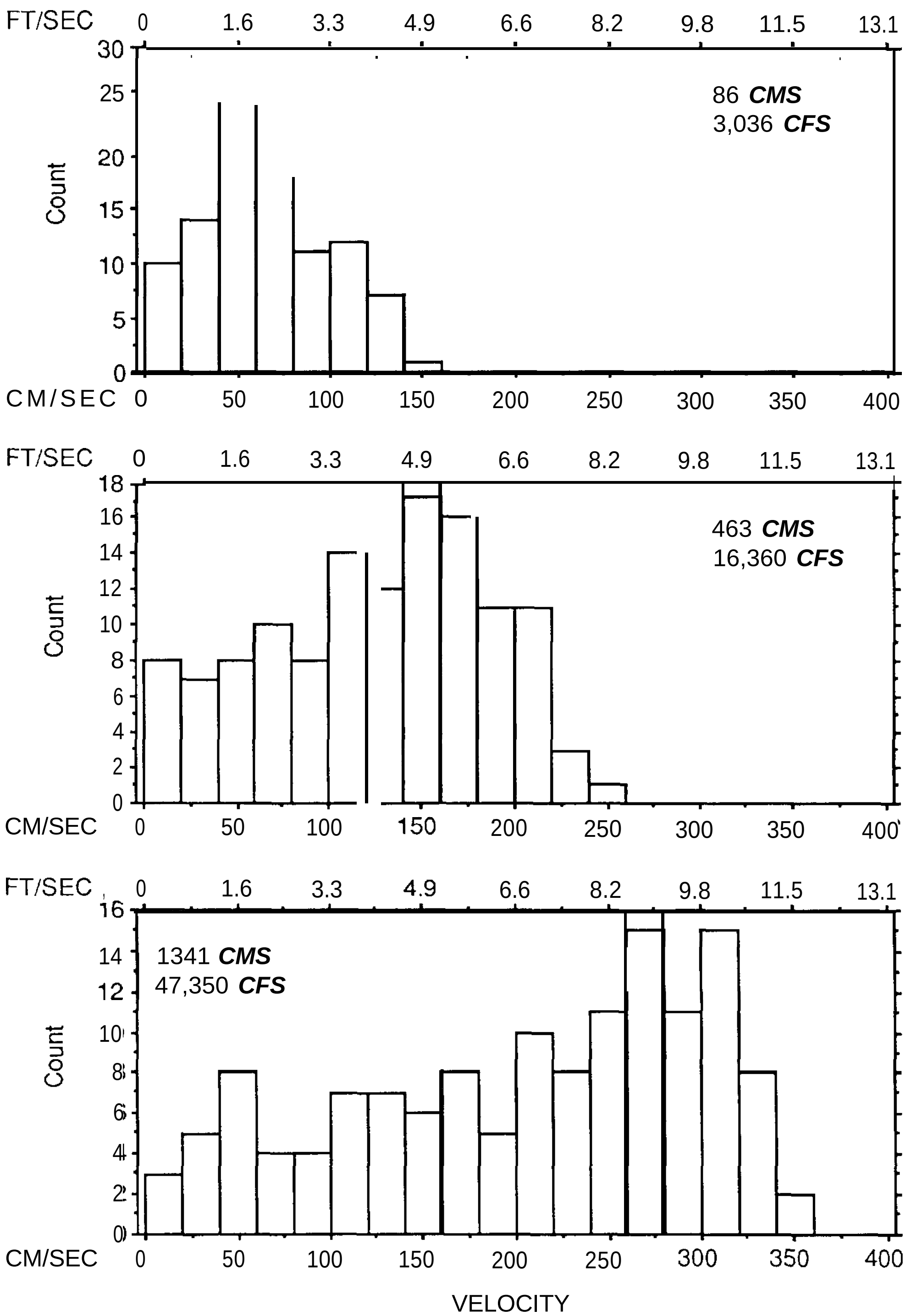

Figure 10. Velocity distribution of Bedrock spawning habitat at low, medium, and high flows.

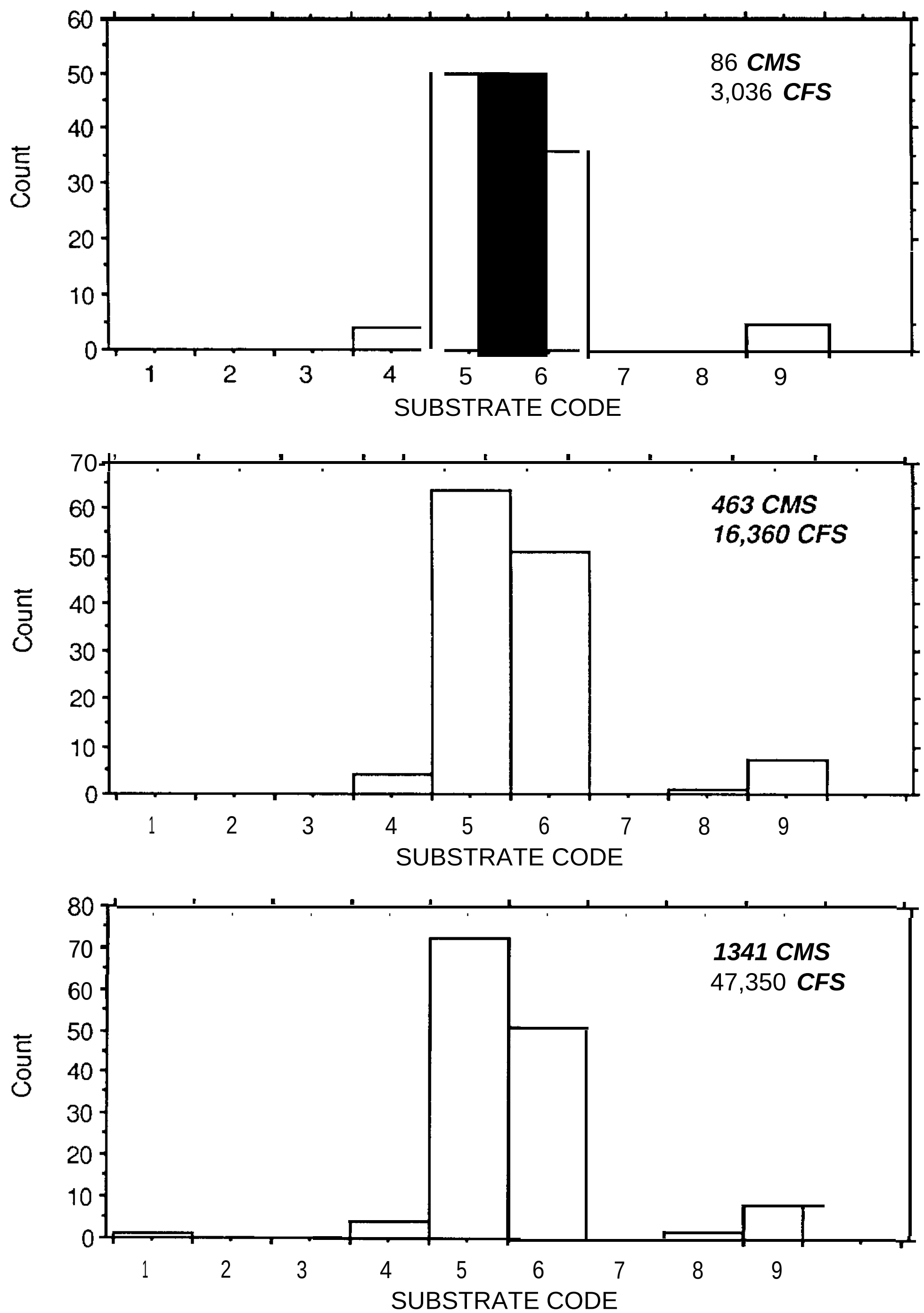

Figure 11. Substrate distribution of Bedrock spawning habitat at low, medium, and high flows.

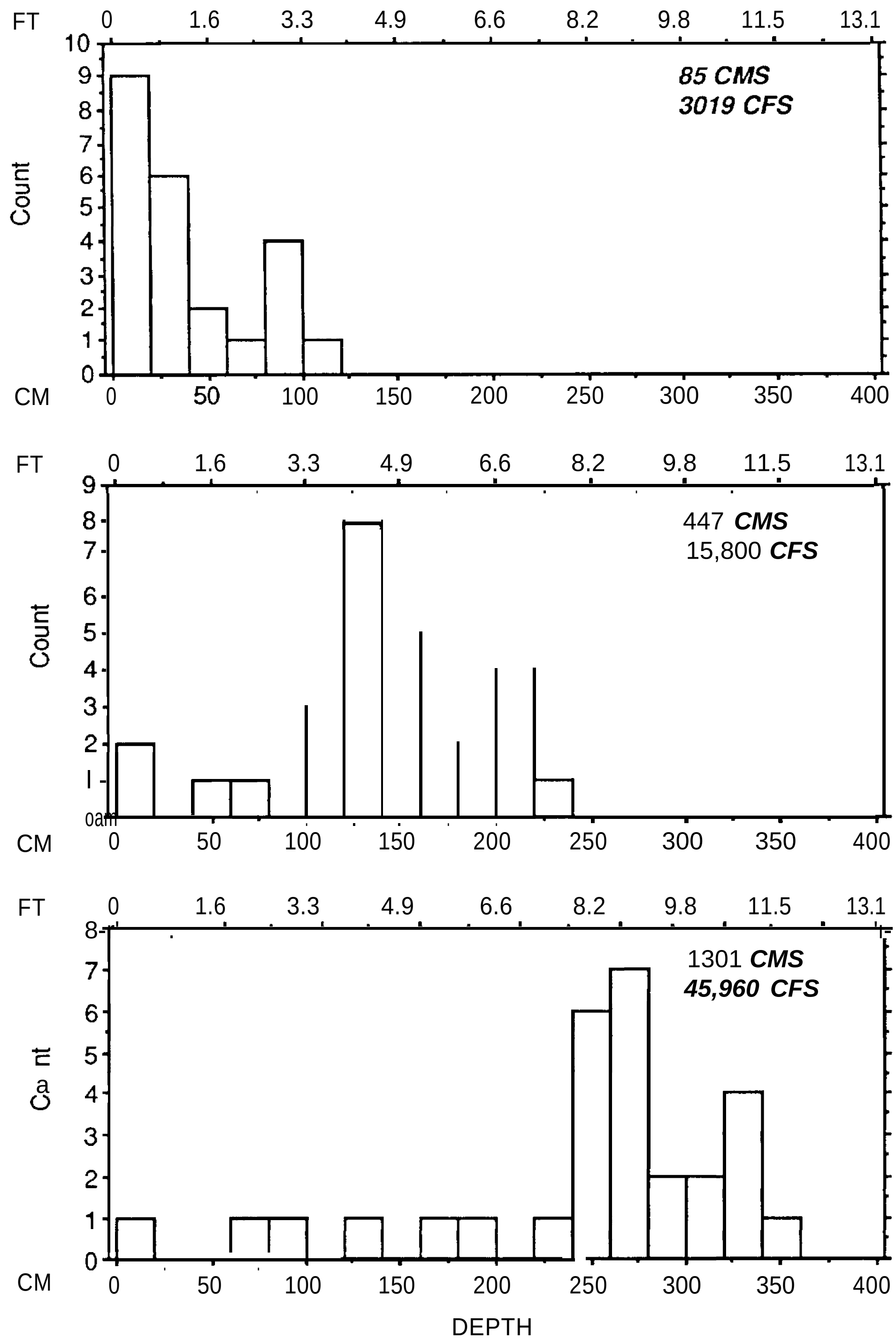

Figure 12. Depth distribution of Big Canyon rapid riffle habitat at low, medium, and high flows.

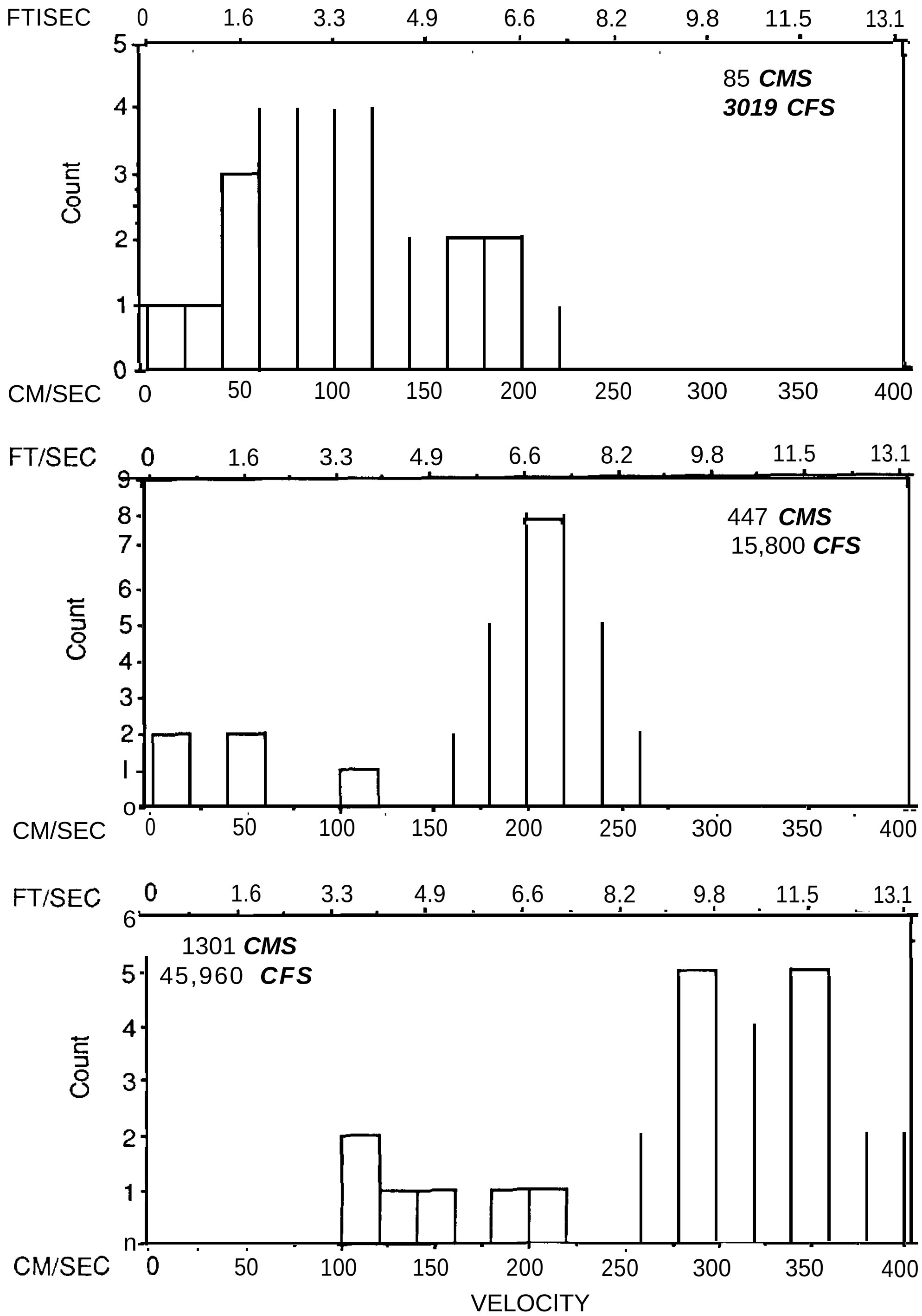

Figure 13. Velocity distribution of Big Canyon rapid riffle habitat at low, medium, and high flows.

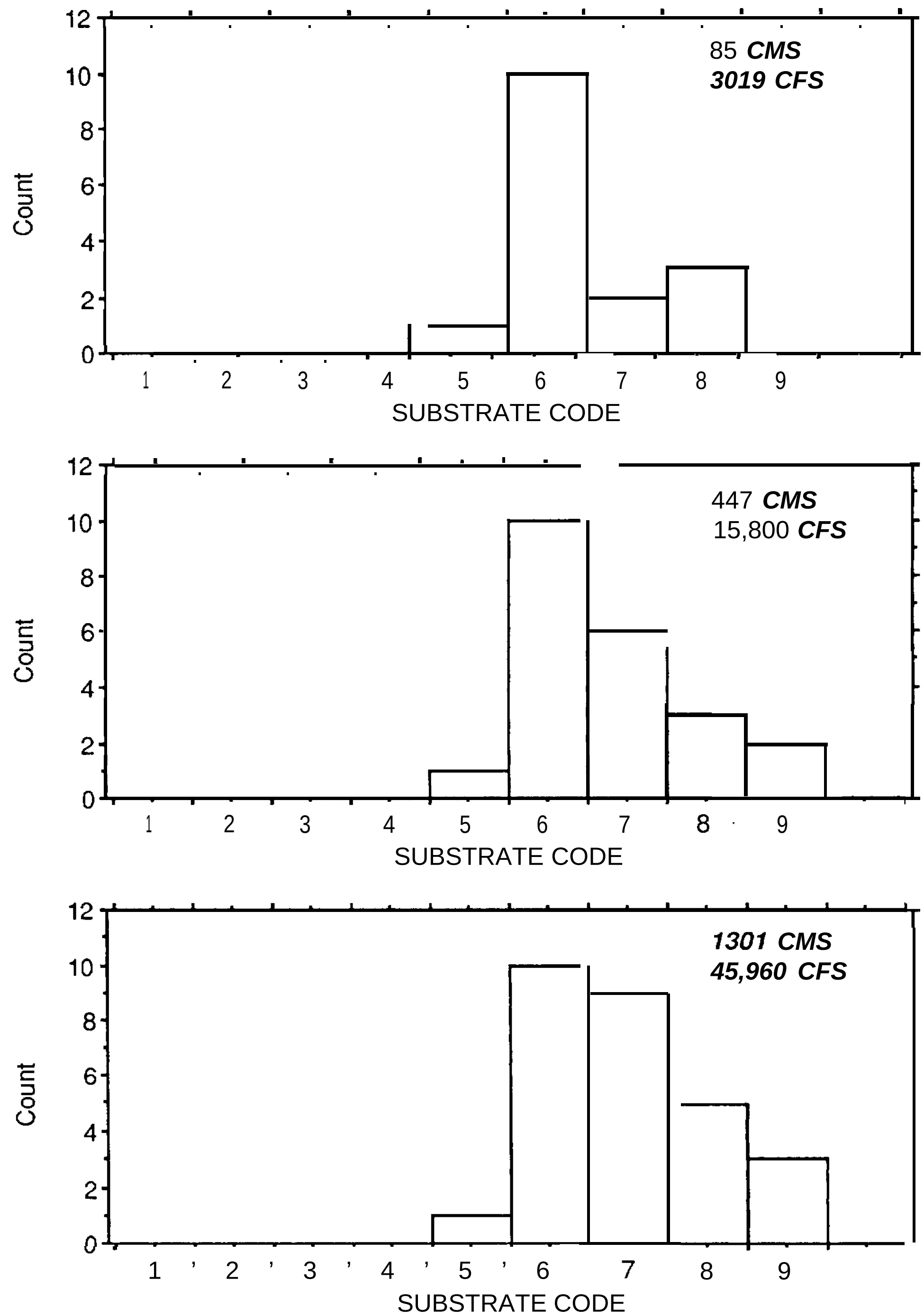

Figure 14. Substrate distribution of Big Canyon rapid riffle habitat at low, medium, and high flows.

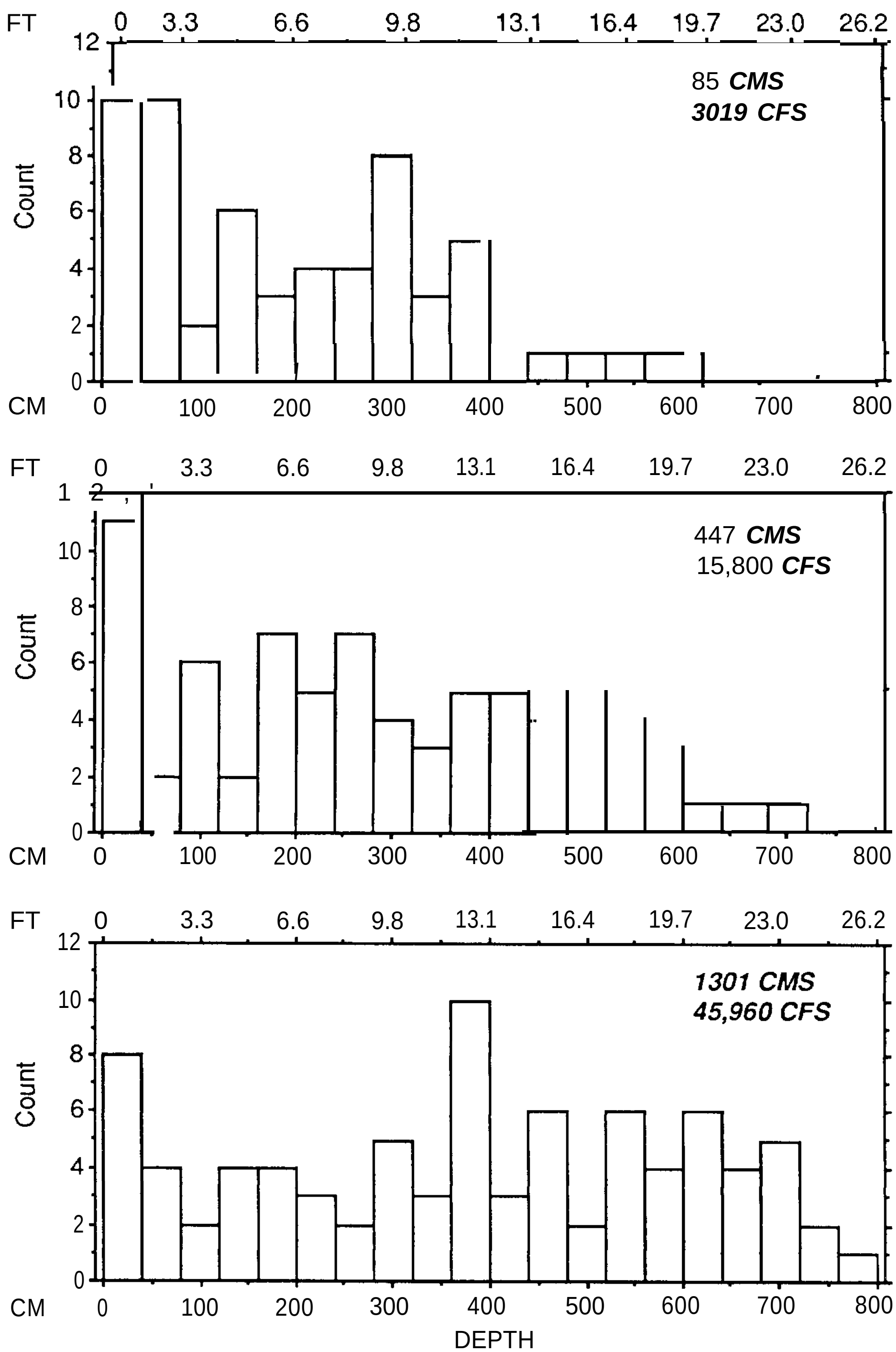

Figure 15. Depth distribution of Big Canyon pool habitat at low, medium, and high flows.

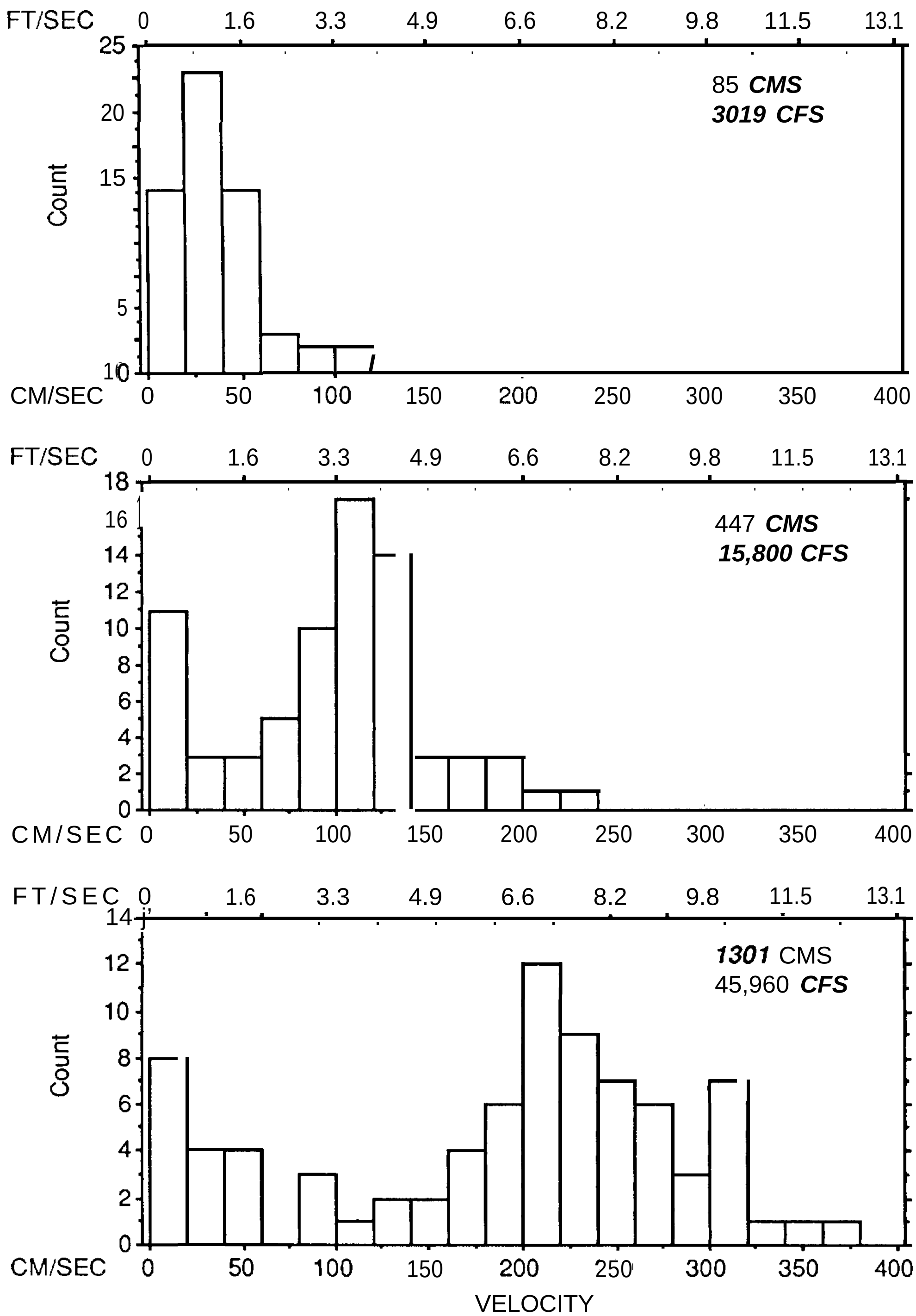

Figure 16. Velocity distribution of Big Canyon pool habitat at low, medium, and high flows.

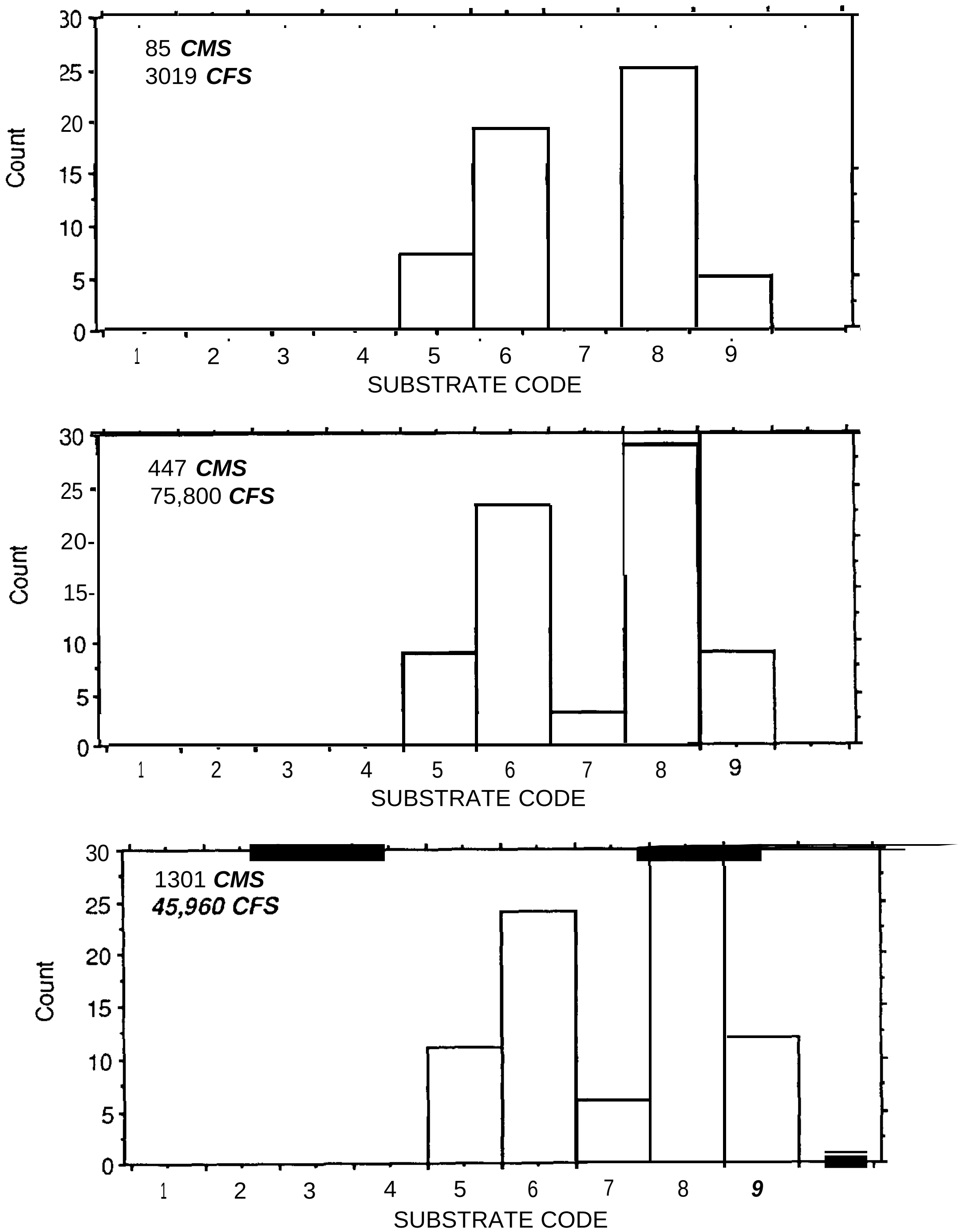

Figure 17. Substrate distribution of Big Canyon pool habitat at low, medium, and high flows.

OBJECTIVE 2: Document the use of the LMCR by anadromous and non-anadromous fish

Direct Observation Lane Assignment:

We assigned four lanes at each study site except for the North Fork study site where we placed two (Appendix C Tables Cl-2 and Figures Cl-8). Intentional and unintentional alterations were made during the final location and measurement of lane lengths at all but the North Fork study site (Appendix C). This affected the accuracy of the data presented in this report. However, it is essential to note that a thoroughly planned sampling strategy limited the resulting biases and the inaccuracies are easily correctable. With this in mind we limited the remaining discussion of our results to the most obvious patterns and trends evident in the following tables and figures.

Collection of Fish Density Data:

We did not depict the chinook salmon parr densities due to the low numbers of these fish we observed. Our first chinook sighting occurred during our tributary survey in June, (Appendix C) when we electrofished five 60 mm (2.4 in) parr at the mouth of Bedrock Creek. Based on the size of these fish we speculated that they were most likely young of the year fall chinook salmon. We recorded the next chinook observation at the Potlatch River study site in October. One 127 mm (5 in) parr was observed in a school of about 7 juvenile whitefish (Prosopium sp.).

Wild rainbow/steelhead parr and residualized hatchery smolt densities were highest in the summer then declined through the fall until winter when none were observed (Table 4 and Figure 18). Hatchery residuals were more abundant than wild parr during all seasons sampled. Both wild parr and hatchery residuals were more abundant in our upriver than down river study sites.

Age 0 redside shiners (Richardsonius balteatus) were abundant at both sites during the summer (Table 4 and Figure 19). By the fall and winter these fish were never observed. Conversely, few age I+ redside shiners were observed in the summer and fall and no observations were recorded in winter (Table 4, Figure 19). More age 0 fish were observed upriver than downriver. Age I+ fish were more abundant downriver than upriver. Overall, age 0 redside shiners were more abundant than age I+ redside shiners.

Mountain whitefish (P. williamsoni) were most abundant in the fall (Table 4 and Figure 20). And whitefish densities were higher in summer than winter. Largescale sucker (Catostomus macrocheilus) upriver densities were highest in the summer and downriver densities were highest in the fall (Table 4 and Figure 20). Overall, whitefish and sucker densities were quite similar.

Other fishes were observed in low numbers including northern squawfish (Pvtochelius oregonensis), smallmouth bass (Micropterus dolomieui), wild adult resident rainbow trout, and ventral fin clipped hatchery rainbow trout released in by the Idaho Department of Fish and Game during the fall of 1989. We expect to collect more data on these species during the 1990 field season.

Table 4. Calculated densities expressed as number per hectare (#/HA) for age 0 wild rainbow/steelhead parr (RBT0), age I+ wild rainbow/steelhead parr (RBT1), hatchery residualized steelhead trout (HRBT), age 0 redside shiners (RS0), age I+ redside shiners (RS1), large scale sucker (S), mountain whitefish (WF) collected in the Potlatch, Bedrock Creek, Big Canyon Creek, and North Fork study sites of the lower mainstem Clearwater (LMCR) project area, 1989.

	Potlatch and Bedrock Creek study sites			North Fork and Big Canyon Creek study sites		
Species	Summer #/HA(SE)	Fall #/HA(SE)	Winter #/HA(SE)	Summer #/HA(SE)	Fall #/HA(SE)	Winter #/HA(SE)
RBT0	0.5(0.0)	0.0(0.0)	0.0(0.0)	2.8(0.2)	0.0(0.0)	0.0(0.0)
RBT1	0.9(0.2)	0.0(0.0)	0.0(0.0)	1.9(0.2)	0.2(0.0)	0.0(0.0)
HRBT	2.1(0.2)	0.2(0.0)	0.0(0.0)	7.6(0.5)	5.6(0.7)	0.0(0.0)
RS0	897.0(163)	0.0(0.0)	1.6(0.2)	2006(202)	0.0(0.0)	0.0(0.0)
RS1	54.9(6.5)	9.5(0.0)	0.0(0.0)	9.3(0.9)	0.0(0.0)	0.0(0.0)
S	43.8(3.0)	73.7(5.3)	10.9(0.9)	159.9(11.6)	19.9(2.8)	2.5(0.5)
WF	26.9(3.2)	72.5(6.0)	7.0(0.7)	51.7(3.7)	65.8(8.1)	8.8(0.7)

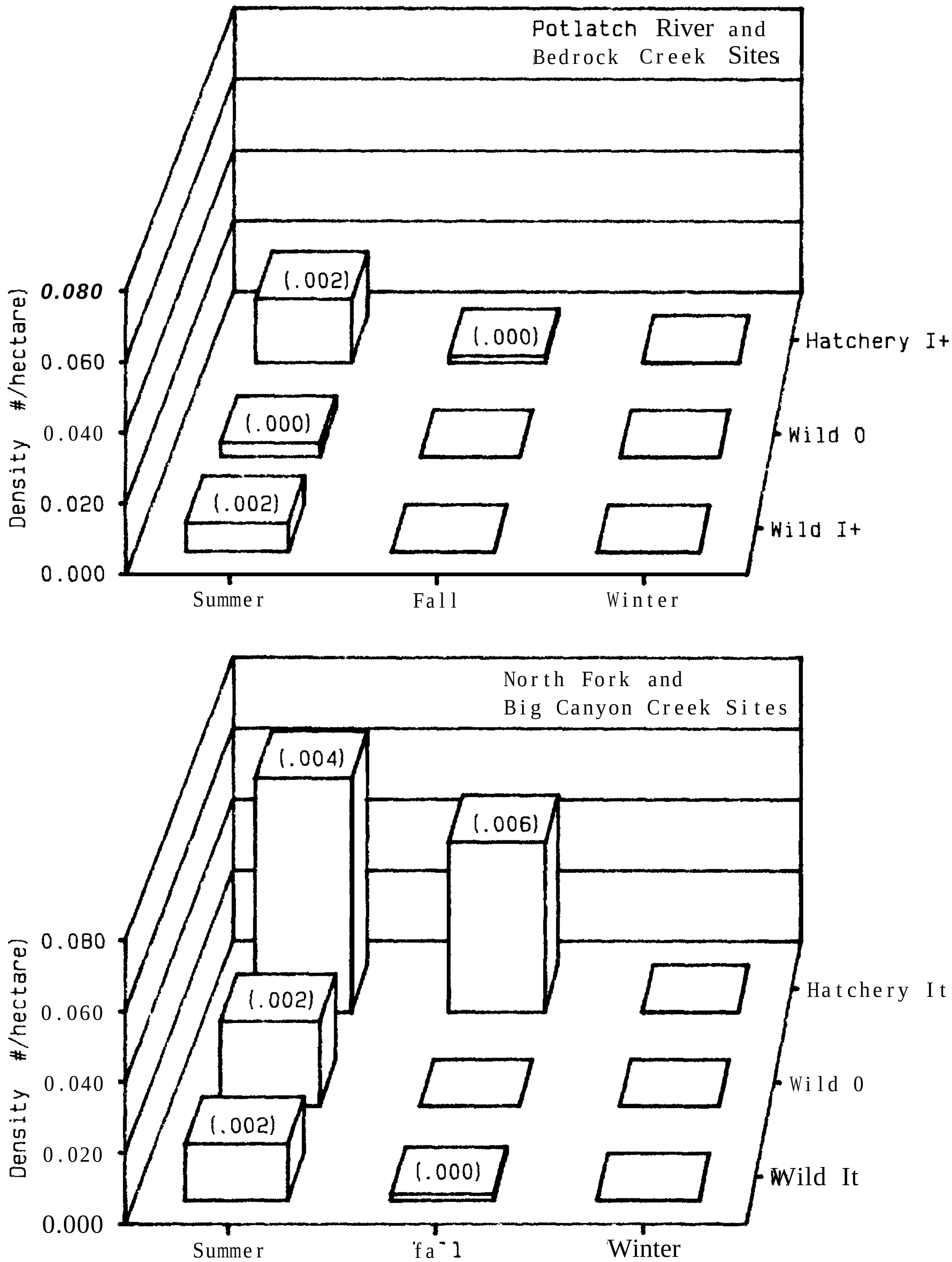

Figure 18. Hatchery and wild rainbow/steelhead trout densities (standard error] for the Potlatch/Bedrock and Big Canyon/North Fork Sites, LMCR project area, 1989.

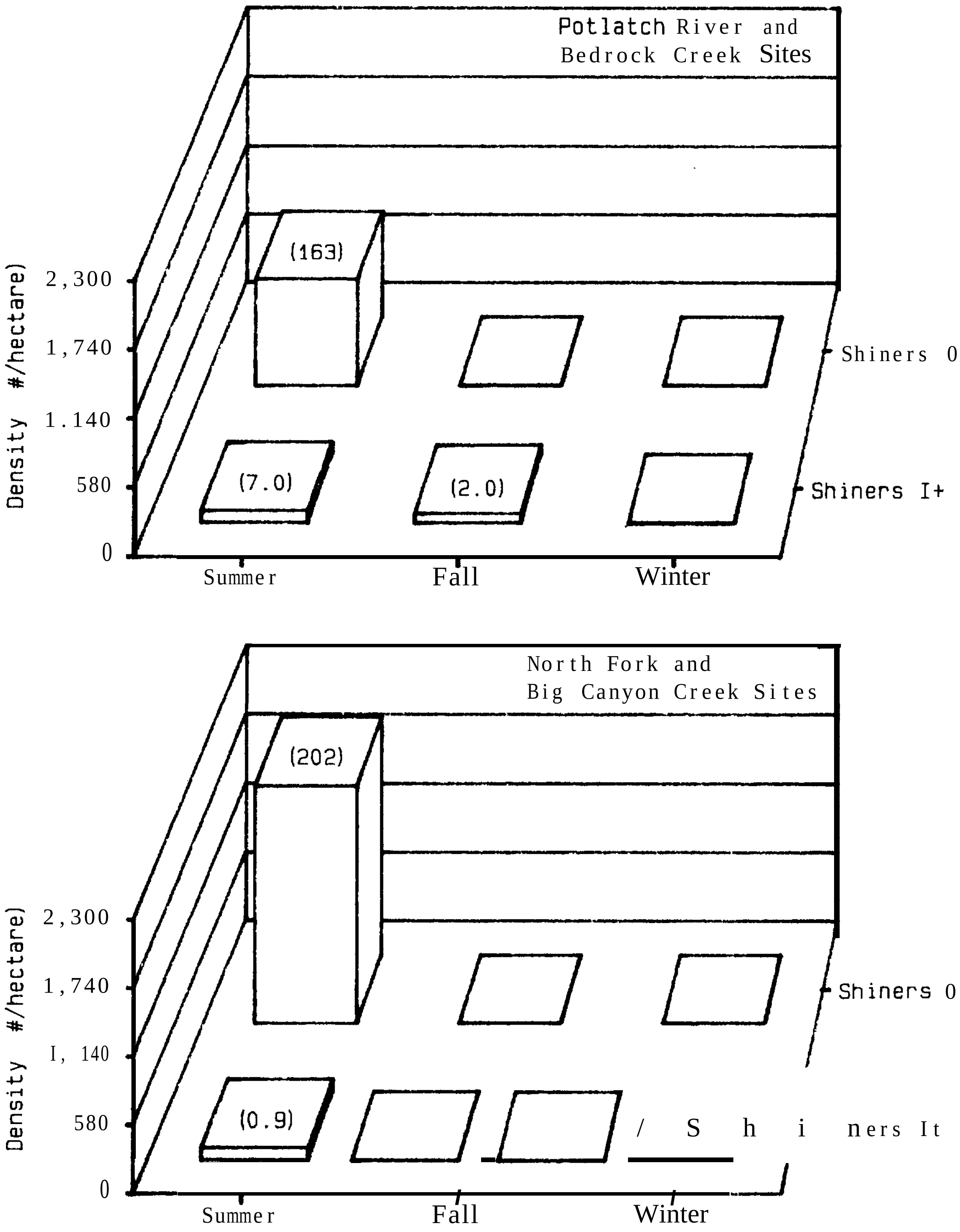

Figure 19. Juvenile and adult redside shiner densities (standard error) for the Potlatch/Bedrock and Big Canyon/North Fork Sites, LMCR project area, 1989.

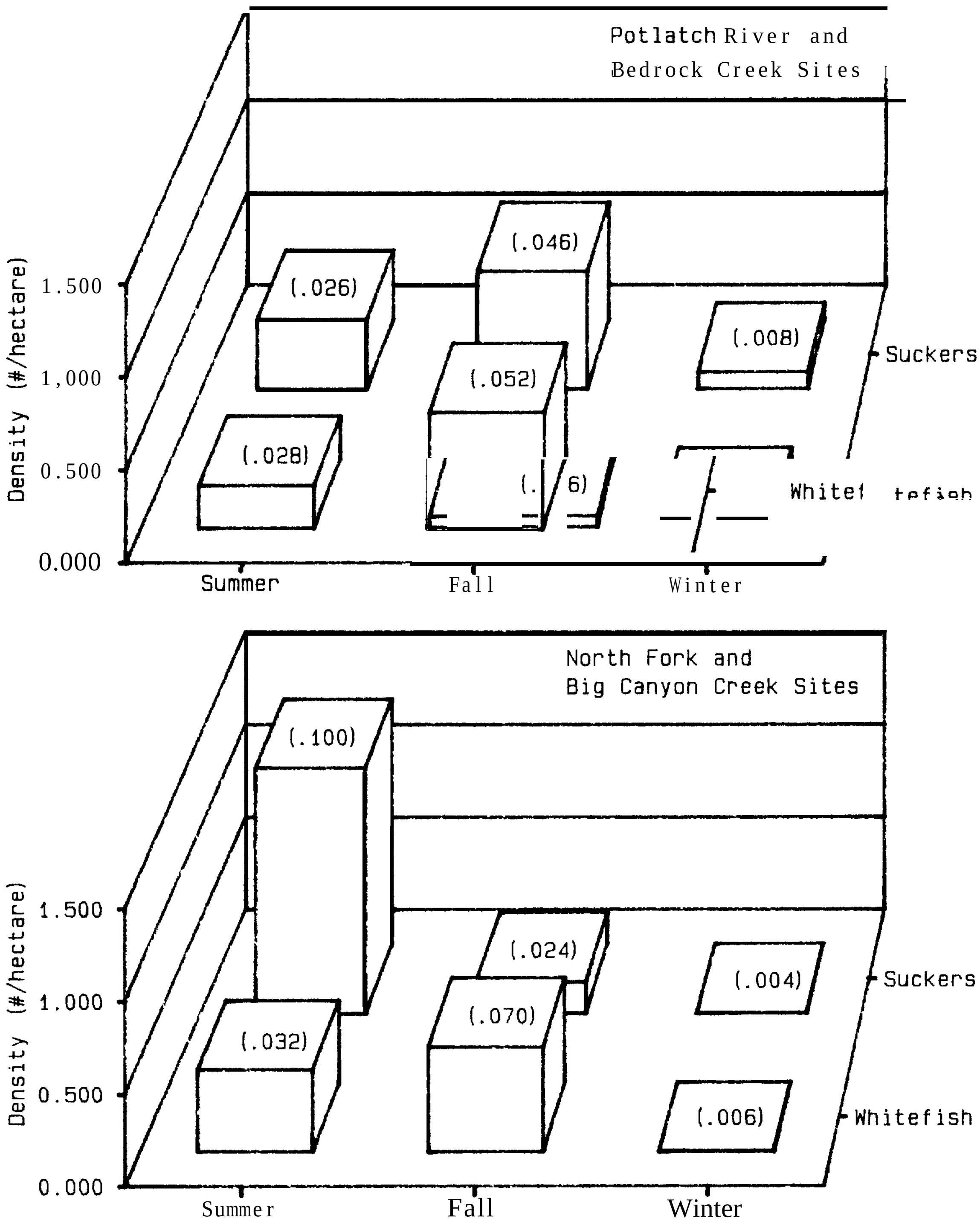

Figure 20. Largescale sucker and mountain whitefish densities (standard error) for the Potlatch/Bedrock and Big Canyon/North Fork Sites, LMCR project area, 1989.

Collection of Fish Microhabitat Preference Data:

Residualized hatchery steelhead smolts selected for specific nose velocities adjacent to higher velocities (Figure 21). Often residuals were within 30 cm (1.0 ft) of the bottom in 120 cm (3.9 ft) of water. Residuals rarely concealed themselves behind velocity cover, but were often found over small boulder substrate.

Because of the low seeding level of the LMCR we collected little microhabitat data for age 0 and I+ wild rainbow\steelhead parr. Subsequently, we did not graph age I+ data. Likewise, histograms for age 0+ parr (Figure 22) are not precise depictions of microhabitat selection since we observed only a small number of these fish. Preliminarily, parr, like smolts selected nose velocities adjacent to higher velocities. Most parr observed were from 10 to 15 cm (0.5 to 0.6 ft) off the bottom. However, no clear relationship is evident with total depth. More parr preferred cover than did not and this cover usually consisted of small cobbles.

Age 0 redside shiners selected positions with low velocity adjacent to slow water (Figure 23). In most cases these shiners were near shore in shallow water within the interstices of small cobble substrate. Histograms were not constructed for age I+ redside shiners due to the small sample size of these fish we obtained.

Largescale suckers selected for moderate water velocities less than 45 cm/sec, (1.5 ft/sec) below higher adjacent velocities (Figure 24). Although suckers were commonly seen in deeper water they always positioned themselves in close proximity to the bottom. Suckers rarely used cover and were found over substrate ranging in size from smaller cobble to large boulder.

Mountain whitefish selected for slightly higher nose velocities than suckers, but adjacent velocities were similar (Figure 25). Whitefish selected positions near the bottom in water between 60 and 90 cm deep (2.0 and 3.0 ft). Whitefish selected cover infrequently and appeared to prefer larger cobble and boulder substrate.

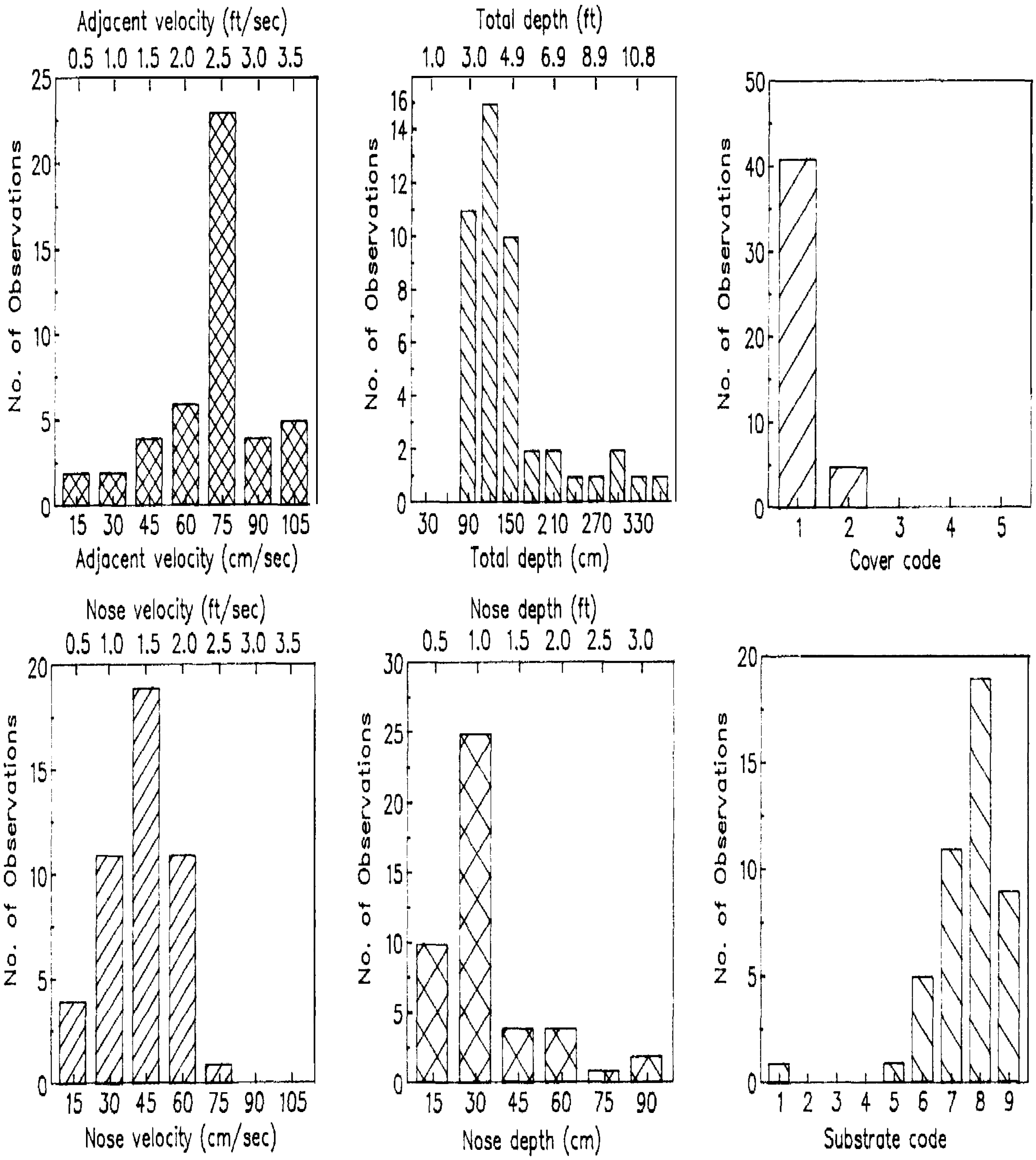

Figure 21. Hatchery residualized steelhead (mean size = 211 ± 48 mm) preliminary microhabitat preference histograms for velocity, depth, cover and substrate constructed by combining data from the Potlatch River, Bedrock Creek, Big Canyon Creek, and North Fork sites, LMCR project area, 1989.

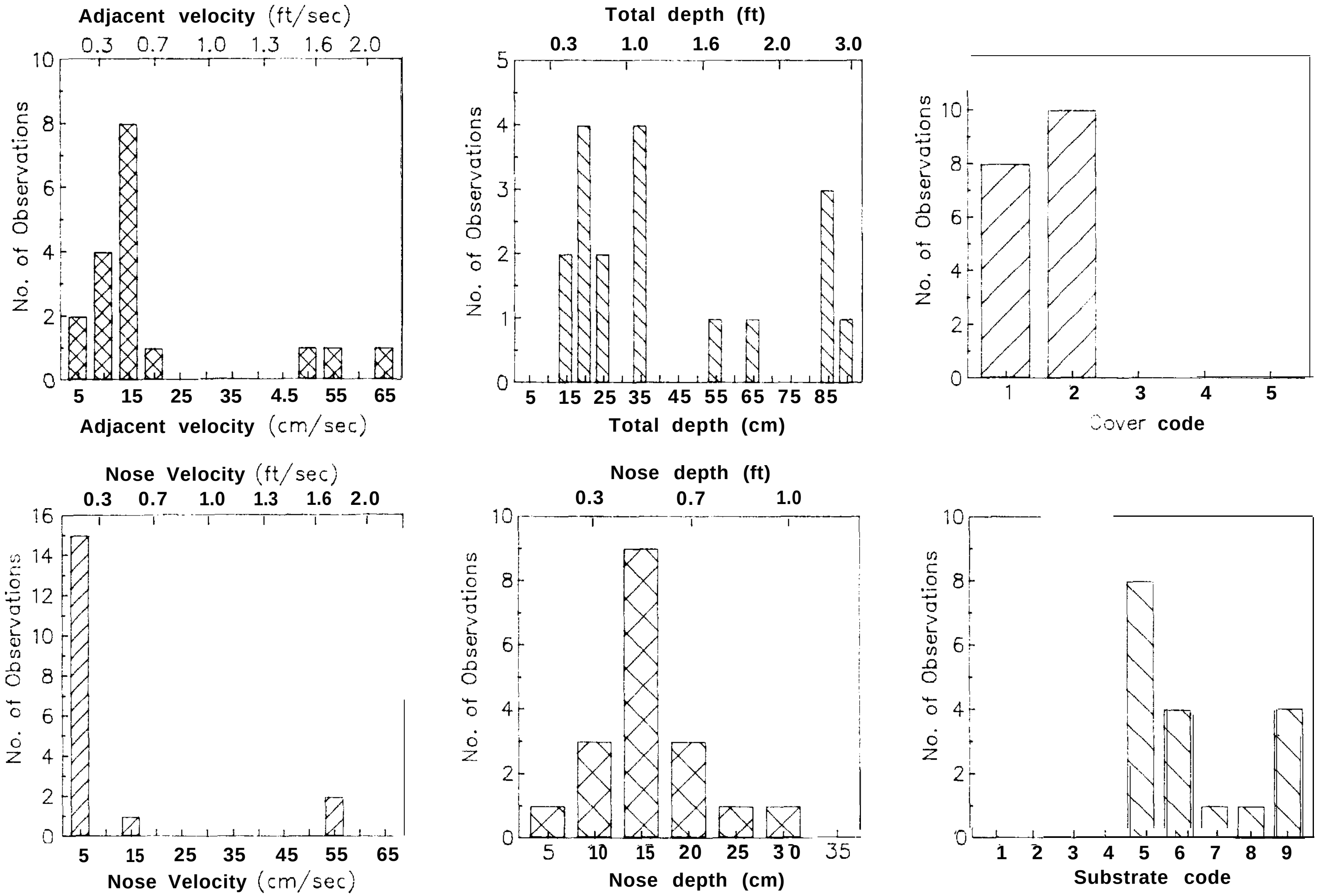

Figure 22. Wild age 0 rainbow/steelhead (mean size = 67 ± 33 mm) preliminary microhabitat preference histograms for velocity, depth, cover and substrate constructed by combining data from the Potiatch River, Bedrock Creek, Big Canyon Creek, and North Fork Sites, LMCR study area, 1989.

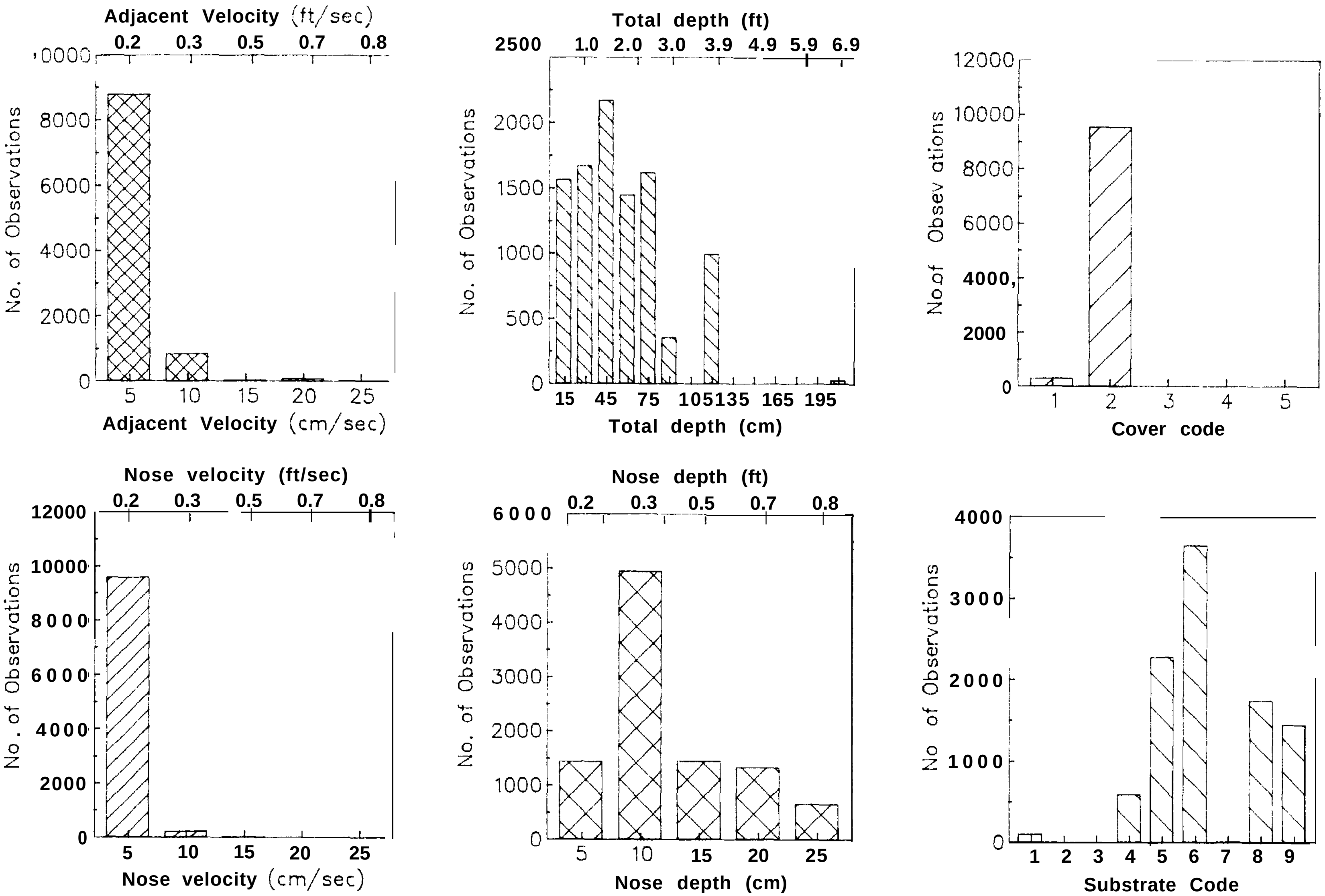

Figure 23. Age 0 shiner (mean size = 17 ± 6 mm) preliminary microhabitat preference histograms for velocity, depth cover and substrate constructed by combining data from the Potlatch River, Bedrock Creek, Big Canyon Creek, and North Fork Sites, LMCR study area, 1989.

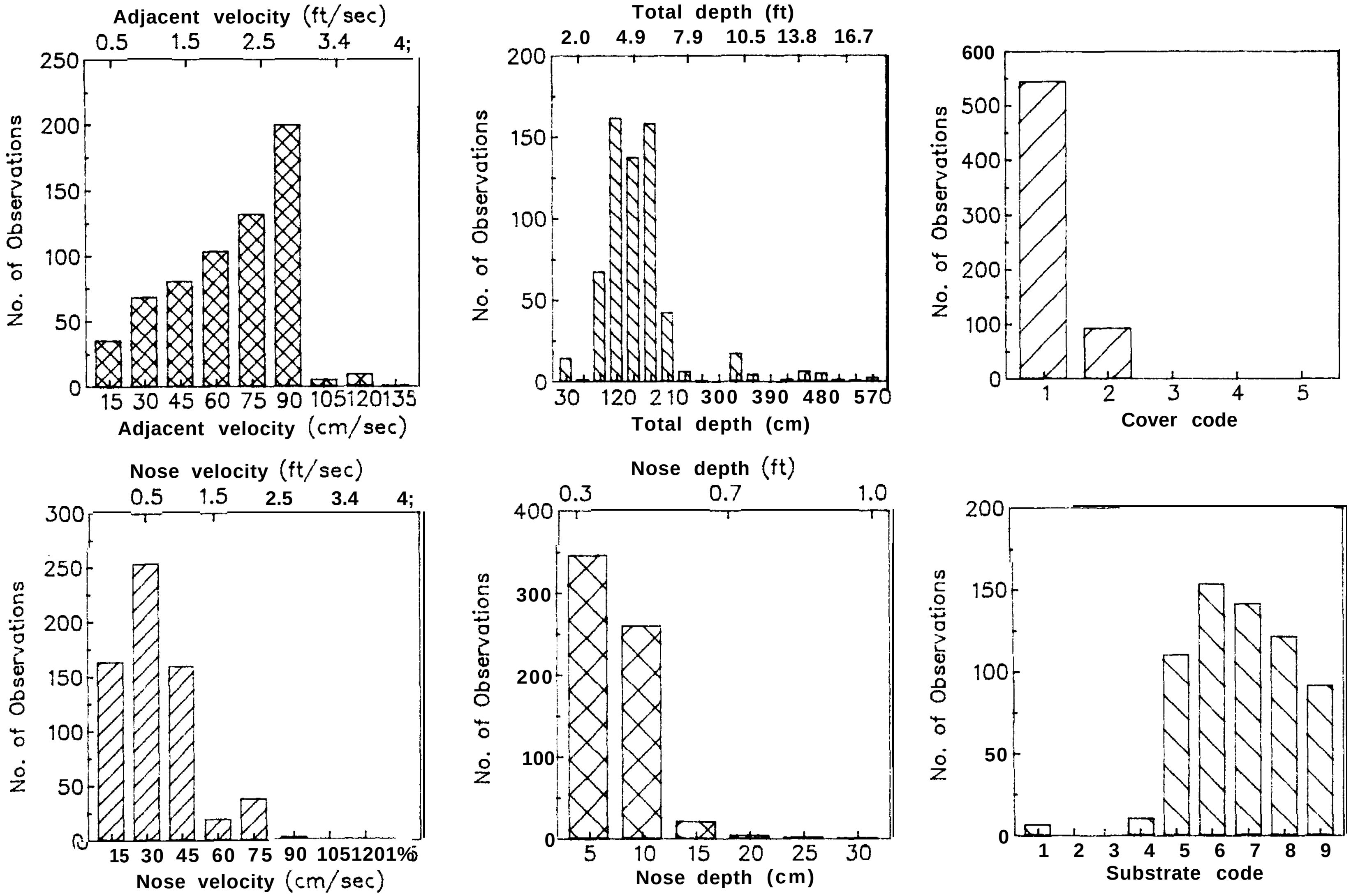

Figure 24. Adult largescale sucker (mean size = 423 ± 29 mm) preliminary microhabitat preference histograms for velocity, depth, cover and substrate constructed by combining data from the Potlatch River, Bedrock Creek, Big Canyon Creek, and North Fork Sites, LMCR study area, 1989.

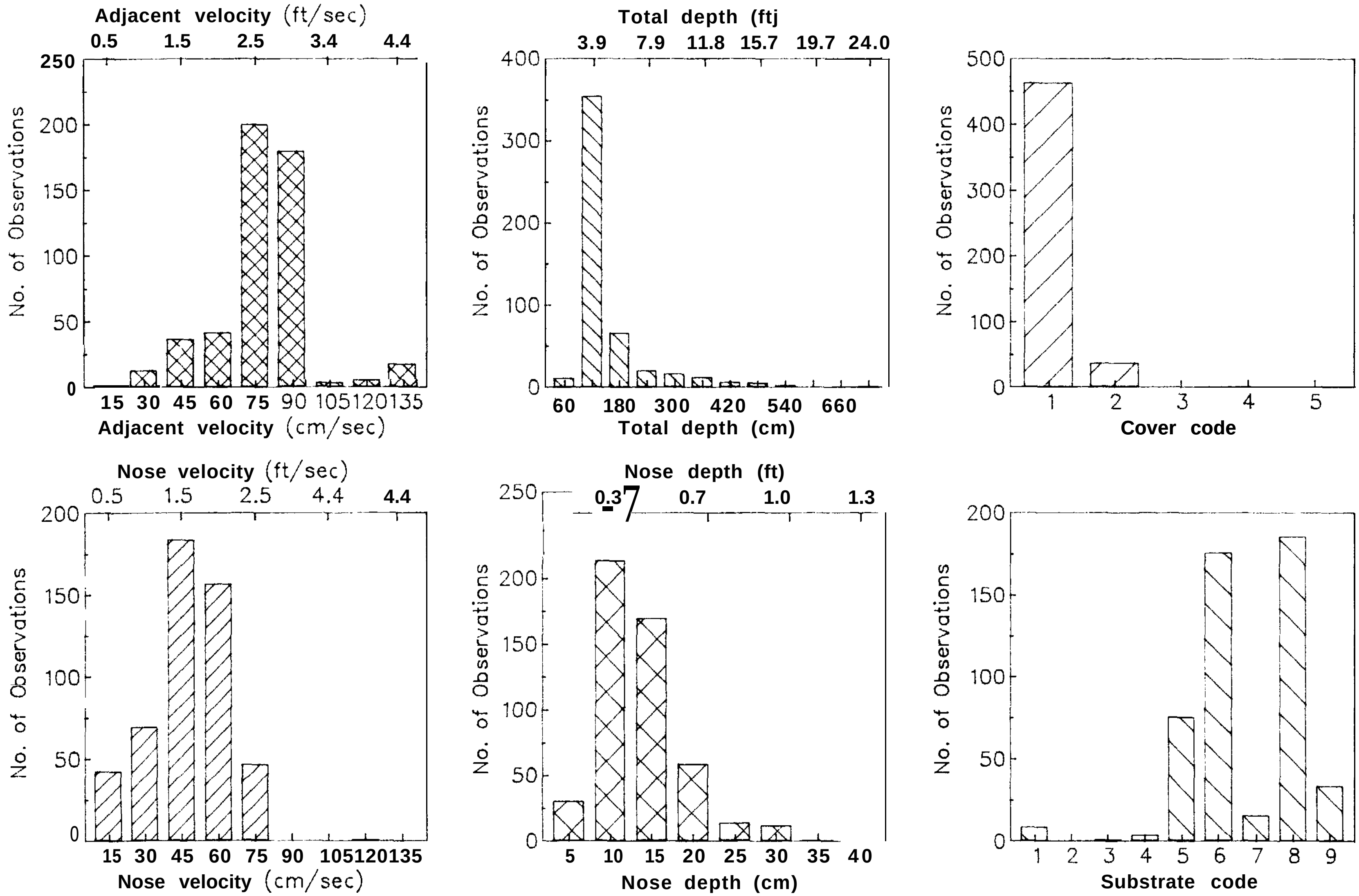

Figure 25. Adult mountain whitefish (mean size = 211 ± 48 mm) preliminary microhabitat preference histograms for velocity, depth, cover and substrate constructed by combining data from the Potlatch River, Bedrock Creek, Big Canyon Creek, and North Fork Sites, LMCR study area, 1989.

SUMMARY

We designed and implemented a habitat quantification study to define the relationship between anadromous fish spawning and rearing habitat in the LMCR and instreamflow. Initially, we stratified the LMCR into three segments for study. Natural fall chinook were observed spawning in the two lowermost segments. Therefore, we established study sites at these spawning areas. In the segment lacking spawning we studied typical habitat.

We measured the hydraulics of these strata and simulated hydraulic conditions over a range of instream flows using the IFG4 hydraulic simulation computer model. Water temperatures were also collected for future evaluation of existing fish habitat in the LMCR using a water temperature simulation model.

From the hydraulic simulations we produced preliminary frequency histograms for velocity, depth and substrate at spawning and rearing areas in the LMCR. Tentatively, it appears that both spawning and rearing requisites of anadromous salmonids are best met low to moderate discharges. Higher discharges may result in depths and velocities which are unsuitable for chinook salmon spawning and salmonid parr rearing.

We did not detect any substantial chinook parr rearing in the LMCR.

Preliminarily, the LMCR parr rearing habitat appears to be underseeded. Residualized Dworshak steelhead smolts were more abundant than wild rainbow/steelhead parr during summer, fall, and winter, but both smolts and parr were observed in low numbers relative to the area sampled. Densities of both fish were highest in summer then declined progressively until winter when few were detected.

The underseedness of the LMCR prevented the acquisition of enough wild rainbow/steelhead parr and residualized Dworshak National Fish Hatchery smolt observations to allow an accurate representation of the microhabitat preferences of these fish. This situation will be remedied in 1990 by altering our sampling strategy.

REFERENCES CITED

Asherin, D.S. and M.L. Orme. 1978. Inventory of riparian habitats and associated wildlife along the Dworshak Reservoir and lower Clearwater River. A report to the U.S. Army Corps of Engineers North Pacific Division by the University of Idaho Cooperative Wildlife Research Unit.

Bovee, K.D. 1988. Use of the instream flow incremental methodology to evaluate influences of microhabitat variability on trout populations in four Colorado streams. Proceedings of Western Division, American Fisheries Society. Albuquerque, New Mexico. July, 1988.

Bovee, K.D. 1986. Development and evaluation of habitat suitability criteria for use in the instream flow incremental methodology. Instream flow information paper 21. U.S. Fish and wildlife Service Biological Report 86(7).

Bovee, K.D. 1982. A guide to stream habitat analysis using the Instream Flow Incremental Methodology. Instream Information Paper 12. U.S.D.I Fish and Wildlife Service, Office of Biological Services. FWS/OBS-82/26.

Bovee, K.D. 1981. A users guide to the instream flow incremental methodology. U.S. Fish and Wildlife Services Biological Services Program. FWS/OBS-80/52.

Bovee, K.D., and R.T. Milhous. 1978. Hydraulic simulation in instream flow studies: theory and techniques. Instream Flow Information Paper No. 5. U.S. Fish and Wildlife Services Biological Services Program. FWS/OBS-78/33.

Buggert, R., P. Seidel, P. LaRiviere, D. Marbach, S. Martin, and L. Ross. 1989. Lower Snake River Compensation Plan Lyons Ferry Evaluation Program. 1988 Annual Report to the U.S. Fish and Wildlife Service Lower Snake River Compensation Plan Office, Boise, Idaho.

Connor, W.P. 1989. Mainstem Clearwater Study: Assessment for salmonid spawning, incubation, and rearing. An annual report to the U.S. Department of Energy, Bonneville Power Administration by the Nez Perce Tribe Department of Fisheries. Contract No. DE-AI79-BP37474, Project No. 88-15.

Fish Passage Center. 1989. Bi-weekly report #89-19. FPC 825 N.E. 20th Avenue, Suite 336, Portland, Oregon 97232-295.

Fulton, L.A. 1968. Spawning areas and abundance of chinook salmon in the Columbia River Basin: past and present. Special Scientific Report of the U.S. Fish and Wildlife Service No. 571.

Gore, J.A., and J.M. Nestler. 1988. Instream flow studies in perspective. Regulated River 2(1988): 93-101.

Griffith, J.S., J.W. Mullan, and T.W. Hillman. 1988. Effects of temperature on the accuracy of underwater counts of juvenile chinook salmon and steelhead trout. M.S.

Haber, D.F., B. Moore, and W. Hicks. 1978. A review of the impacts of fluctuating flows on the lower Clearwater River and recommendations for future studies. Contract No. DACW68-76M-2586, Idaho Water Resources Research Institute, University of Idaho, Moscow, Idaho.

Hill, T.W., D.W. Chapman, and J.S. Griffith. 1988. Summer and winter ecology of juvenile chinook salmon and steelhead trout in the Wenatchee River, Washington. A report to Chelan County Public Utility District, Washington.

Howell, P., K. Jones, D. Scarnecchia, L. Lavoy, W. Kendra, D. Ortman. 1985. Stock assessment of Columbia River anadromous salmonids. Volume I: Chinook, Coho, Chum and Sockeye Salmon Stock Summaries. Final Report to the U.S. Department of Energy Bonneville Power Administration. Contract No. DE-AI79-84BP12737.

Horner, N. and T.C. Bjornn. 1981. Status of upper Columbia and Snake River summer chinook salmon in relation to the Endangered Species Act. Idaho Cooperative Fishery Research Unit, University of Idaho, Moscow, Idaho.

Irving, J.S. and T.C. Bjornn. 1980. Status of Snake River fall chinook salmon in relation to the Endangered Species Act. Idaho Cooperative Fishery Research Unit, University of Idaho, Moscow, Idaho.

Kronemann, L.A. and K. Lawrence. 1987. Wildlife protection, mitigation, and enhancement planning - Dworshak Reservoir. A report to the U.S. Department of Energy Bonneville Power Administration by the Nez Perce Tribe Department of Wildlife Resources. Contract No. DE-AI79-87BP35333.

Kucera, P.A. and D.B. Johnson. 1986. A biological and physical inventory of the streams within the Nez Perce Reservation. Juvenile steelhead survey and factors that affect abundance in selected streams in the lower Clearwater River Basin, Idaho. Final Report to the U.S. Department of Energy, Bonneville Power administration, Division of Fish and Wildlife. Contract No. DE-AI79-83BP10068, Project No. 82-l.

Li, S. 1988. Proceedings of a workshop on the development and evaluation of habitat suitability criteria. Bovee, D., and J.R. Zuboy eds. U.S. Fish and Wildlife Service. Biological Report 88(11). 407 p.

Milhous, R.T. 1984. The use of one velocity calibration set with IFG4. PHABSIM Technical note No. 4. U.S. Fish and Wildlife Service, National Ecology Research Center. Fort Collins, Colorado.

Milhous, R.T. 1985. The use of the stage-discharge relationship and one data set with the IFG4 simulations program. PHABSIM Technical note No. 18: U.S. Fish and Wildlife Service, National Ecology Research Center. Fort Collins, Colorado.

Milhous, R.T., M.A. Updike, and D.M. Schneider. 1989. Computer reference manual for the Physical Habitat Simulation System (PHABSIM) - Version II. U.S. Fish and Wildlife Service, National Ecology Research Center. Fort Collins, Colorado.

Milhous, R.T., T. Wegner, and T. Waddle. 1984. User's guide to the Physical Habitat Simulations System (PHABSIM). Instream Flow Information Paper No. 11. U.S. Fish and Wildlife Services Biological Services Program. Revision FWS/OBS-81/43.

Morhardt, J.E. 1986. Instream flow methodologies. Electric Power Research Institute, EPRI EA-4819.

Orth, D.J., and O.E. Maughan. 1982. Evaluation of the incremental methodology for recommending instream flows for fishes. Transactions of the American Fisheries Society 111(4): 413-445.

Murphy, P.K. 1989. Chinook salmon spawning ground surveys Selway River drainage, mainstem Clearwater drainage, Clearwater River Subbasin, Idaho 1988. Technical Report 89-l. Department of Fisheries Management, Nez Perce Tribe, Lapwai, Idaho.

Murphy, P.K. 1986. Water quality status report for lower Clearwater River Tributaries, Nez Perce Reservation, Idaho Water Year 1986. Submitted to The Bureau of Indian Affairs, Department of Fisheries Resource Management, Nez Perce Tribe, Lapwai, Idaho.

Murphy, P.K., Johnson, D.B. 1986. A review of the 1986 fish kill in Lapwai Creek, Lower Clearwater River Subbasin, Nez Perce Reservation, Idaho. Nez Perce Tribe Technical Report 86-7. Department of Fisheries Resource Management, Nez Perce Tribe.

North West Power Planning Council. 1987. Columbia River Basin Fish and Wildlife Program. NWPPC, 850 S.W. Broadway, Suit 1100, Portland, Oregon 97205.

Osborne, L.L, M.J. Wiley, and R.W. Larimore. 1988. Assessment of the water surface profile model: accuracy of predicted instream flow habitat conditions in low-gradient, warmwater streams. Regulated River 2(1988): 619-631.

Parkhurst, Z.E. 1950. Survey of the Columbia River and its tributaries. Special Scientific Report No. 39, Part 6. United States Department of the Interior Fish and Wildlife Service, Washington, D.C.

Schill, D.J. and J.S. Griffith. 1984. Use of underwater observations to estimate cutthroat trout abundance in Yellowstone River. North American Journal of Fisheries Management 4:479-487.

Seidel, P., B. Buggert, P. LaRiviere, D. Marbach, S. Martin, and L. Ross. 1989. Lower Snake River Compensation Plan Lyons Ferry Evaluation Program. 1988 Annual Report to the U.S. Fish and Wildlife Service Lower Snake River Compensation Plan Office, Boise, Idaho.

Theurer, F.D., K.A. Voos, and W.J. Miller. 1984. Instream water temperature model. Instream Flow Information Paper 16. U.S. Fish and Wildlife Service. FWS/OBS-84/15.

Trihey, E.W., and D.L. Wegner. 1981. Field data collection procedures for use with the Physical Habitat Simulations System of the Instream Flow Group. Cooperative Instream Flow Service Group, Fort Collins, Colorado. Partial Revision 1983.

U.S. Army Corps of Engineers. 1975. Final environmental impact statement - Dworshak Reservoir, North Fork Clearwater River, Idaho.. Walla Walla District.

U.S. Army Corps of Engineers. 1986. Water Control Manual for Dworshak Dam and Reservoir, North Fork Clearwater River, Idaho. Walla Walla District.

APPENDIX A
River Stratification

Segment Division by Flow Regime:

Discharge data for the major tributaries of the LMCR is scarce. USGS gaging stations are located on the mainstem at Orofino, Peck, Spalding, and in Lapwai Creek. USACE records Dworshak Dam Discharge on the North Fork. All other information was collected from technical reports. Discharge data indicate that the North Fork Clearwater River increases mainstem Clearwater discharge by 40.8 % (Table Al). Therefore we placed a segment boundary at this location.

There are no diversions in the lower mainstem Clearwater River that would equal 10% of annual discharge (40 CMS or 1,400 CFS).

Table Al. Annual measured discharges from the LMCR and major tributaries used to estimate flow accretions in the river.

Water source	Average annual discharge (cms)	(cfs)	Percent accretion
Mainstem at Orofino[a]	246	8,686	N/A
North Fork[b]	171	6,038	40.8%
Mainstem at Peck[a]	406	14,336	N/A
Big Canyon[c]	0.2	7	<1%
Jacks[c]	4.6	162	<1%
Bedrock[c]	2.1	74	<1%
Cottonwood[c]	3.8	134	<1%
Potlatch[a]	10.1	357	4.8%
Mainstem at Spalding[a]	418	14,760	N/A
Lapwai[a]	2.5	88	1%

a = USGS gaging station data
b = USACE
c = Kucera and Johnson 1986

Segment Division by Channel Morphology
Longitudinal Profile:

The slope of the LMCR from the North Fork confluence to Lewiston is only .14%. The only noticeable change in slope occurs at Big Eddy Below Lenore (Figure Al). Therefore, no segment boundaries were placed based on river gradient.

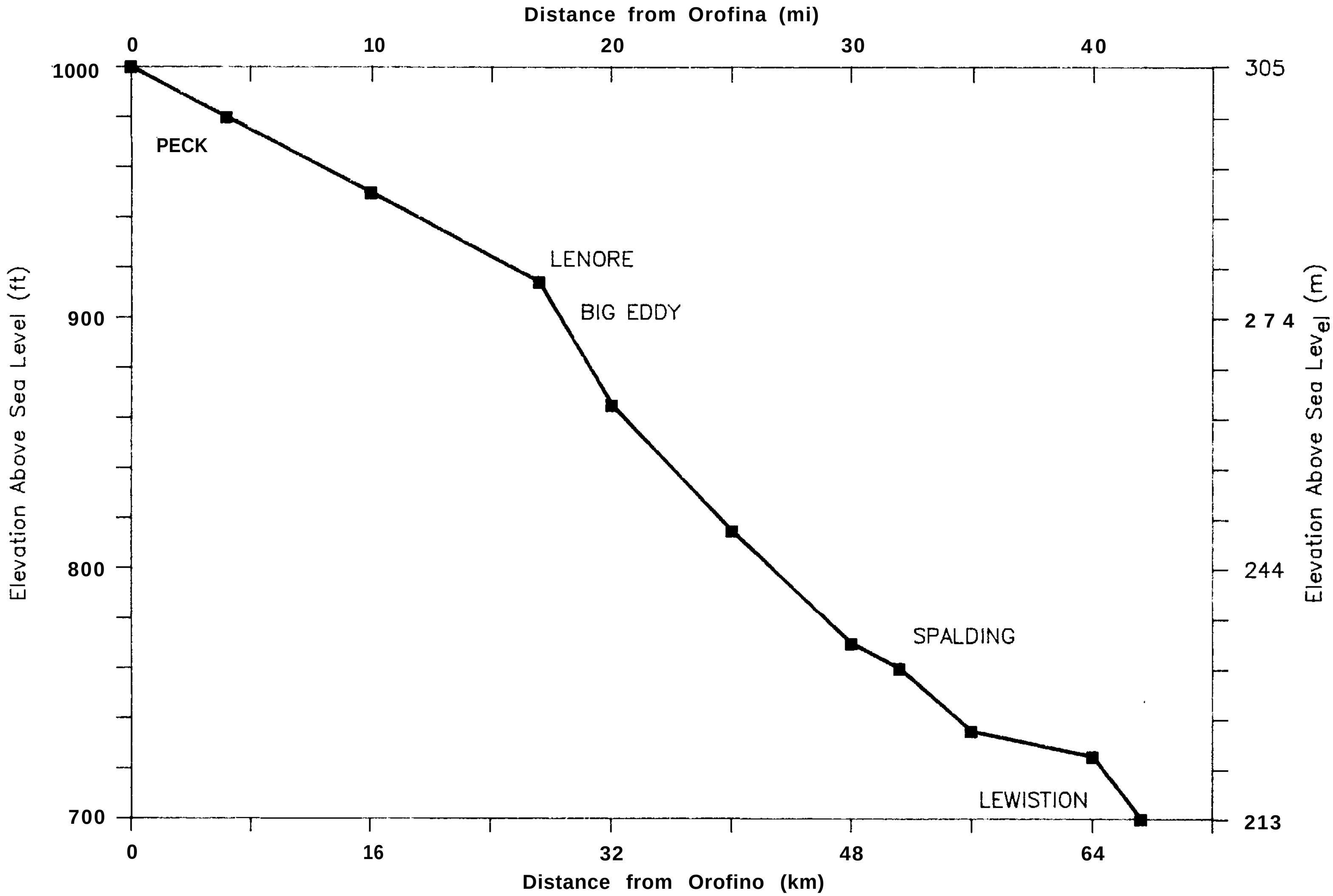

Figure Al. Longitudinal profile of the lower mainstem Clearwater River (LMCR) project area constructed using USGS topographic map elevations.

Channel Pattern:

The channel is relatively straight from the North Fork confluence to Big Canyon Creek and exemplifies the typical riffle/pool sequence (Table A2). Sinuosity increases between Big Canyon Creek and Bedrock Creek. The most obvious pattern change begins below Bedrock Creek where braiding, reflected in islanded reaches, becomes common. Although differences in sinuosity are not great, it is important to incorporate the single versus braided channel distinction into overall river segmentation.

Table A2. Stratification of the LMCR based on channel sinuosity.

Tributary name	Thalweg distance (km)	Thalweg distance (mi)	Down valley distance (km)	Down valley distance (mi)	Channel sinuosity
Potlatch	19.5	11.7	18.7	11.2	1.1
Bedrock	16.0	9.6	13.0	7.8	1.2
Big Canyon	13.8	8.3	11.4	6.8	1.2
North Fork	8.0	4.8	7.5	4.5	1.1

Sediment Supply:

Sediment problems in the LMCR have received much written attention (Haber et al. 1978, Lane, Lane, and Nash 1981, Murphy 1986, Murphy and Johnson 1986). All lower river tributaries contribute large sediment loads to the mainstem (Murphy 1986). The volume of water, however, contributed by most of these tributaries is small and it is not feasible to segment the river at each tributary mouth, as described above. At best a segment boundary could be placed at the Potlatch River confluence since this is the largest lower mainstem tributary and is capable of flash flooding. Special consideration may be warranted at Bedrock Creek since an ongoing watershed planning project is being conducted there by the Soil Conservation Service (SCS) and the confluence is located near an obvious change in channel pattern.

Bank Materials, Topography, and Vegetation:

A detailed discussion of bank materials of the LMCR is the subject of ongoing study by the Nez Perce Tribe and the SCS (Dave Eby pers. comm.) and is well beyond the scope of this report. Nonetheless, some differences in the longitudinal distribution of soils is evident in our study area (Table A3).

Table A3. Longitudinal distribution of soil classifications along the lower mainstem Clearwater River from Orofino to Lewiston, Idaho.

River section	Aspect	Soil class
North Fork confluence to Bedrock Creek	North	Jnl
	South	Rnl
Hatwai Creek to Lewiston	North	CD4
	South	Prl

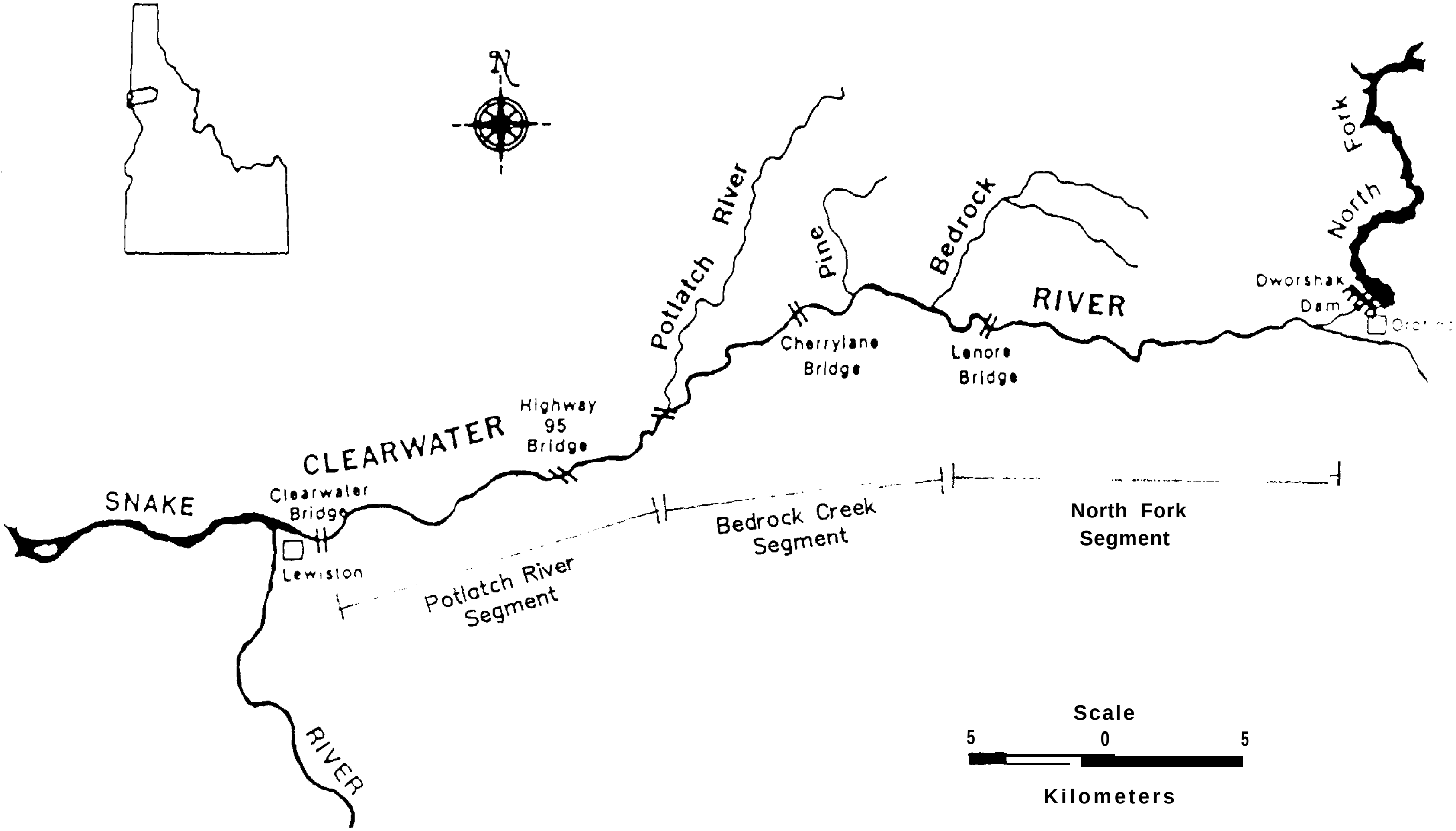

Figure A2. Lower mainstem Clearwater River (LMCR) project area divided into the Potlatch River, Bedrock Creek, and North Fork Segments based on geomorphologic and hydraulic characteristics.

Spawning Habitat:

Twenty-eight areas were located and mapped from the Potlatch Mill to North Fork/LMCR confluence with substrate of suitable size, embeddedness, and friability for fall and summer chinook salmon spawning (Table A4). Subsequently, 21 fall chinook redds and four fall chinook carcasses were counted during our helicopter flight. All redds counted were in the Potlatch River and Bedrock Creek Segments within potential spawning areas mapped prior to the redd survey (Figures A3 and A4). Nine redds were located within the Hog Isle complex. The Cherry Lane Island Complex contained eight redds.

Table A4. Spawning gravel information from the Potlatch Mill confluence to North Fork/lower mainstem Clearwater confluence.

Location	Code
G1	45.2
G2	45.0
G3	54.5
G4	54.2
G5	45.2
G6	54.0
G7	54.2
G8	45.0
G9	45.0
G10	42.0
G11	42.0
G12	56.5
G13	45.2
G14	45.0
G15	42.0
G16	54.2
G17	45.2
G18	54.0
G19	54.5
G20	45.2
G21	45.0
G22	54.2
G23	24.5
G24	56.2
G25	54.2
G26	45.0
G27	62.2
G28	42.0

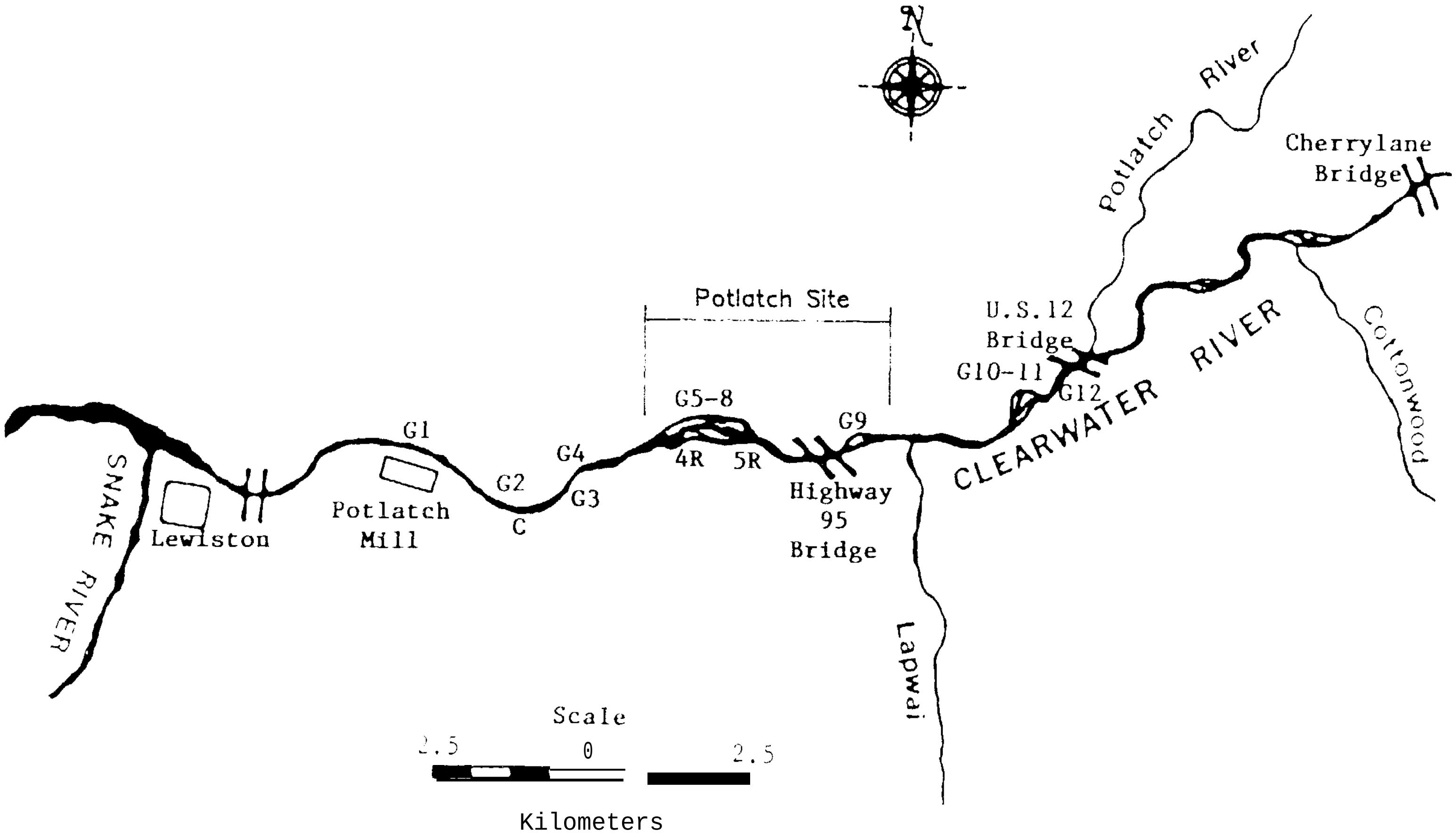

Figure A3. Spawning gravel (G#), redds (#R), fall chinook carcass (#C), and study site location within the Potlatch River Segment of the lower mainstem Clearwater River (LMCR) project area.

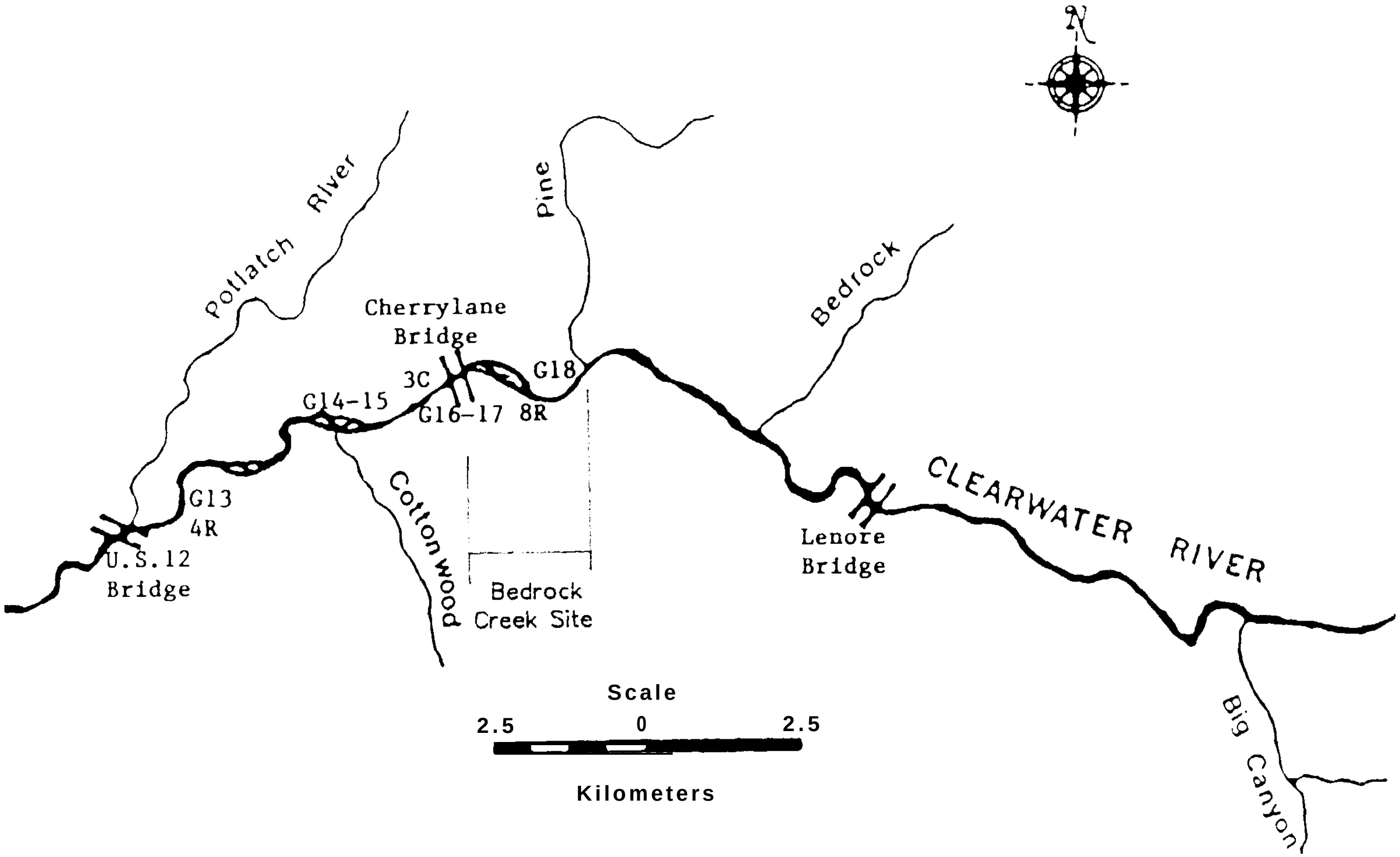

Figure A4. Spawning gravel (G#), redds (#R), fall chinook carcass (#C), and study site location within the Bedrock Creek Segment of the lower mainstem Clearwater River (LMCR) project area.

Table A5. Habitat type area by segment and site within the lower mainstem Clearwater River (LMCR) project area.

Habitat type	Potlatch River		Bedrock Creek		North Forka	
	Segment area (HA)	Site area (HA)	Segment area (HA)	Site area (HA)	Segment area (HA)	Site area (HA)
Run	172.3	66.2	162.1	29.4	0.0	0.0
Rapid run	4.7	0.0	20.9	5.8	16.3	2.2
Rapid riffle	13.7	0	4.4	3.2	66.0	37.6
Pool	0.0	0	13.0	0.0	116.5	48.1
Eddy	0.0	0	7.2	0.0	5.6	0.0
Side channel	23.4	17.4	23.5	7.7	2.3	0.0
Intermittent side channel	7.4	7.4	0.0	2.7	0.0	0.0
Total	221.5	91.0	231.1	48.8	206.7	87.9

Site area calculated by combining both the North Fork and Big Canyon data

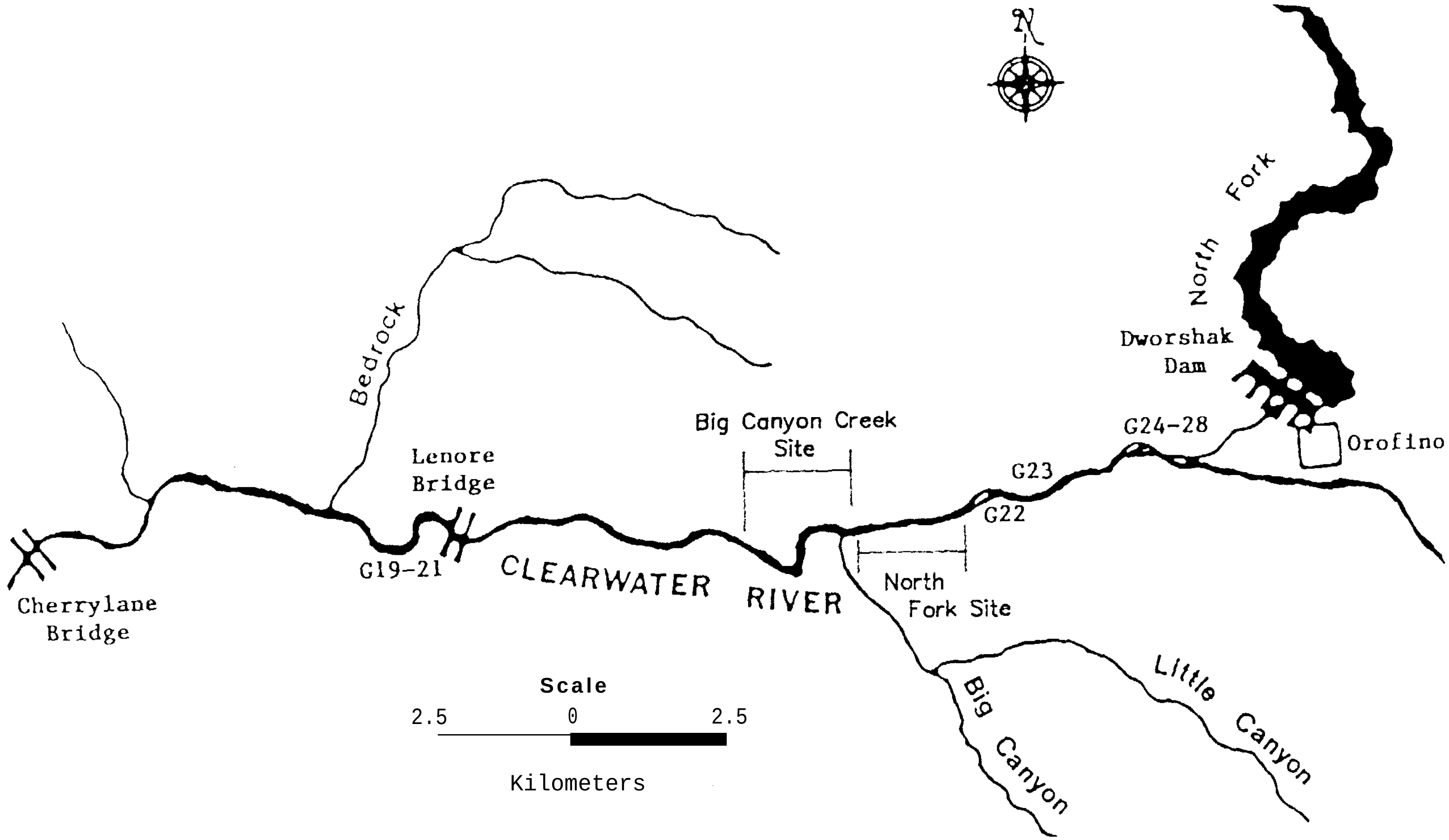

Figure A5. Spawning gravel (G#), and study site locations within the North Fork Segment of the lower mainstem Cleat-water River (LMCR) project area.

Table A6. Habitat representation by cross-section at the lower area of the Potlatch Site, Potlatch River Segment, lower mainstem Clearwater River (LMCR) project area, 1989.

Cross-section number	Habitat and hydraulic characteristics
LP-1	Run
LP-2	Run
LP-3	Rapid riffle, spawning gravel
LP-4	Spawning gravel
LP-5	Run, spawning gravel
LP-6	Run, spawning gravel
LP-7	Run, spawning gravel
LP-8	Run
LP-9	Stage of zero flow for side channel, not measured but surveyed
LP-10	Intermittent side channel
LP-11	Intermittent side channel
LP-12	Side channel
LP-13	Side channel
LP-14	Stage of zero flow, not measured, but surveyed
LP-15	Side channel
LP-16	Rapid riffle containing stage of zero flow for side channel

Table A7. Habitat representation by cross-section at the upper area of the Potlatch Site, Potlatch River Segment, lower mainstem Clearwater River (LMCR) project area, 1989.

Cross-section number	Habitat and hydraulic characteristics
UP-1	Run
UP-2	Run
UP-3	Run, spawning gravel
UP-4	Side channel

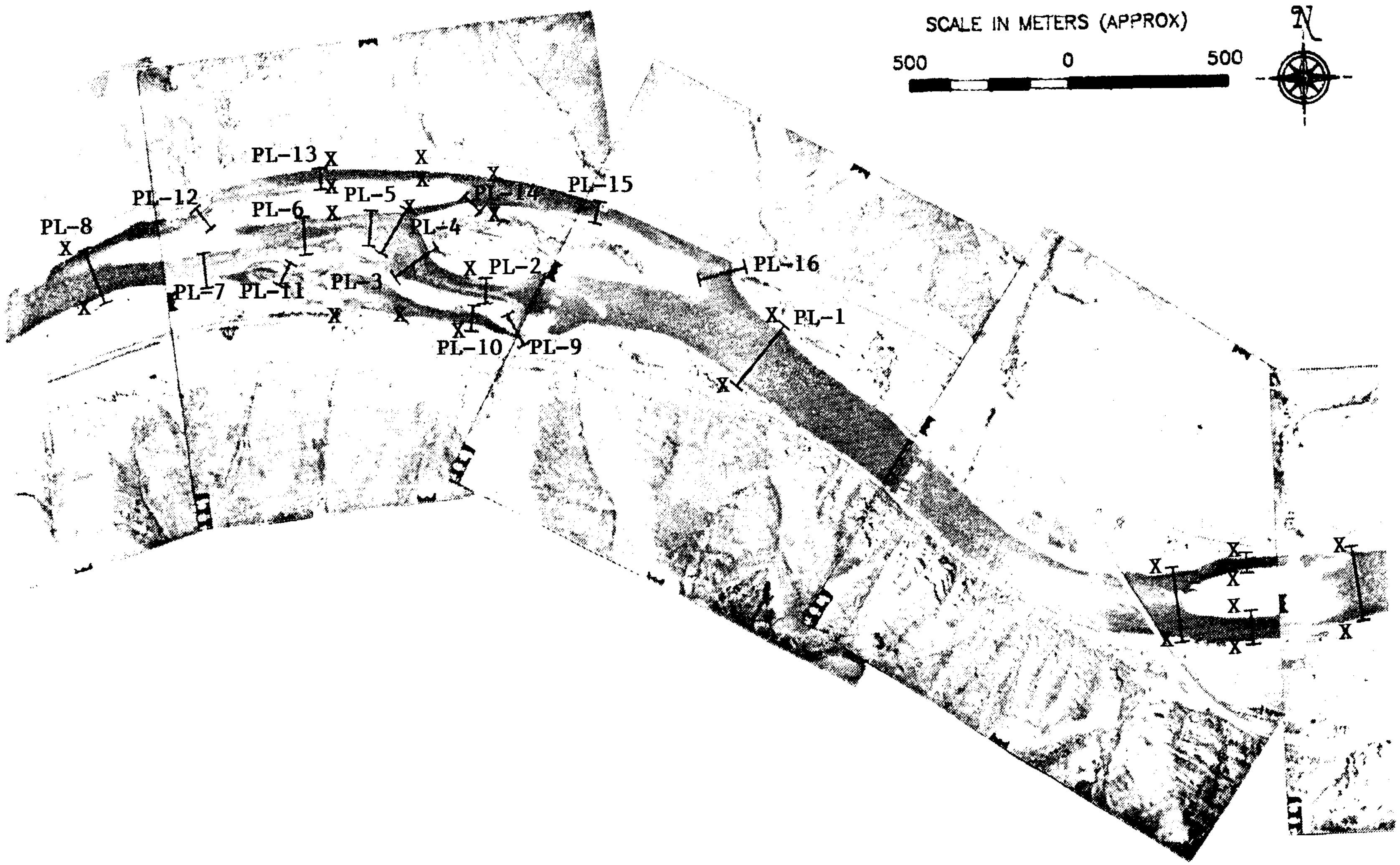

Figure A6. Assignment of hydraulic cross-sections (PL#, UPL#) and locations of water surface elevation rebar (X) within the Potlatch River Site of the Potlatch River segment, lower mainstem Clearwater River (LMCR) project area.

Table A8. Habitat representation by cross-section at the Bedrock Creek Site, Bedrock Creek Segment, lower mainstem Clearwater River (LMCR) project area, 1989.

Cross-section number	Habitat and hydraulic characteristics
BDR-1	Rapid run, not measured
BDR-2	Run, significant spawning gravel ability
BDR-3	Run, significant spawning habitat availability
BDR-4	Run, spawning habitat
BDR-5	Run, spawning habitat
BDR-6	Run
BDR-7	Run
BDR-8	Side channel
BDR-9	Side channel

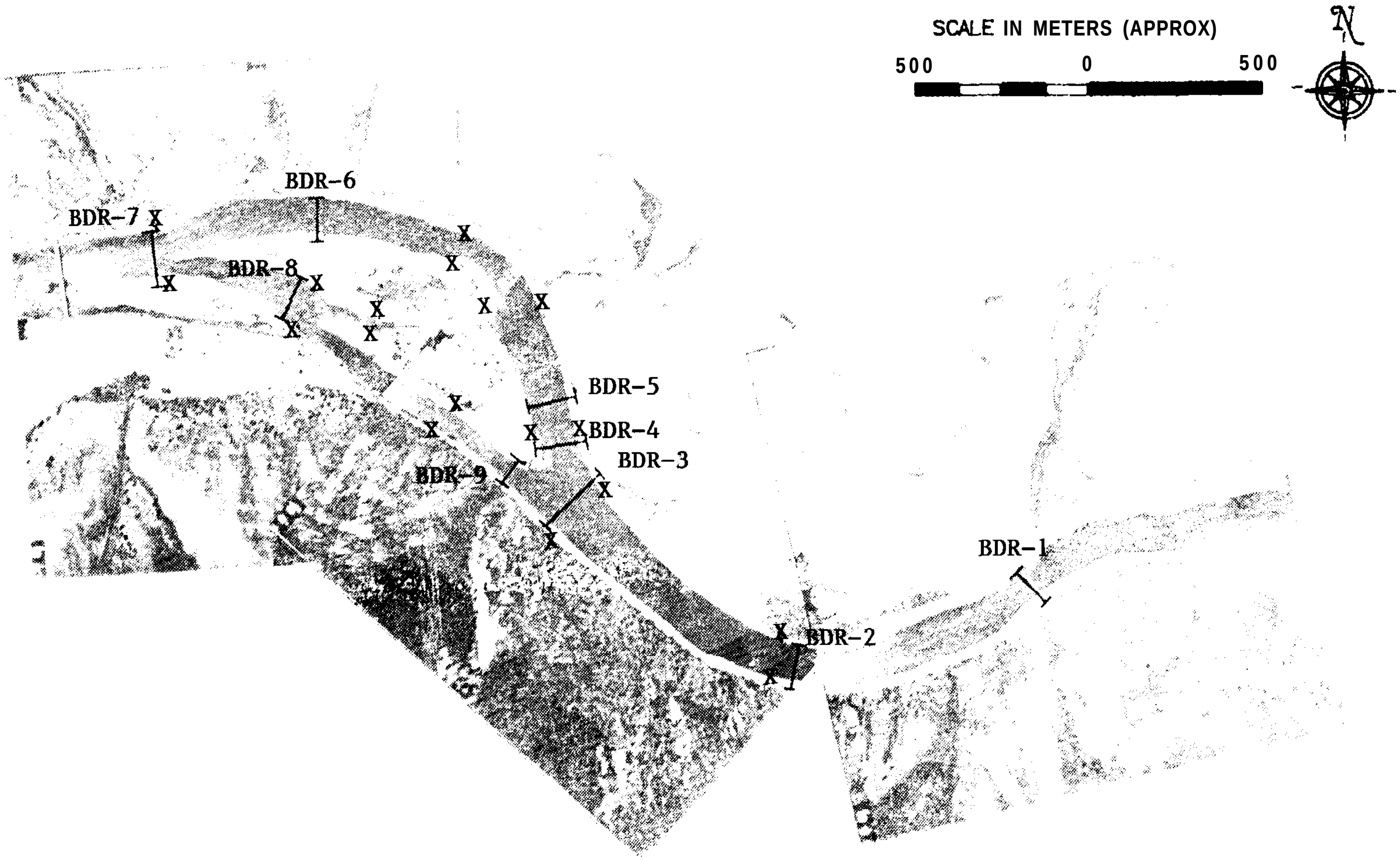

Figure A7. Assignment of hydraulic cross-sections (BDR#) and locations of water surface elevation rebar (X) within the Bedrock Creek segment, lower mainstem Clearwater River (LMCR) project area,

Table A9. Habitat representation by cross-section at the North Fork Site, North Fork Segment, lower mainstem Clearwater River (LMCR) project area, 1989.

Cross-section number	Habitat and hydraulic characteristics
BGC-1	Pool, triangular channel
BGC-2	Rapid, riffle
BGC-3	Pool, triangular channel
NF-1	Rapid riffle, not measured
NF-2	Pool

Figure A8. Assignment **of hydraulic** cross-**sections** (BGC#) and locations of water surface elevation rebar (X) within **the** Big Canyon Creek **site** of the **North** Fork segment, lower mainstem Clearwater River (LMCR) project area.

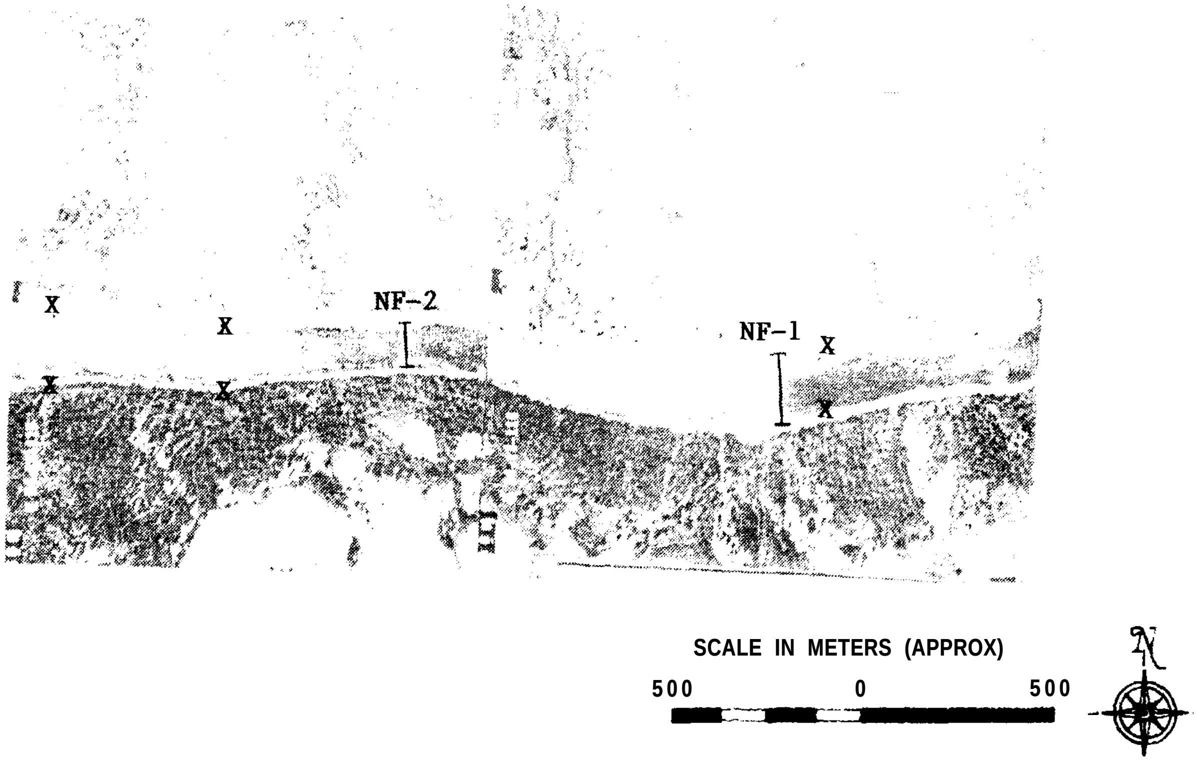

Figure A9. Assignment of hydraulic cross-sections (NF#) and locations of water surface elevation rebar (X) within the North Fork Site of the North Fork segment, lower mainstem Cleat-water River (LMCR) project area.

APPENDIX B
Hydraulic Simulation

Stage-Discharge Relationship:

Discharges obtained from USGS gages at Peck and Spalding at presented in Table B1. These discharges were used by IFG4 for calculation of stage-discharge relationships. Discharge readings provided correspond to the dates and times at which water surface elevation rebar where placed on the LMCR.

Several different modeling options are available with respect to the discharge used by IFG4 for calculating the stage-discharge relationship for a given cross-section. These modeling options are specified different combinations of Input-Output Card (IOC) Options 5 and 8 in the IFG4 data deck. Several options are provided for special situations when discharge is not consistent among transects, such as caused by subsurface flows. Additional options allow the use of discharges calculated by the program at velocity calibration flows for subsequent calculations of stage-discharge relationships.

For IFG4 hydraulic simulations of the LMCR, we set IOC Option 5 to 1, IOC Option 8 to 0. This combination of IOC options invokes the use of a stage-discharge relationship based upon given discharges, such as provided by USGS gaging station data, instead of discharges calculated by IFG4 from velocity calibration data (Milhous et al 1984). These discharges are specified on the WSL-discharge calibration (CAL) lines of the input data deck. This hydraulic simulation option is appropriate when gaging station data is thought to provide the best estimate of discharge, or when velocity measurements obtained at cross-section may be inaccurate (Milhous et al 1984).

We concluded that this IFG4 modeling option was most appropriate for hydraulic simulations applied to the LMCR for three reasons. First, because the Spalding and Peck USGS gaging stations were both rated as "excellent", we concluded that they would provide more accurate discharge readings than the discharges calculated at IFIM cross-sections from velocity measurements. Some of the cross-sections employed in our study were probably susceptible to velocity measurement errors due to complex hydraulics (e.g. standing waves; vertical eddy currents associated with large boulders) encountered at the 323 cms (11,400 cfs) velocity calibration discharge, or due to an irregular cross-sectional profile. Second, discharge was very consistent among cross-section during the placement of water surface elevation rebar because of the extremely minor contribution of tributary inflows to the mainstem river. Consequently, discharge readings from the Peck Gage could be applied to all North Fork and Big Canyon Creek study site cross-sections, and from the Spalding Gage for all Bedrock Creek and Potlatch River study site cross-sections. For islanded reaches of the Bedrock Creek and Potlatch River study sites, total river discharges obtained from USGS gages provided the basis for partial discharge calculations for side channels. Third, steady flow conditions existed during rebar placement and velocity calibration measurements due to controlled flow releases from Dworshak Reservoir. Steady state discharge conditions were verified by temporary staff gages placed at each study site during water surface elevation and velocity calibration measurements. Steady discharge conditions were also evident from hourly flow data obtained from the USGS. These conditions allowed us to assume the discharge was consistent between cross-sections and the USGS gaging station at any given time.

Table B1. Lower mainstem Clearwater river discharge data obtained from USGS GOES stations at Peck and Spalding.

Station	Date	Time	Discharge (cms)	Discharge (cfs)
Peck	6/7/89	10:08 am	1294.2	45,698
		10:35 am	1295.9	45,758
		10:44 am	1301.6	45,959
		11:15 am	1301.6	45,959
		12:38 pm	1301.6	45,959
		2:04 pm	1301.6	45,959
Spalding	6/7/89	3:43 pm	1340.9	47,347
		4:50 pm	1340.9	47,347
Peck				
	6/13/89	9:21 am	984.1	34,749
		9:58 am	990.6	34,978
		10:05 am	990.6	34,978
		10:42 am	990.6	34,978
		12:42 pm	1007.1	35,561
		1:15 pm	1007.6	35,578
Spalding	6/13/89	2:26 pm	1026.3	36,239
		4:14 pm	1026.3	36,239
Peck	6/29/89	8:00 am	447.5	15,801
		8:43 am	447.5	15,801
		9:07 am	447.5	15,801
		9:25 am	447.5	15,801
		10:25 am	447.5	15,801
		11:45 am	444.1	15,801
Spalding	6/29/89	1:00 pm	463.3	16,359
		3:45 pm	463.3	16,359
Peck	7/6/89	11:15 am	312.7	11,041
		11:40 am	312.7	11,041
		12:40 pm	312.7	11,041
		1:12 pm	312.7	11,041
		1:30 pm	312.7	11,041
		2:30 pm	312.7	11,041

Table B1 (cont). Lower mainstem Clearwater river discharge data obtained from USGS GOES stations at Peck and Spalding.

Station	Date	Time	Discharge (cms)	Discharge (cfs)
Spalding	7/6/89	4:00 pm	325.7	11,500
		4:30 pm	325.7	11,500
Peck	7/25/89	10:20 am	228.7	8,075
		10:52 am	228.7	8,075
		11:15 am	228.7	8,075
		11:50 am	228.7	8,075
		12:40 pm	228.7	8,075
		1:58 pm	228.7	8,075
Spalding	7/25/89	2:33 pm	230.4	8,135
		5:11 pm	230.4	8,135
Peck	8/5/89	9:45 am	85.5	3,019
		7:45 pm	85.5	3,019
Spalding	8/6/89	7:45 am	86.5	3,054
		2:30 pm	85.9	3,033
Peck	8/6/89	2:30 pm	83.7	2,955
		8:59 pm	83.7	2,955
Spalding	8/14/89	12:00 pm	111.9	3,951
		1:00 pm	111.9	3,951
Peck	8/14/89	7:00 am	111.6	3,941
		12:00 pm	111.6	3,941

Hydraulic Geometry:

Hydraulic geometry relationships between width, average depth, average velocity, and discharge are presented in Figures Bl-B30. Several general patterns in hydraulic geometry can be observed from these figures which specifically reflect the shape of the cross-section profile. For example, Lower Potlatch cross-section 1 (Figure B1) has a profile representative of many main channel sections of the river. Width does not increase much with increasing discharge, since the channel is fully wetted even at low discharges of approximately 85 cms (3,000 cfs). Since main channel sections of the LMCR has relatively steep banks, depth instead increases substantially with increasing flow to approximately 500 cms (17,655 cfs). Above this point, velocity shows the greatest increase with respect to discharge. Increased velocities result from lowered overall channel roughness at higher stages of flow. This pattern in hydraulic geometry is to a greater extreme in Bedrock cross-section 2 (Figure B19), which has a fully wetted channel during low flow conditions, and which has very steep side slopes attributed to highway riprap on the left bank, and a railroad grade on the right bank. Steep banks are typical of main channel sections of the Bedrock Creek, Big Canyon Creek, and North Fork study sites.

An opposite pattern in hydraulic geometry is observed in islanded channel sections, which have relatively broad floodplains. Lower Potlatch cross-section 3 (Figure B3) provides a good example of this channel type, which has a relatively narrow wetted channel at low discharge conditions. In this case, width increases greatly with increasing discharge to about 400 cms (14,124 cfs). At this point, the channel becomes fully wetted. Beyond this point, depth and velocity increased considerably with increasing discharge while width remains fairly constant.

Unusual patterns in hydraulic geometry are seen in several cross-sections. For example, velocity decreases with increasing discharge in Lower Potlatch cross-section 2 (Figure B2) beyond 750 cms (26,483 cfs). Analysis of water surface slopes indicates that a considerable backwater effect occurs beyond this discharge due to a constriction in the channel several hundred meters downstream. Another unusual pattern is observed at Lower Potlatch cross-section 16 (Figure B14), in which average velocity is greatest at the lower measured discharge. Analysis of calibration data indicates that this transects has a highly irregular cross-sectional shape, having a deep inner channel located within a broad, flat outer channel. Consequently, high average velocities are experienced in the inner channel at low discharges. However, lower average velocities are experienced when discharge is sufficient to fill the inner channel and expand into the broad outer channel. Decreased average velocity results from increased overall channel roughness experienced in the outer channel at higher discharges.

VAF Analysis:

Plots of VAF (velocity adjustment factor) verse discharge are presented in figures B31-34. These plots are commonly used for calibration of IFG4 hydraulic simulations. Analysis of VAF's suggested possible stage-discharge calibration problem at certain islanded transects. Specifically, the velocity adjustment factor should normally increase with increasing discharge, indicating decreasing channel roughness with increased flow. The VAF should normally approximate unity at the velocity calibration discharge. However, for several transects the VAF decreased as discharge increased. This is evident for Lower Potlatch cross-sections 13 and 15, and Bedrock Creek cross-sections 6 and 8. This inverse VAF plot is probably caused by the channel shape of these transects, indicating that a stage-discharge relationship may not be appropriate for these transects. These particular transects have an irregular cross-section, having a defined, steep-sided inner channel which is located within a wide, shallow overflow channel.

This problem can be corrected by an hydraulic modelling option of the IFG4 program which essentially bypasses the use of the regression based stage-discharge relationship. Instead, of predicting water surface elevations (WSE's) for each discharge, the WSE's used in the IFG4 data deck are those actually measured in the field at known discharges. Since field WSE's are used instead of predicted WSE's, this modeling procedure is referred to as an "empirical modelling approach". Additional water surface elevations can be obtained for intermediate discharges by interpolating between two measured stage-discharge pairs. Proper application of the option requires measurement of a relative large number of stage-discharge pairs. Since six stage-discharge pairs were obtained for each transect on the LMCR, this empirical modelling approach may provide a more appropriate method for simulating hydraulic conditions at certain cross-sections.

This empirical approach will be applied in future IFG4 calibration runs to those transects identified as problematic. This modeling approach is achieved by the following IFG4 Input-Output Card (IOC) Options:

IOC 5 = 0 (turns off use of stage-discharge relationship):

IOC 8 = 1 (water surface elevation is supplied on WSL lines for each discharge entered).

This combination of IOC options specify that for each discharge (QARD) provided in the IFG4 data deck, a corresponding water surface elevation will be provided on a WSL input data line.

Inverse VAF plots can also indicate an overestimation of discharge at low water surface elevations. VAF's for these transects will be further analyzed after additional discharge measurements are obtained in islanded side channels during low flow conditions.

Grouping of Cross-Sections:

As mentioned we separated the cross-sections into groups to simplify simulation (Table B2). Separation into these groups was most extreme for the highly complex Lower Potlatch area, which consists of three separate channels which diverged and merged at different points. Grouping of cross-sections in the Upper Potlatch area and the Bedrock Creek study site was much more simple, since these sites possessed islanded reaches with a main channel and single side channel. The Big Canyon Creek and North Fork sites consisted only of main channel transects. These latter two sites were grouped together due to their close proximity.

Table B2. Channel groupings employed in IFG4 hydraulic simulations.

Code	Description	Cross-sections
LPMC	Lower Potlatch Main Channel	1,8
LPCC1	Lower Potlatch Center Channel, upstream section	2,3
LPCC2	Lower Potlatch Center Channel, middle section	4,5,6
LPCC3	Lower Potlatch Center Channel, lower section	7
LPRC1	Lower Potlatch Right Channel, upper section	15,16
LPRC2	Lower Potlatch Right Channel, lower section	12,13
LPLC1	Lower Potlatch Left Channel, upper section	10
LPLC2	Lower Potlatch Left Channel, lower section	11
UPMC	Upper Potlatch Main Channel	1,3
UPRC	Upper Potlatch Right Channel	2
UPLC	Upper Potlatch Left Channel	4
BRMC	Bedrock Main Channel	2,3,7
BRRC	Bedrock Right Channel	8,9
BRLC	Bedrock Left Channel	4,5,6
BCMC	Big Canyon Main Channel and North Fork Main Channel (combined)	1,2,3 1

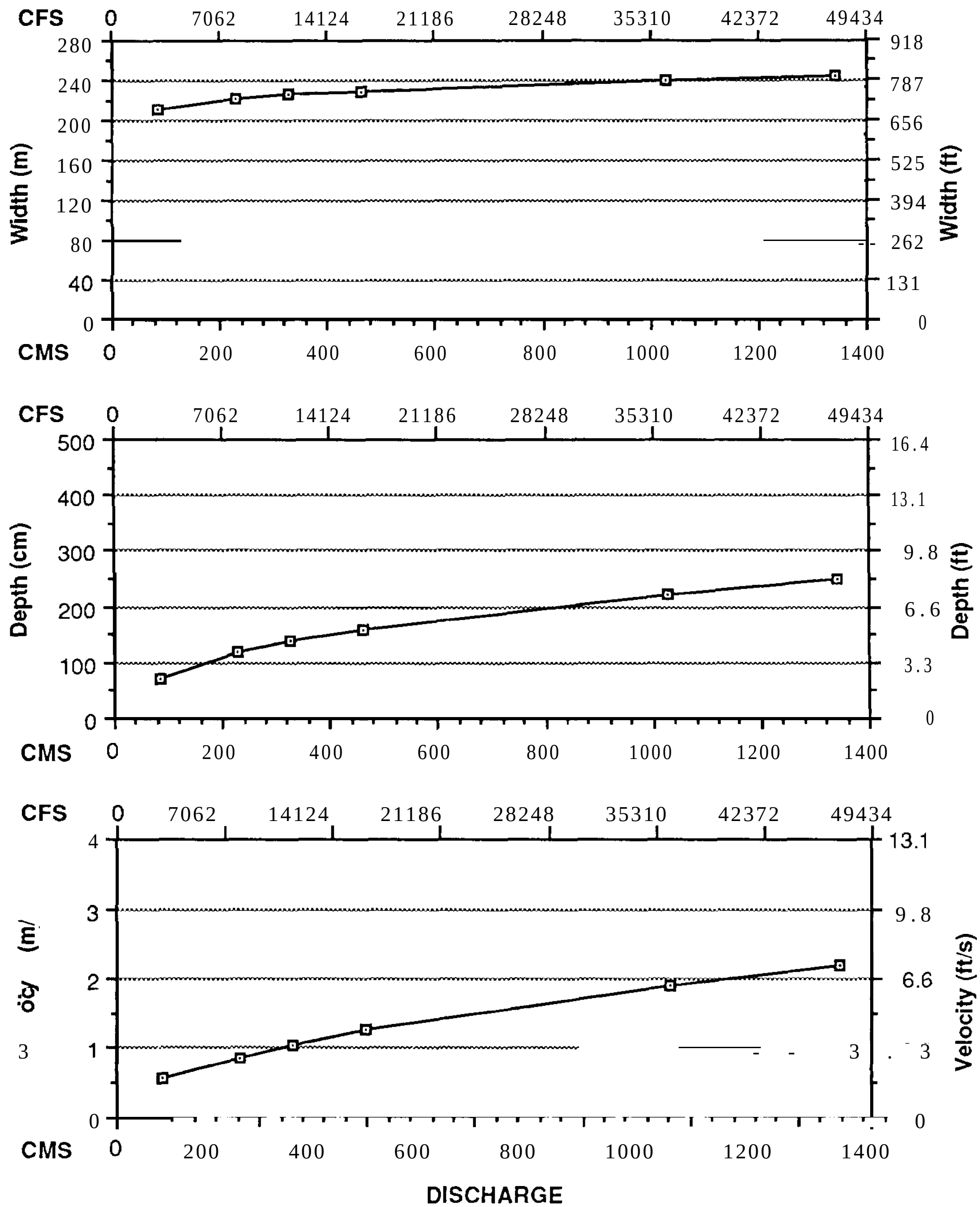

Figure B1. Hydraulicgeometry for Lower Potlatch Transect 1.

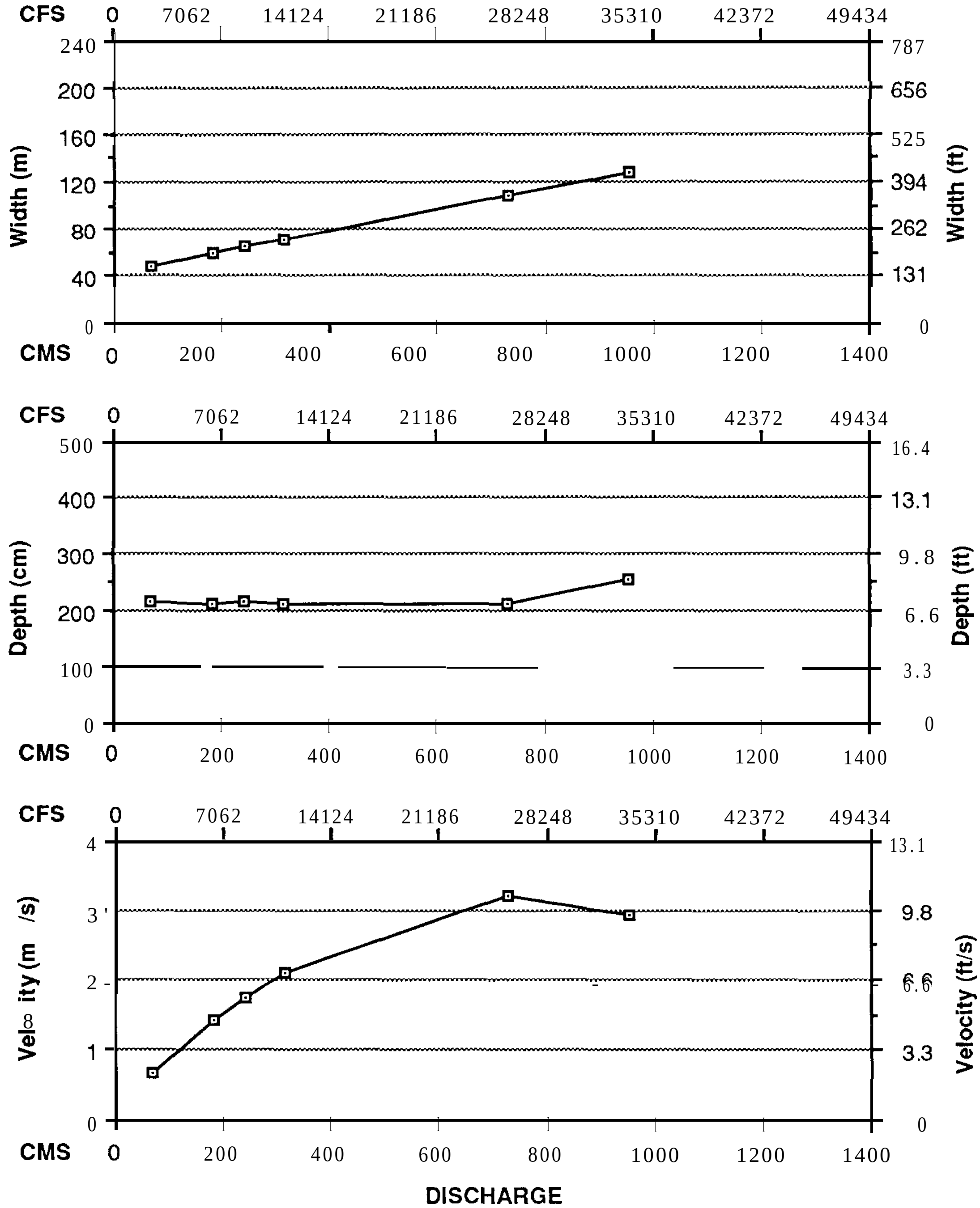

Figure B2. Hydraulic geometry for Lower Potlatch Transect 2.

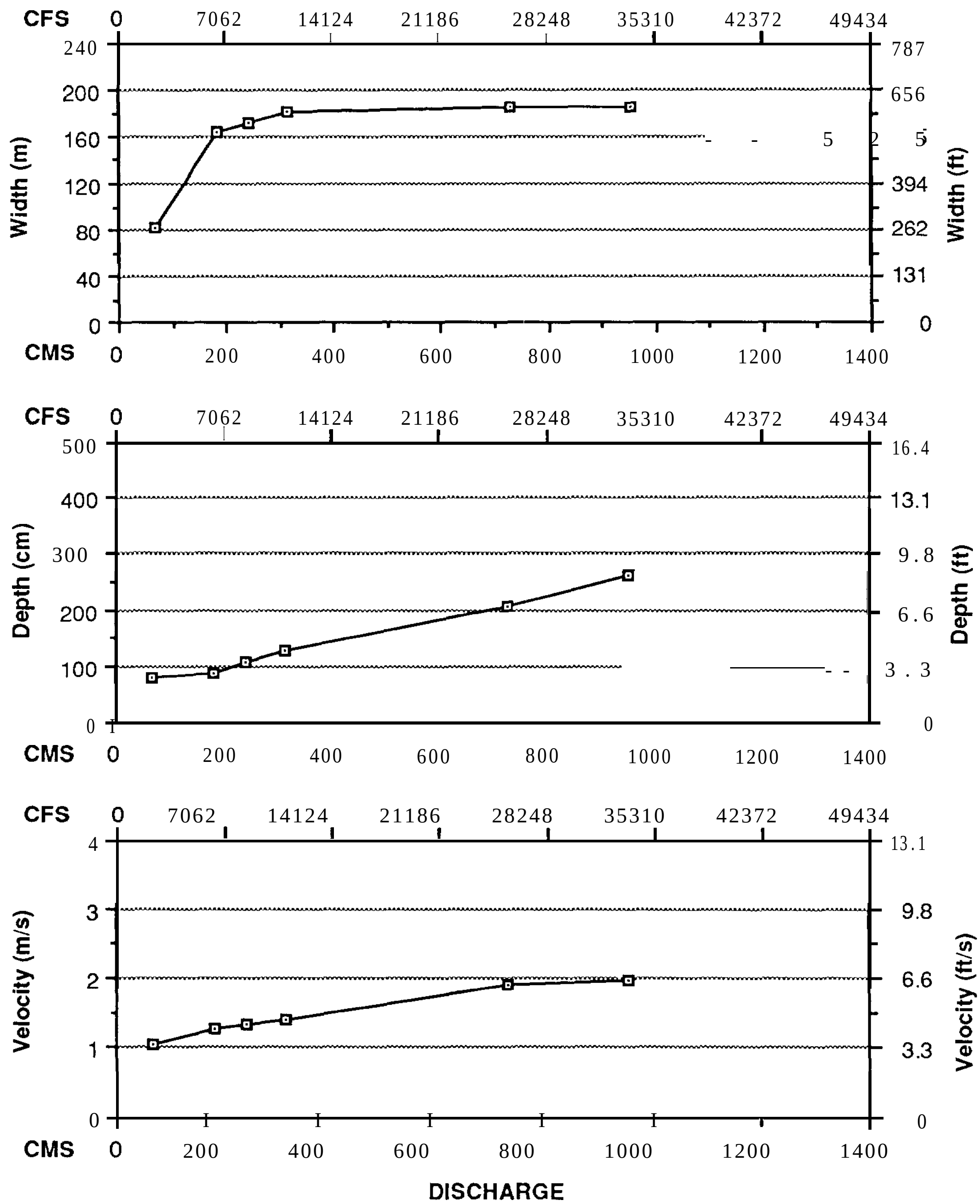

Figure B3. Hydraulicgeometry for Lower Potlatch Transect 3.

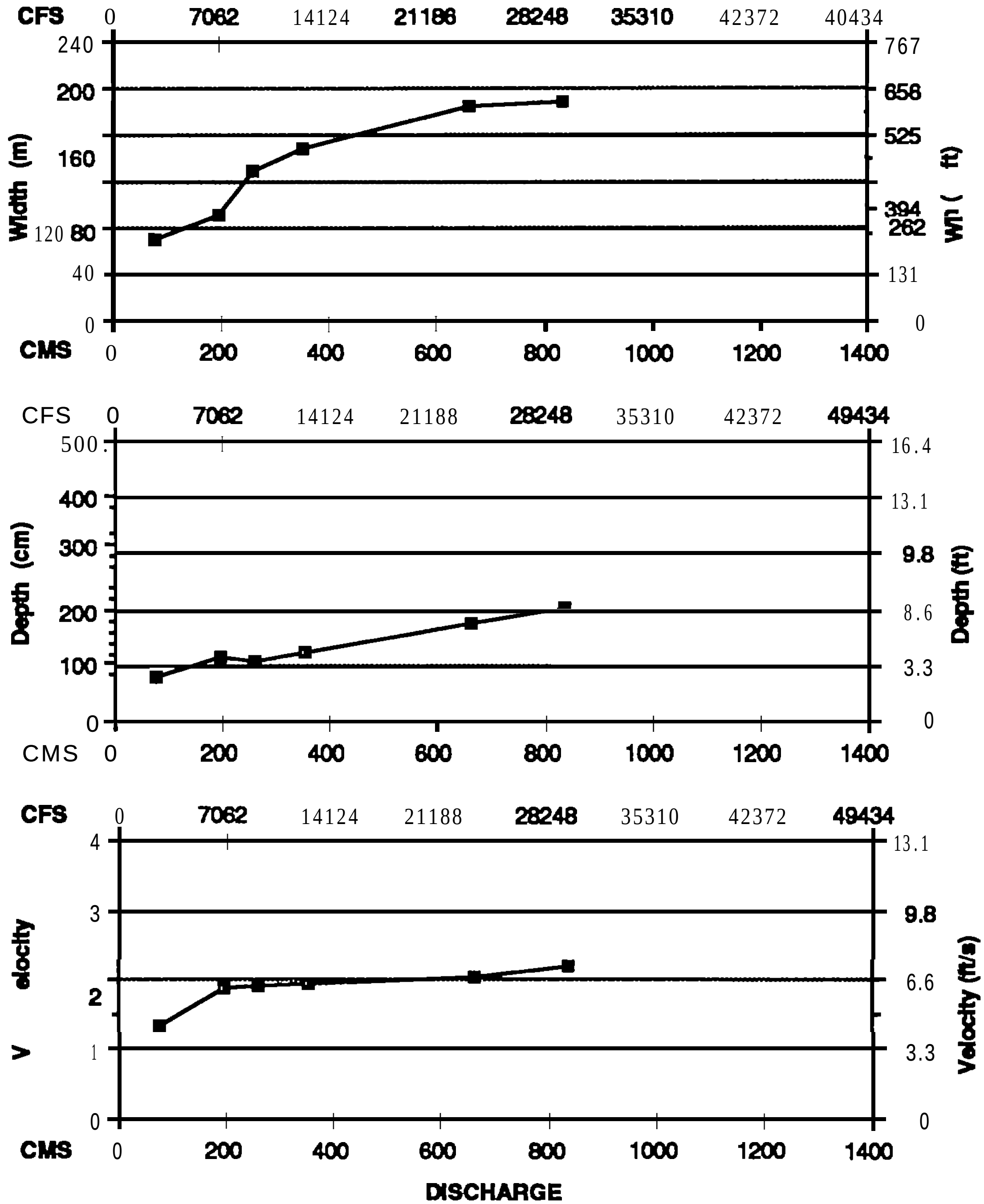

Figure 84. Hydraulic geometry for Lower Potlatch Transect 4.

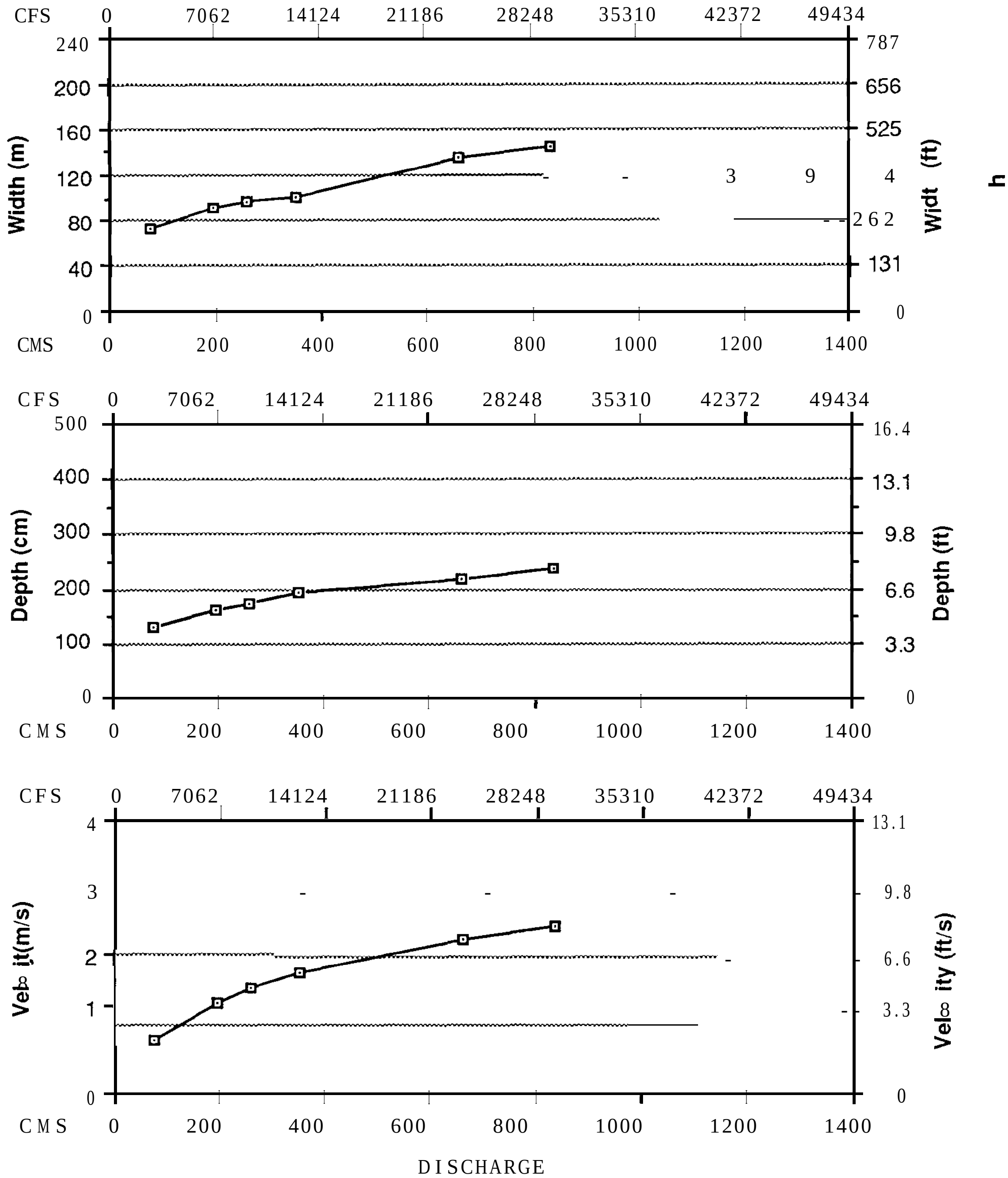

Figure B5. Hydraulicgeometry for Lower Potlatch Transect 5.

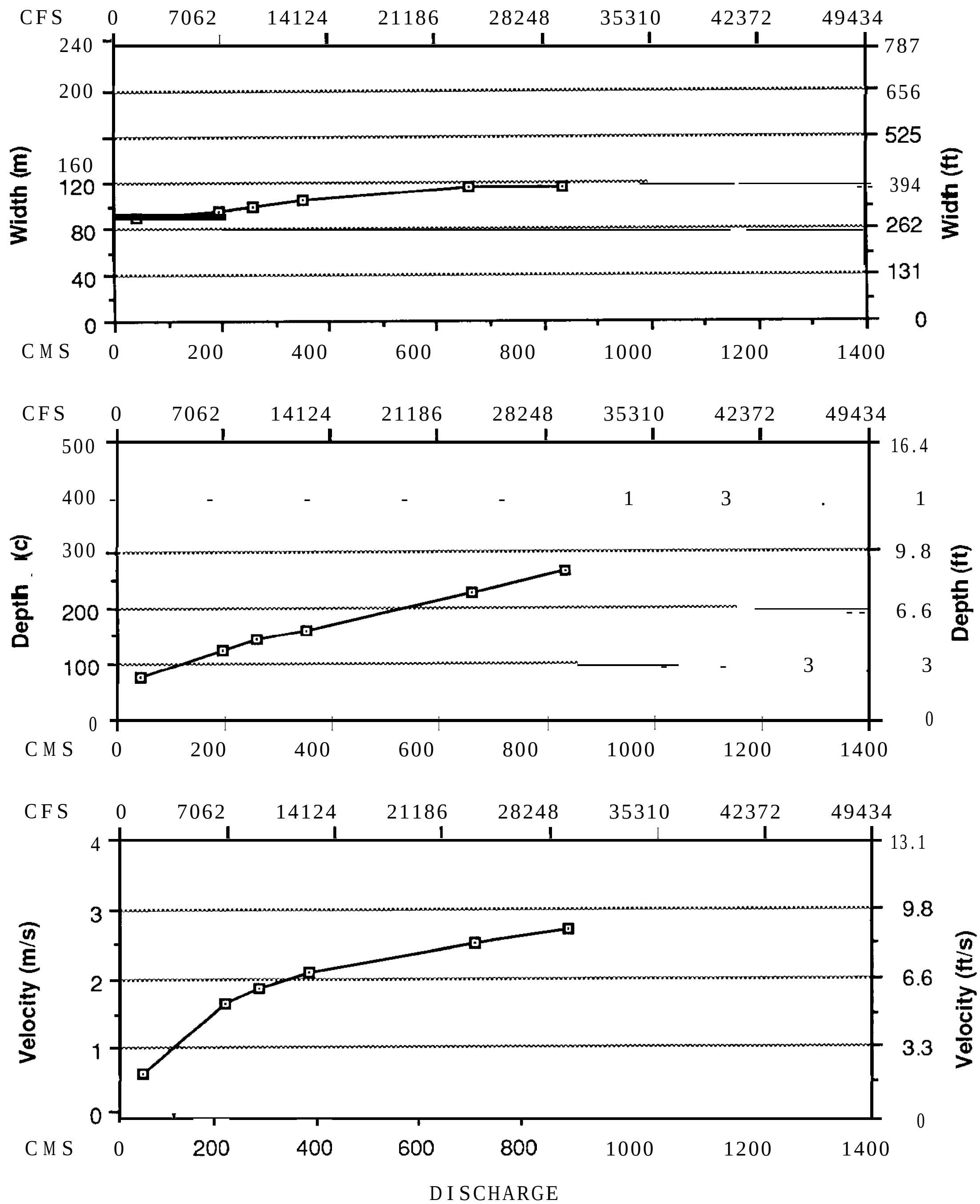

Figure B6. Hydraulic geometry for Lower Potlatch Transect 6

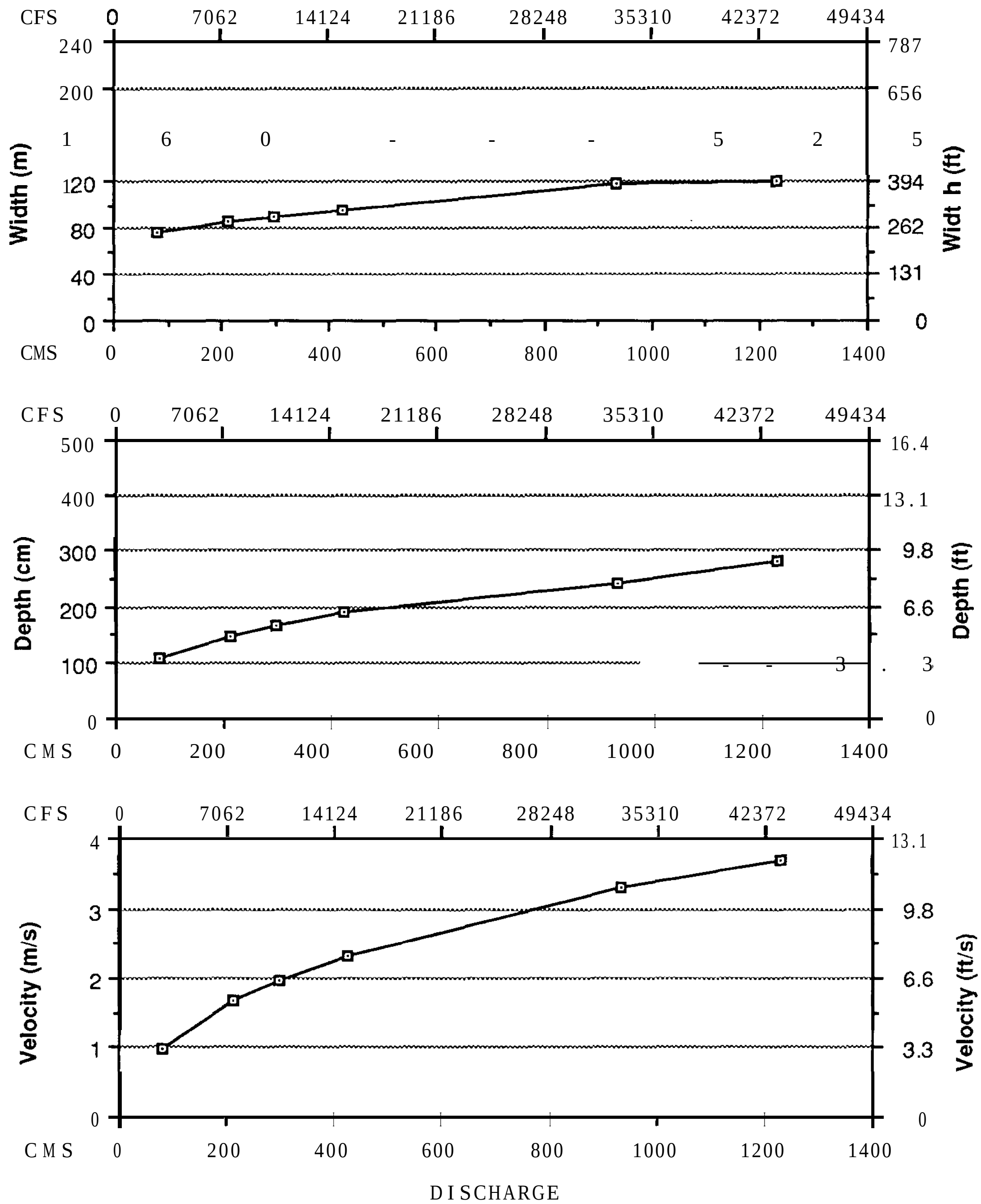

Figure B7. Hydraulic geometry for Lower Potlatch Transect 7.

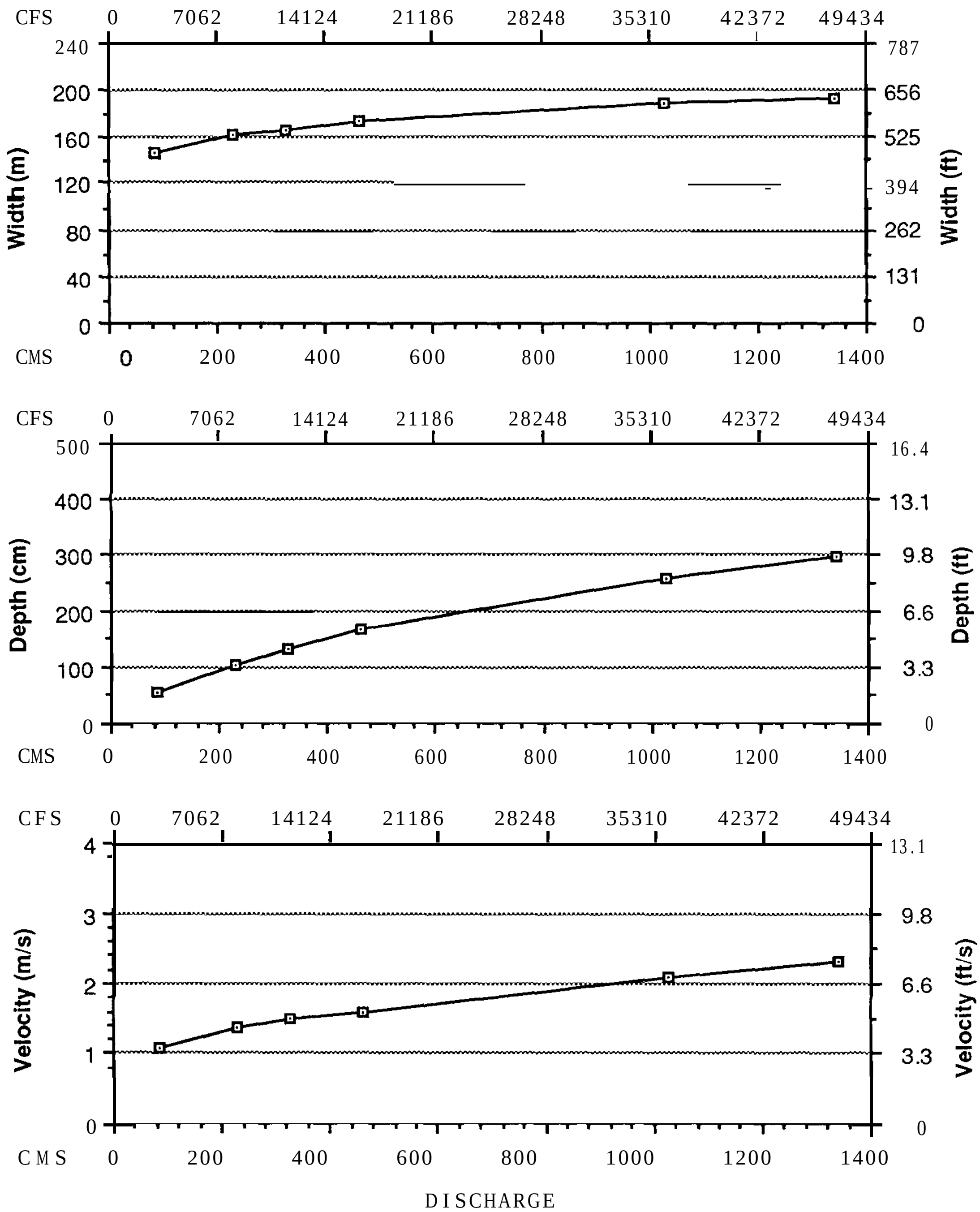

Figure B8. Hydraulic geometry for Lower Potlatch Transect8

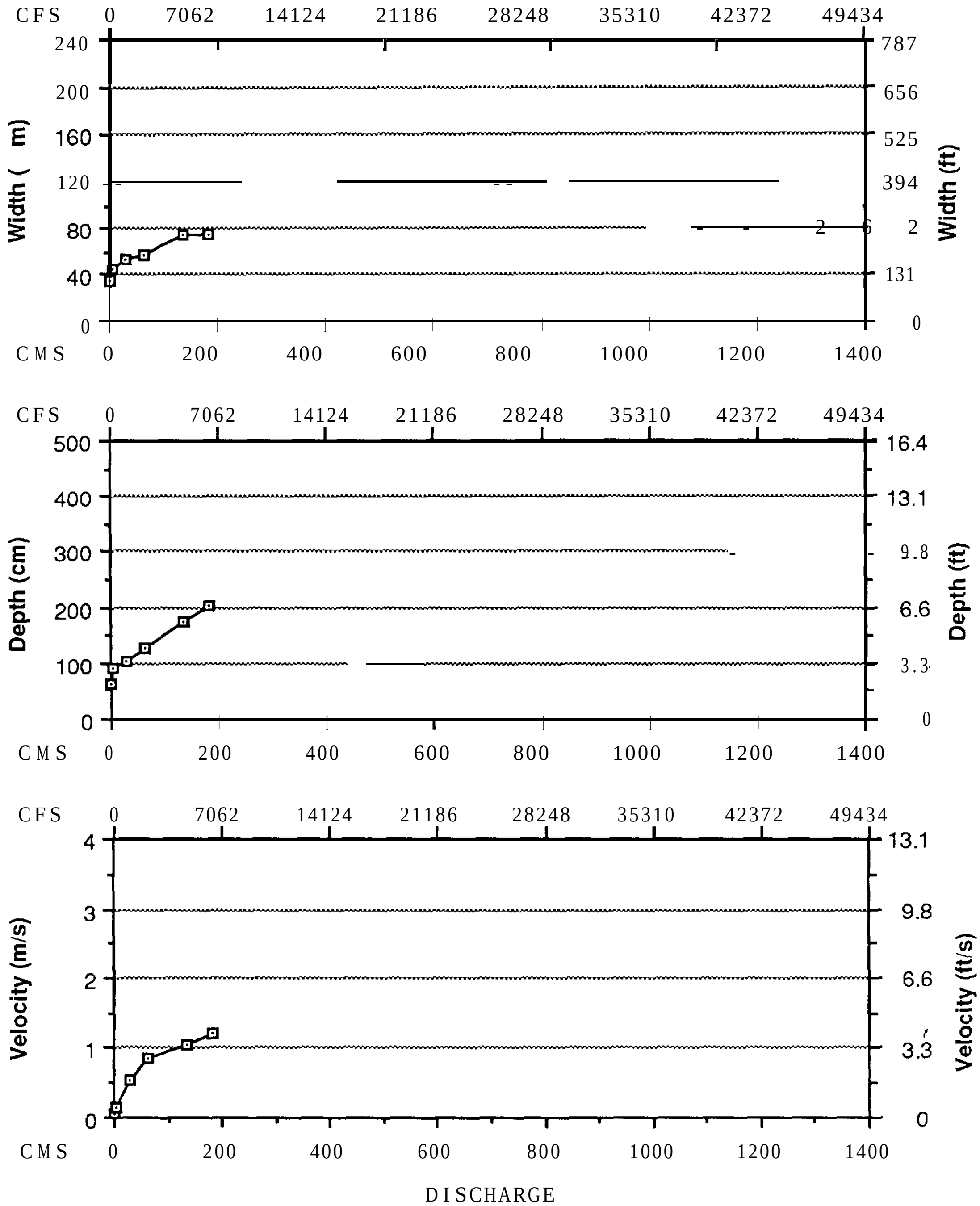

Figure B9. Hydraulic geometry for Lower Potlatch Transect 10.

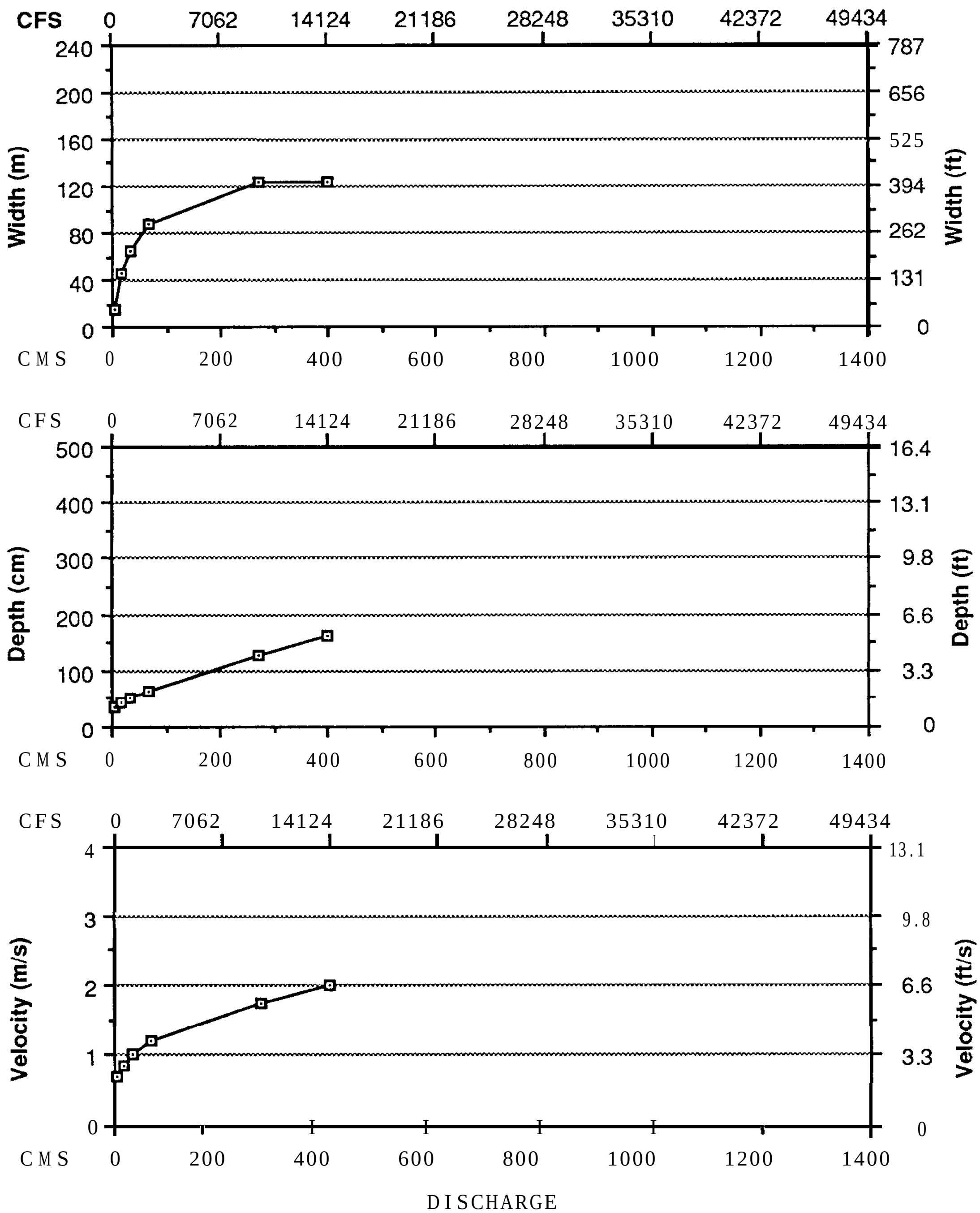

Figure B10. Hydraulic geometry for Lower Potlatch Transect 11.

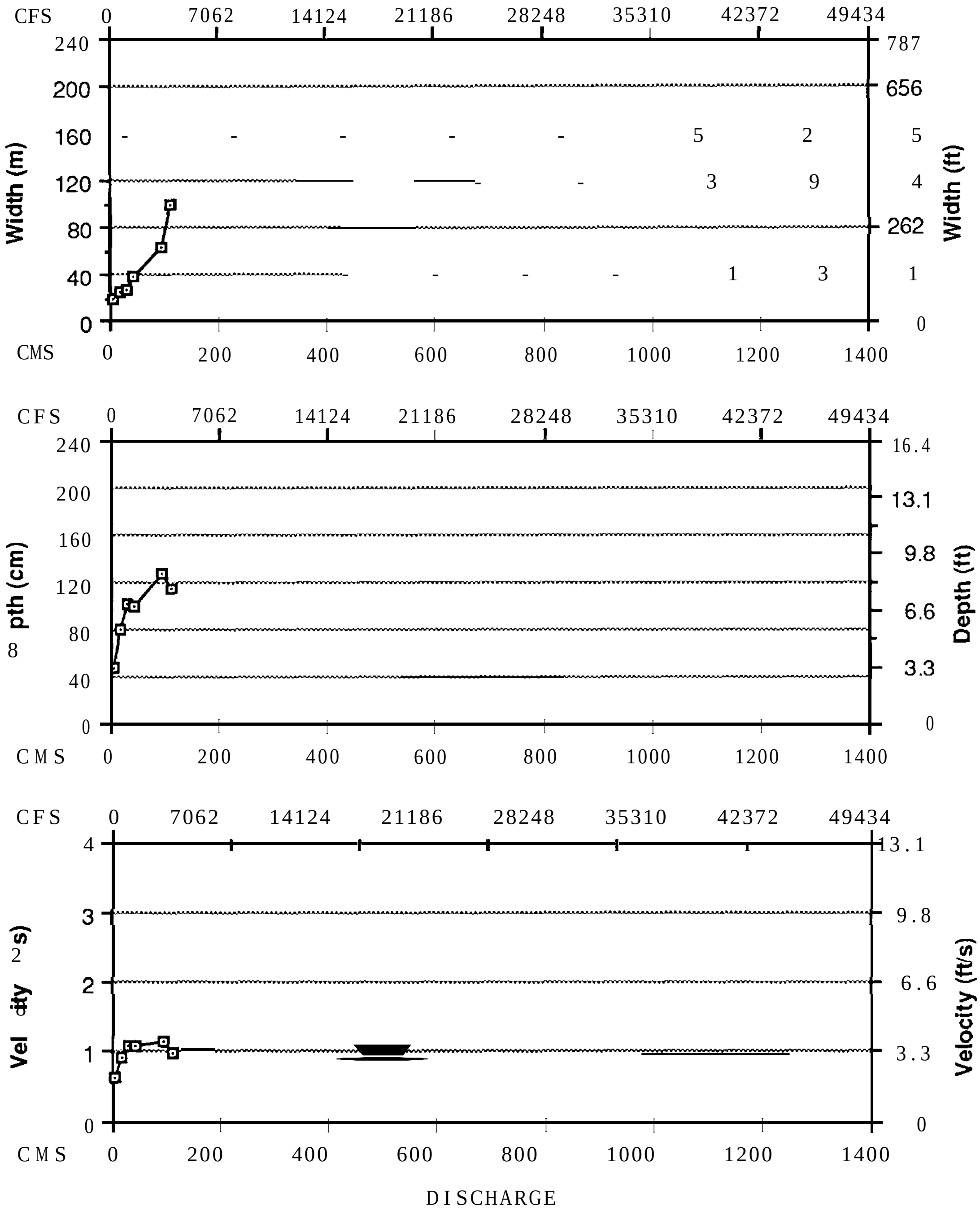

Figure B11. Hydraulic geometry for Lower Potlatch Transect 12.

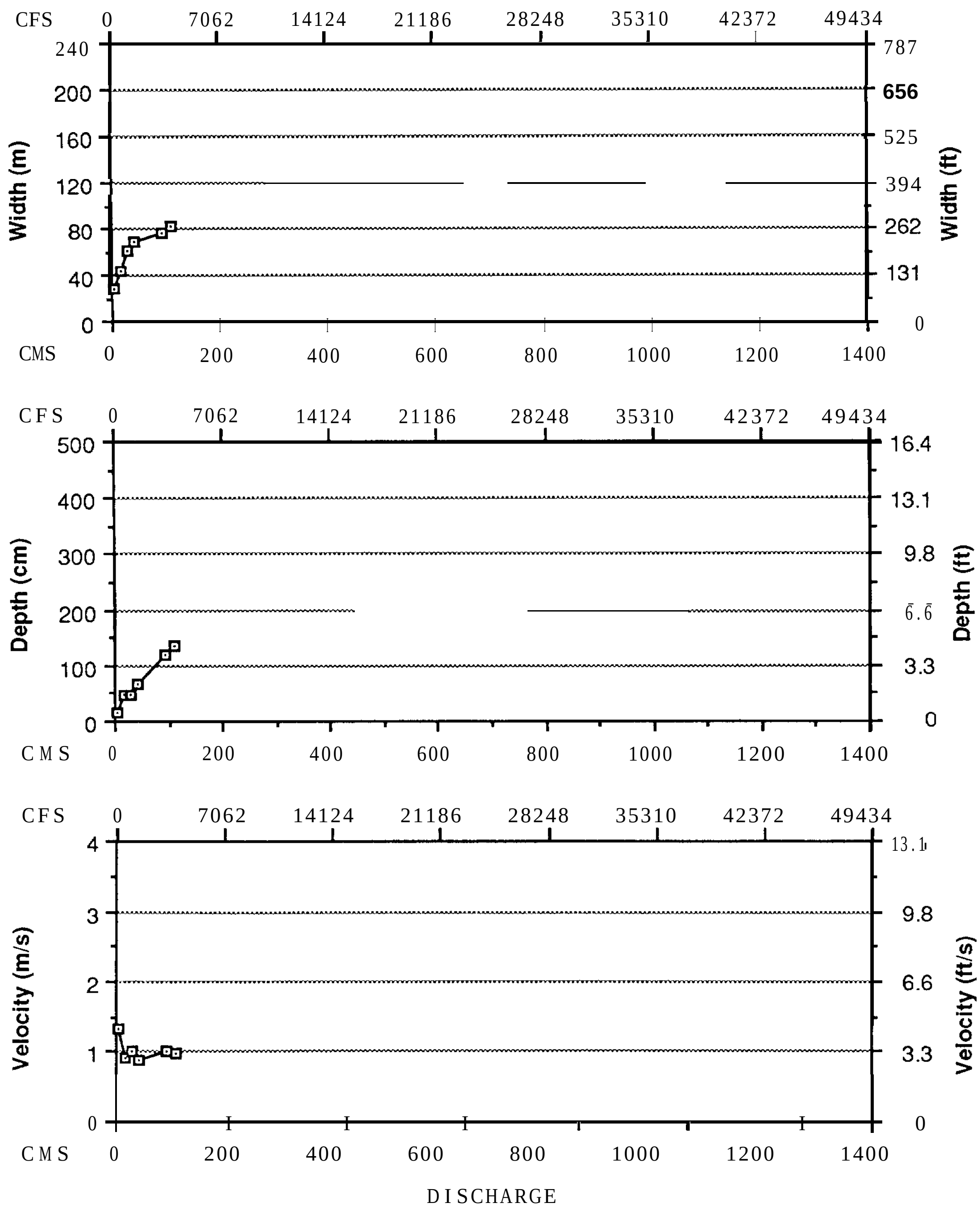

Figure B12. Hydraulicgeometry for Lower Potlatch Transectl3.

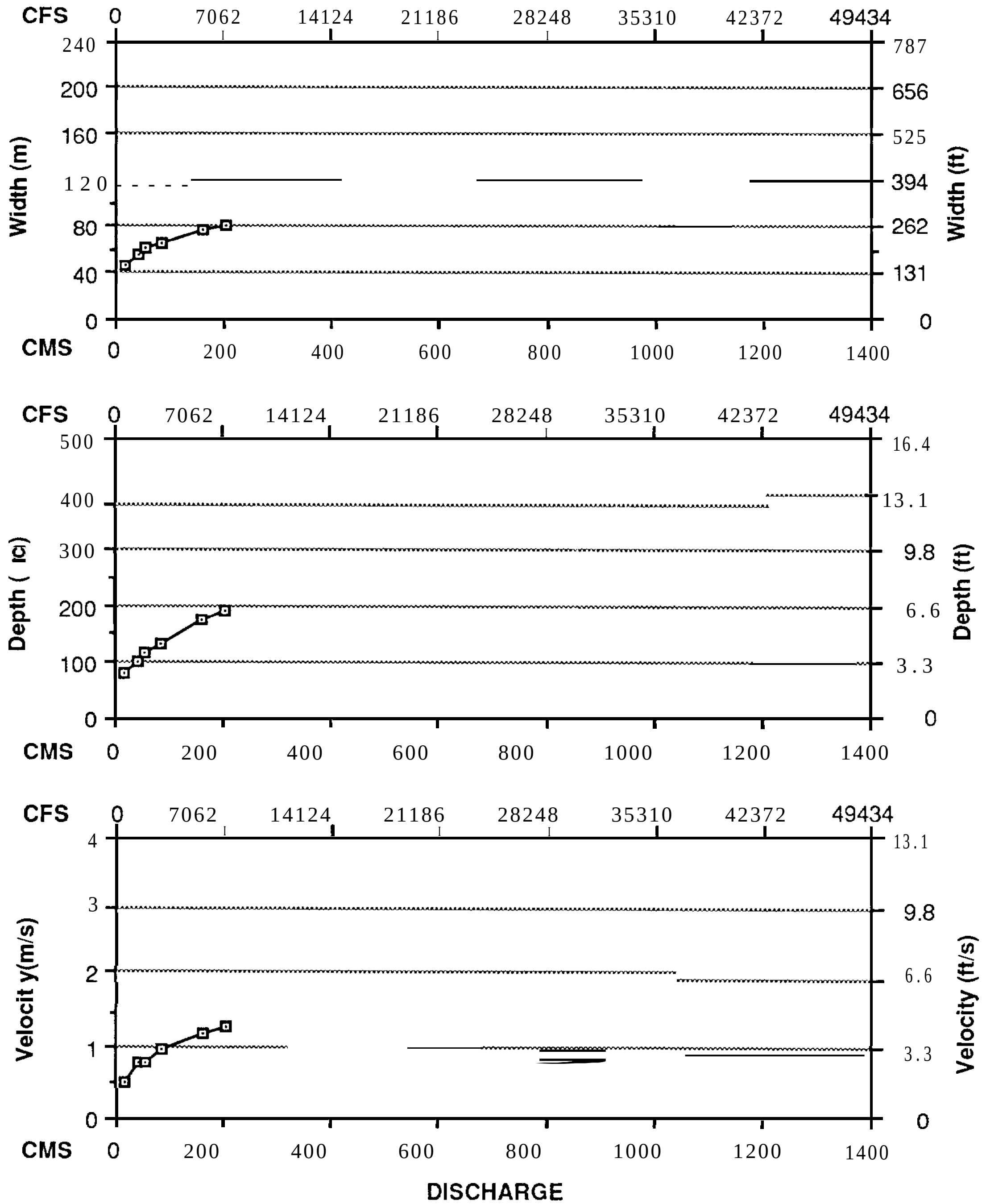

Figure B13. Hydraulic geometry for Lower Potlatch Transect 15.

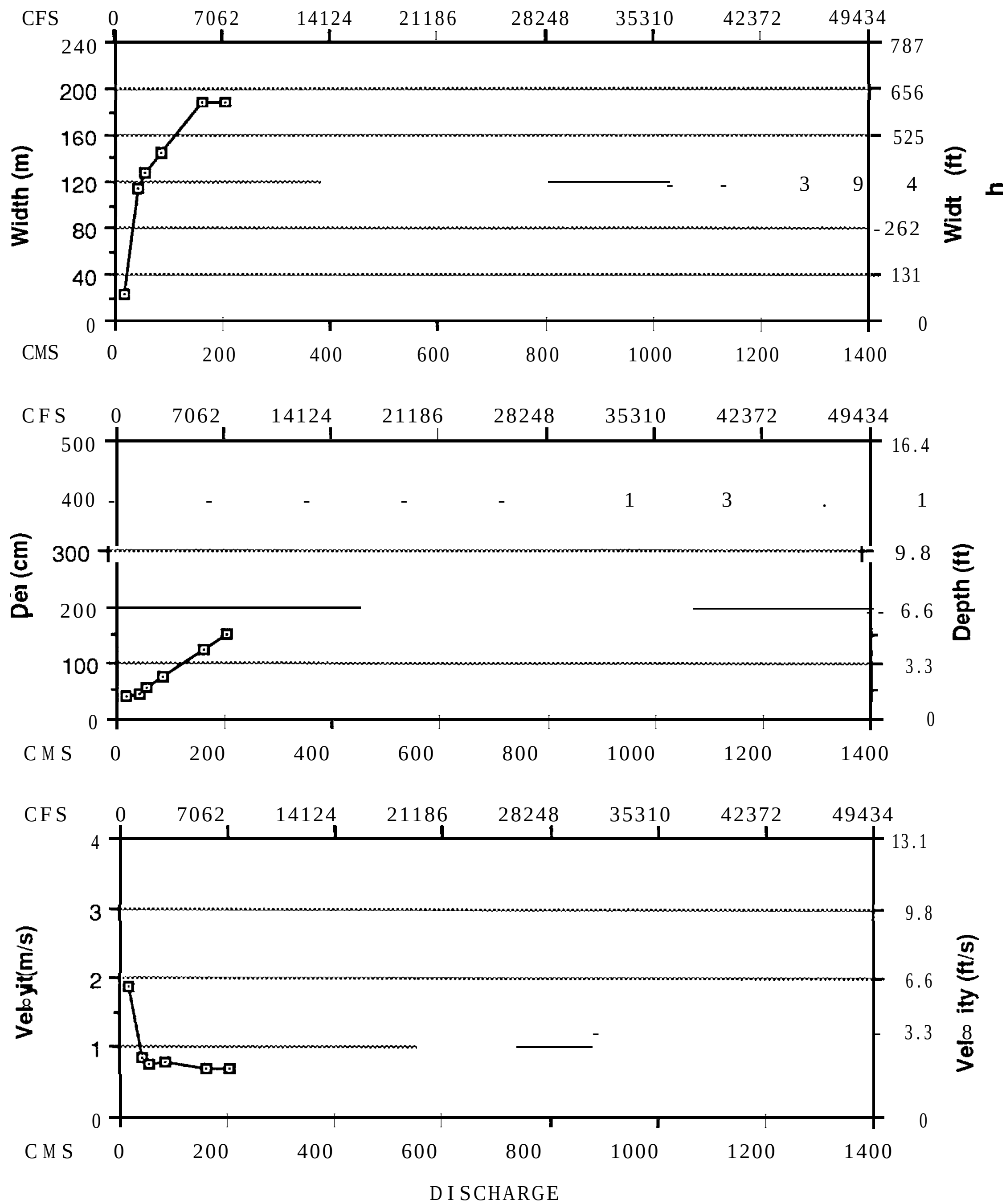

Figure B14. Hydraulic geometry for Lower Potlatch Transect 16.

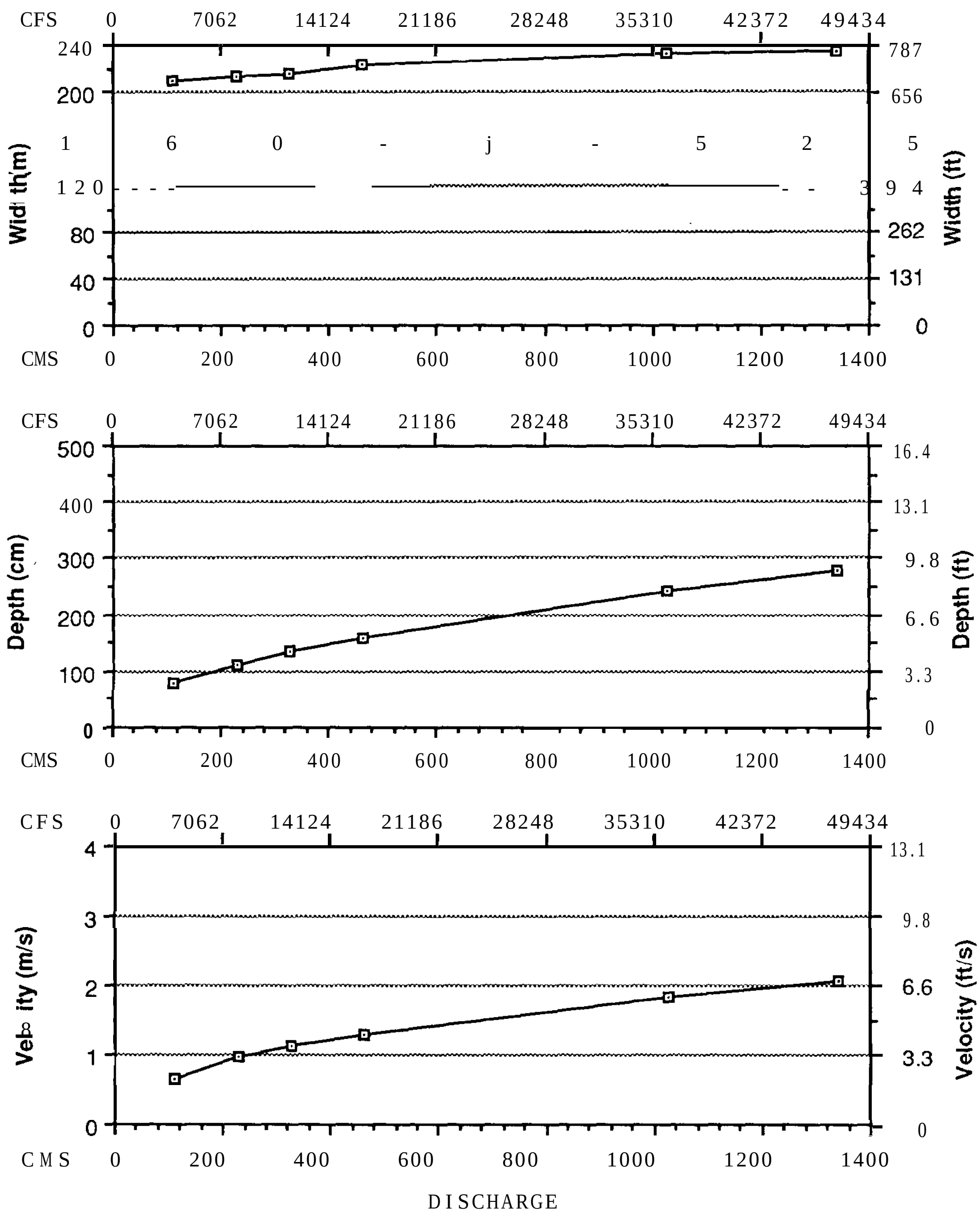

Figure B15. Hydraulic geometry for Upper Potlatch Transect 1.

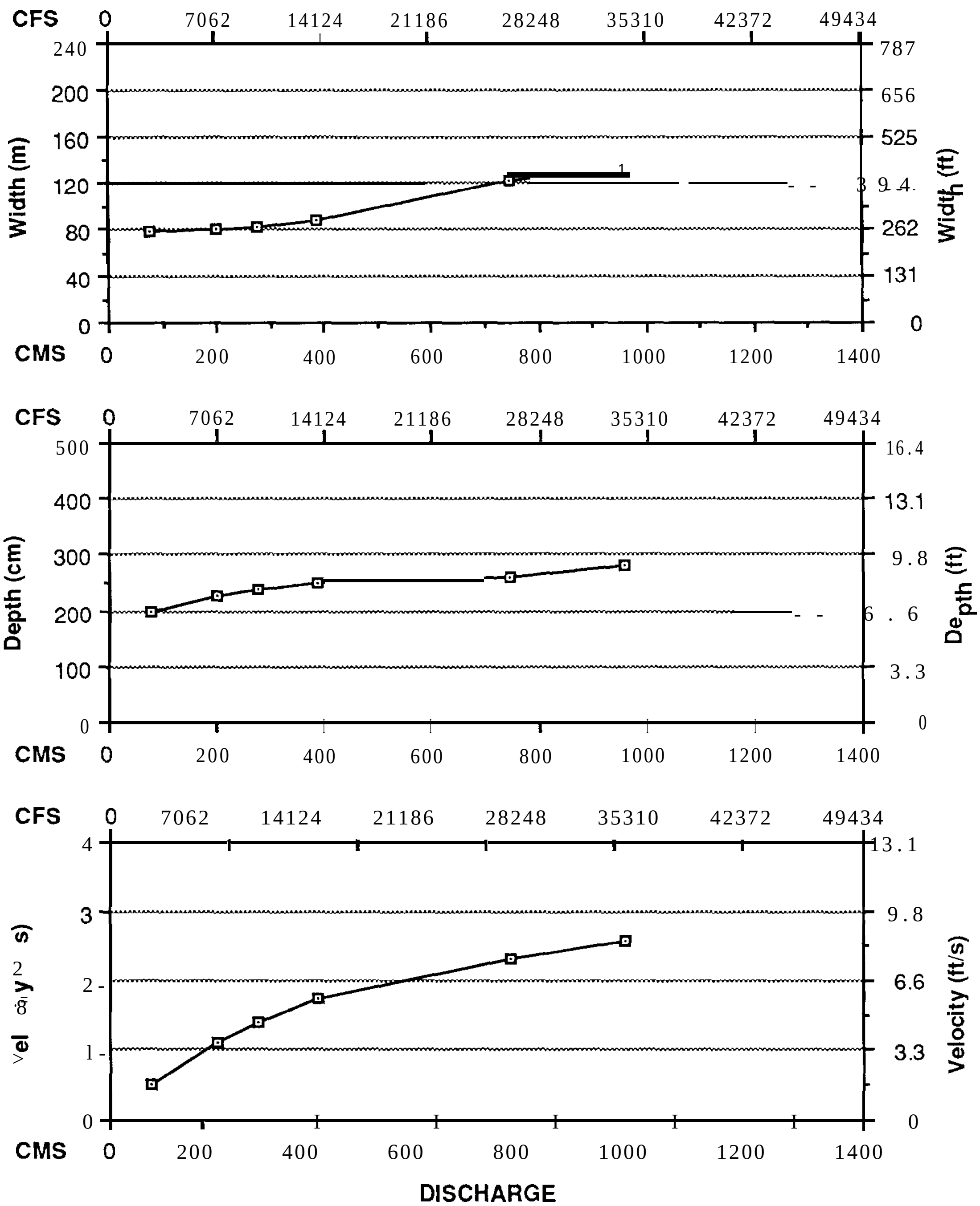

Figure B16. Hydraulicgeometty for Upper Potlatch Transect 2.

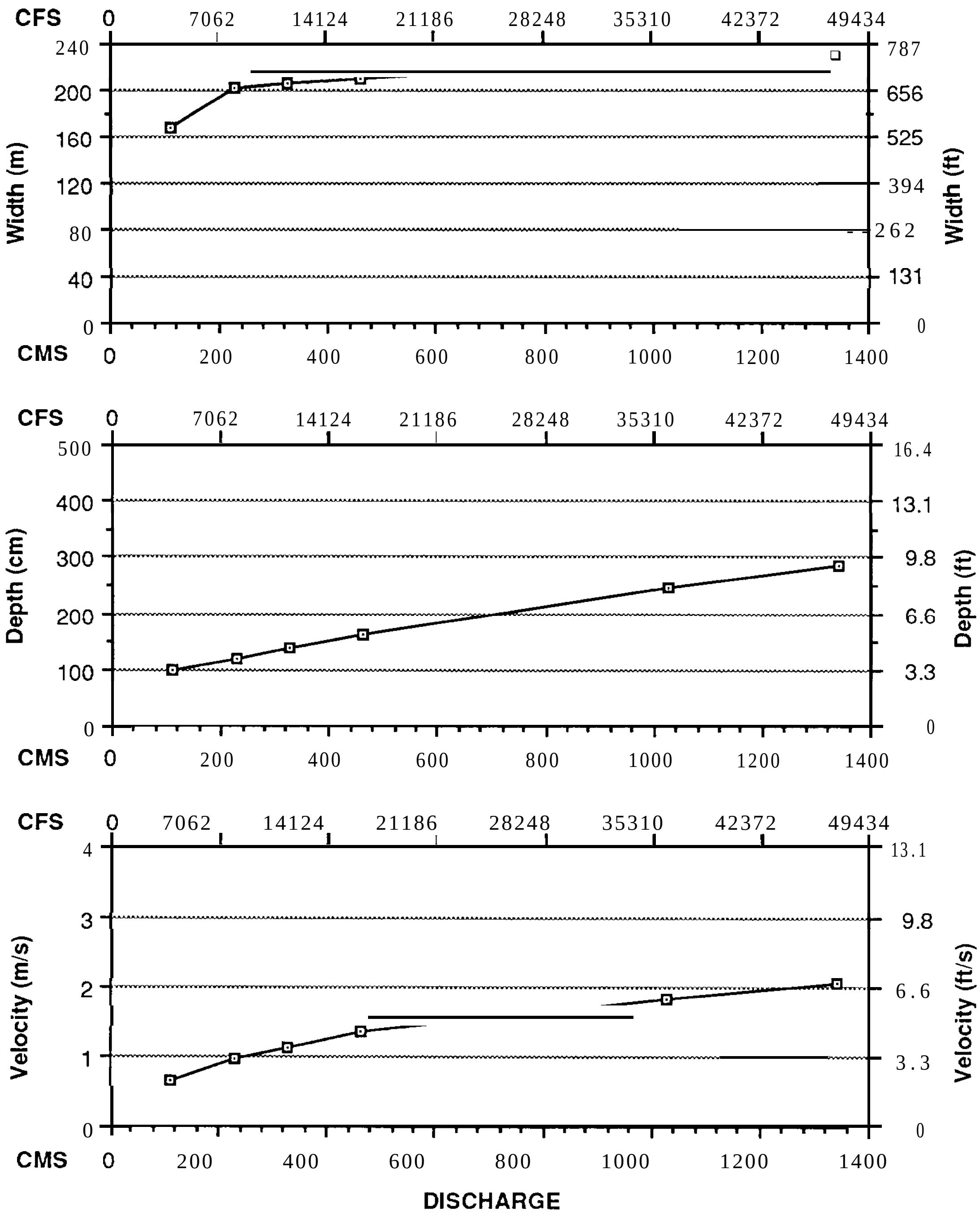

Figure 817. Hydraulicgeometry for Upper Potlatch Transect 3.

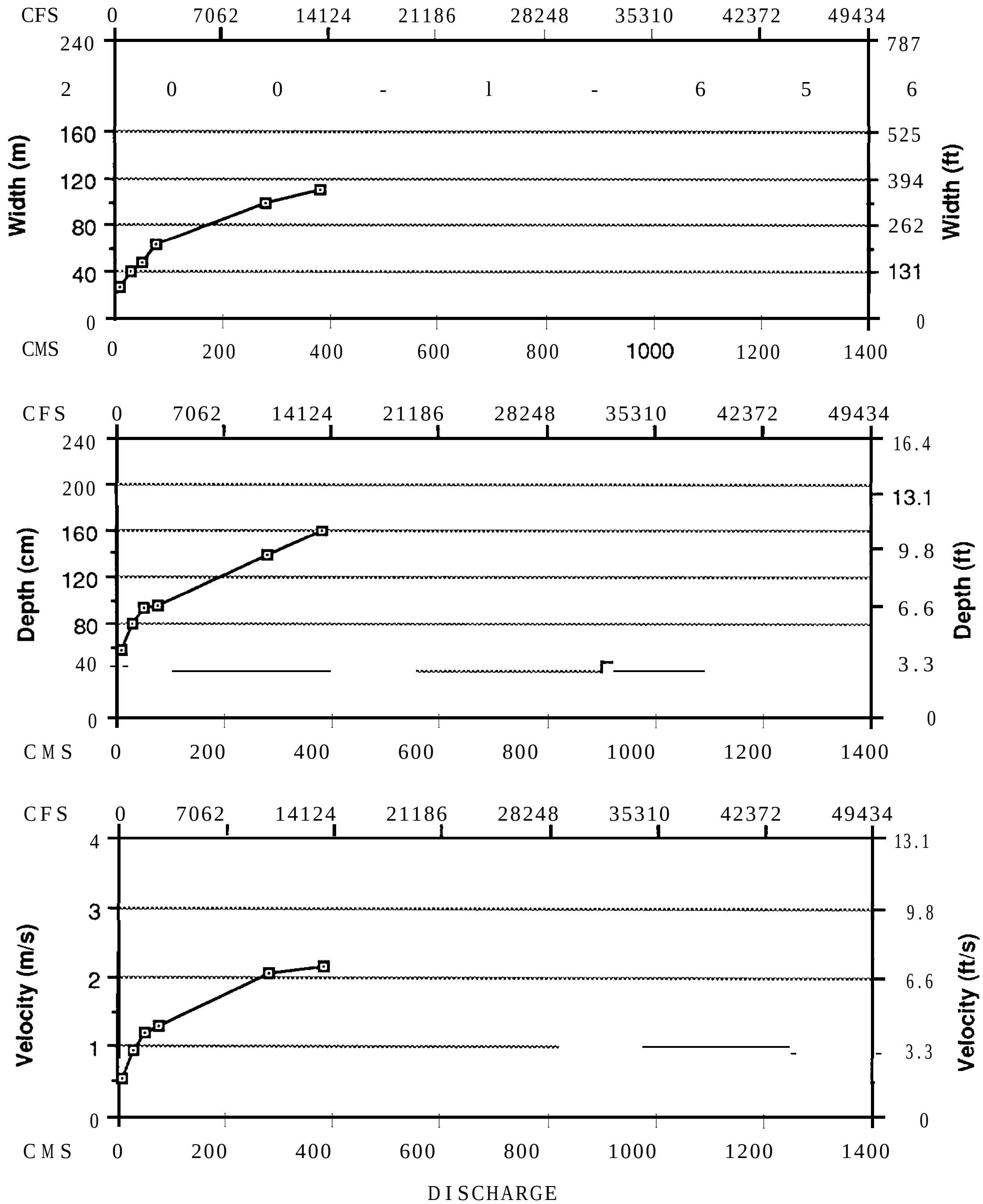

Figure B18. Hydraulicgeometryfor Upper Potlatch Transect 4.

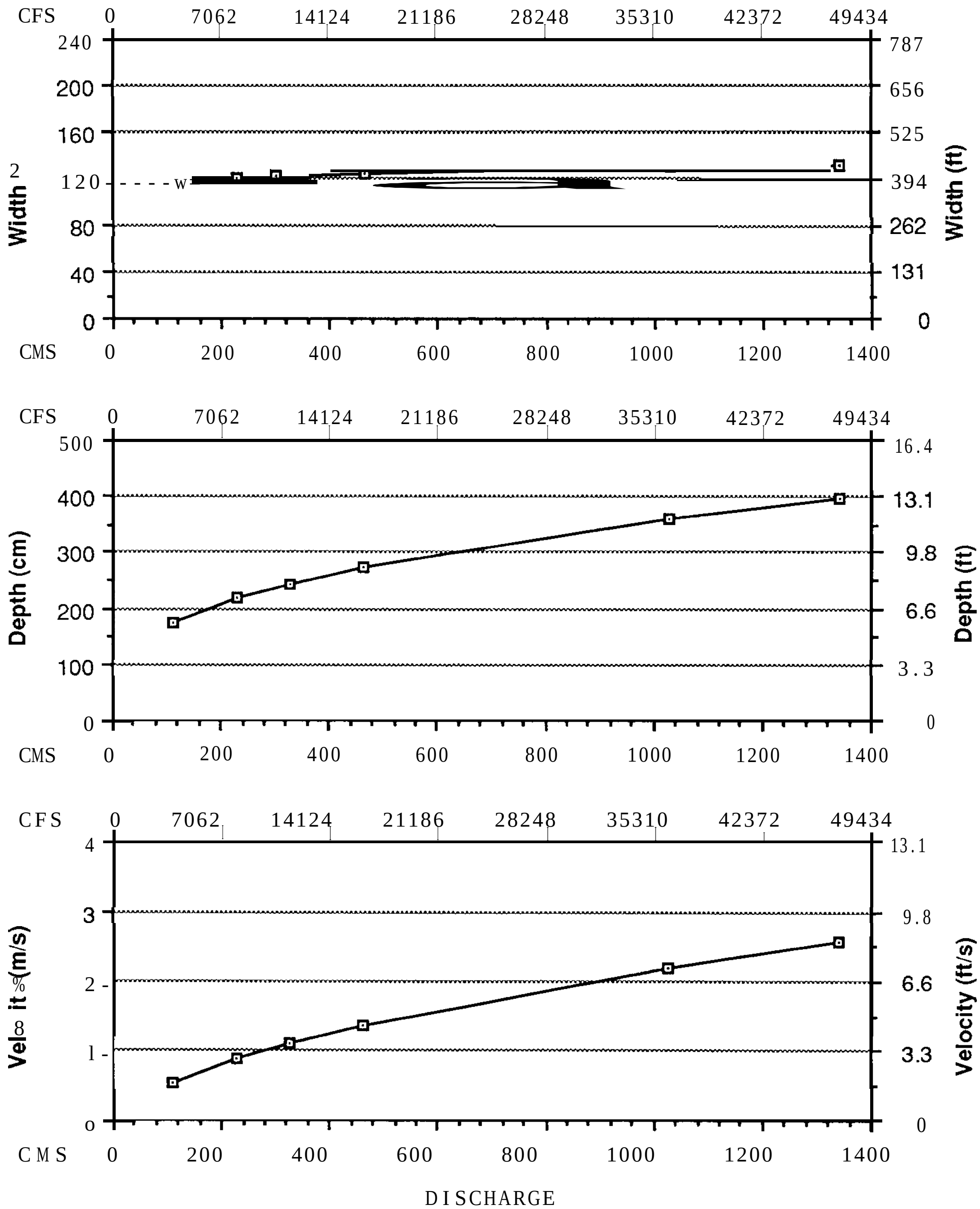

Figure B19. Hydraulic geometry for BedrockTransect2.

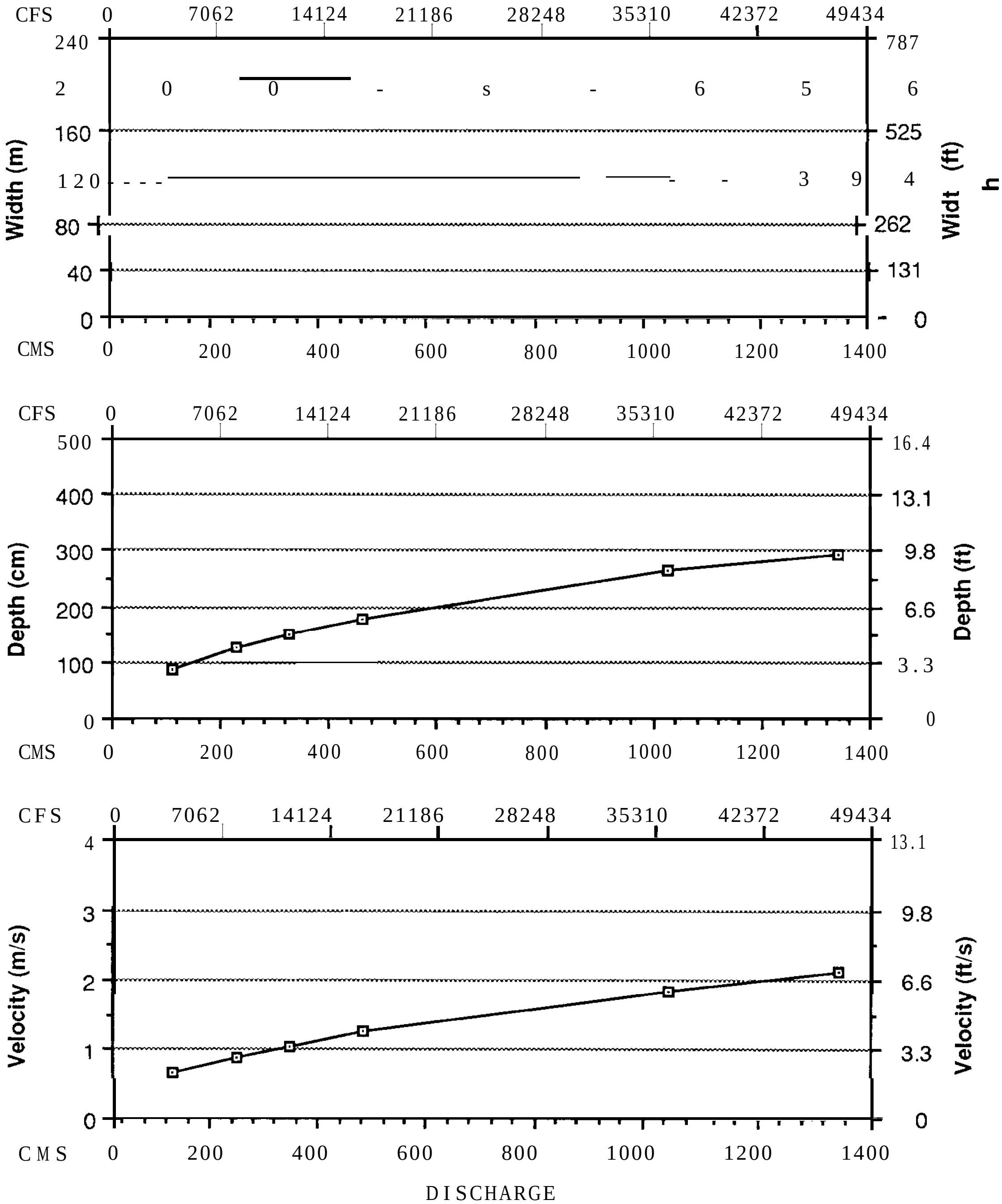

Figure 820. Hydraulic geometry for BedrockTransect3.

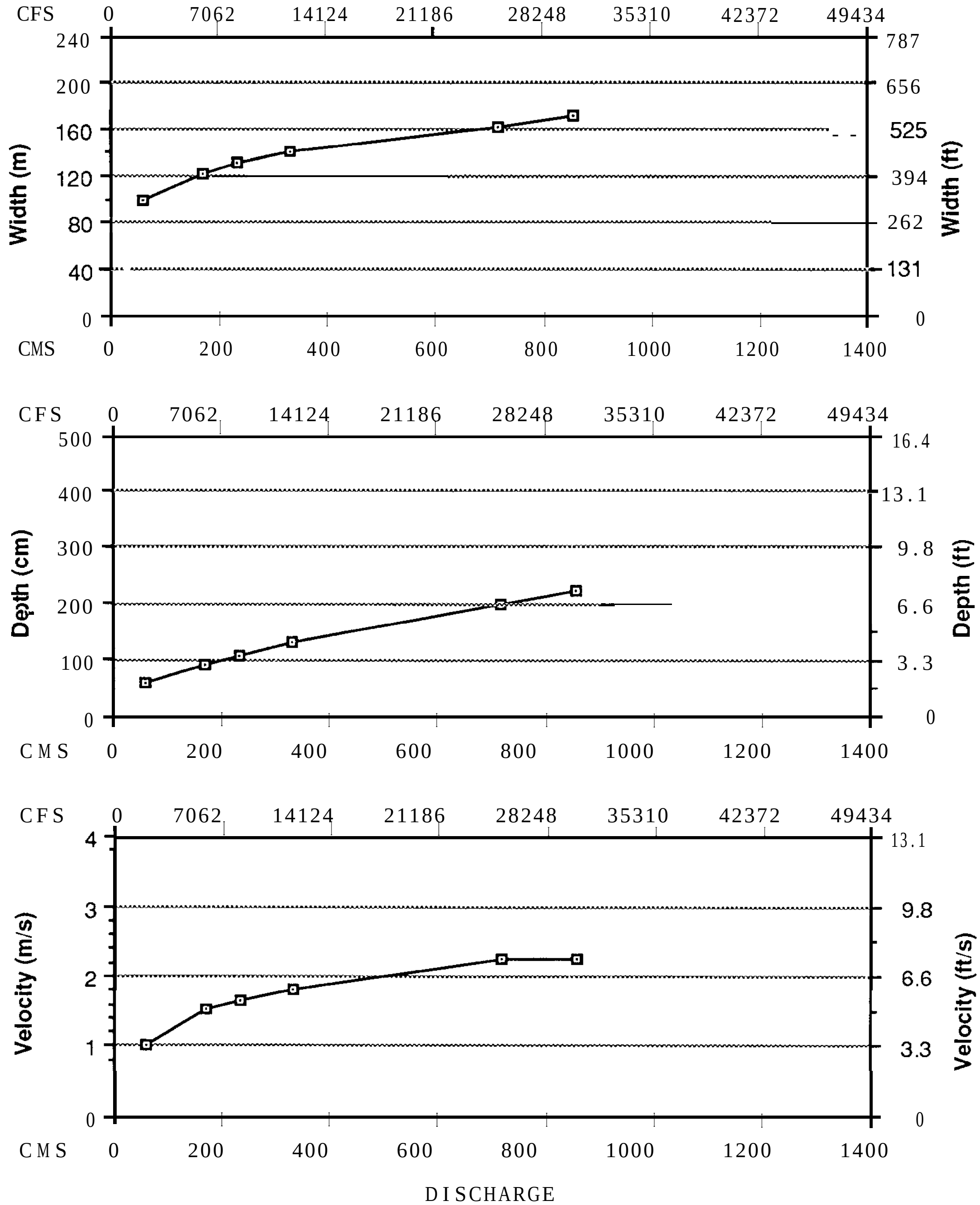

Figure B21. Hydraulic geometry for Bedrock Transect 4.

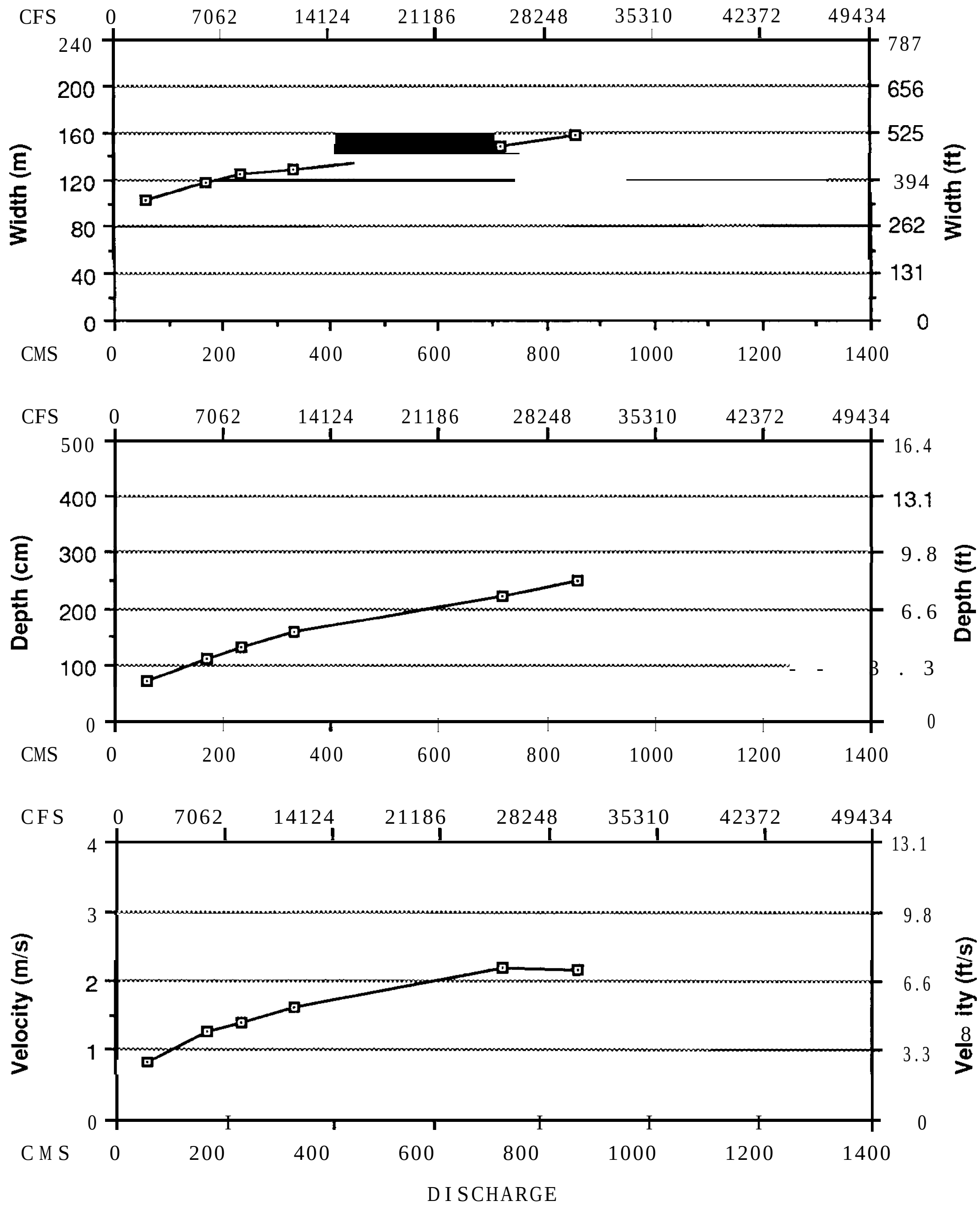

Figure B22. Hydraulic geometry for BedrockTransect5.

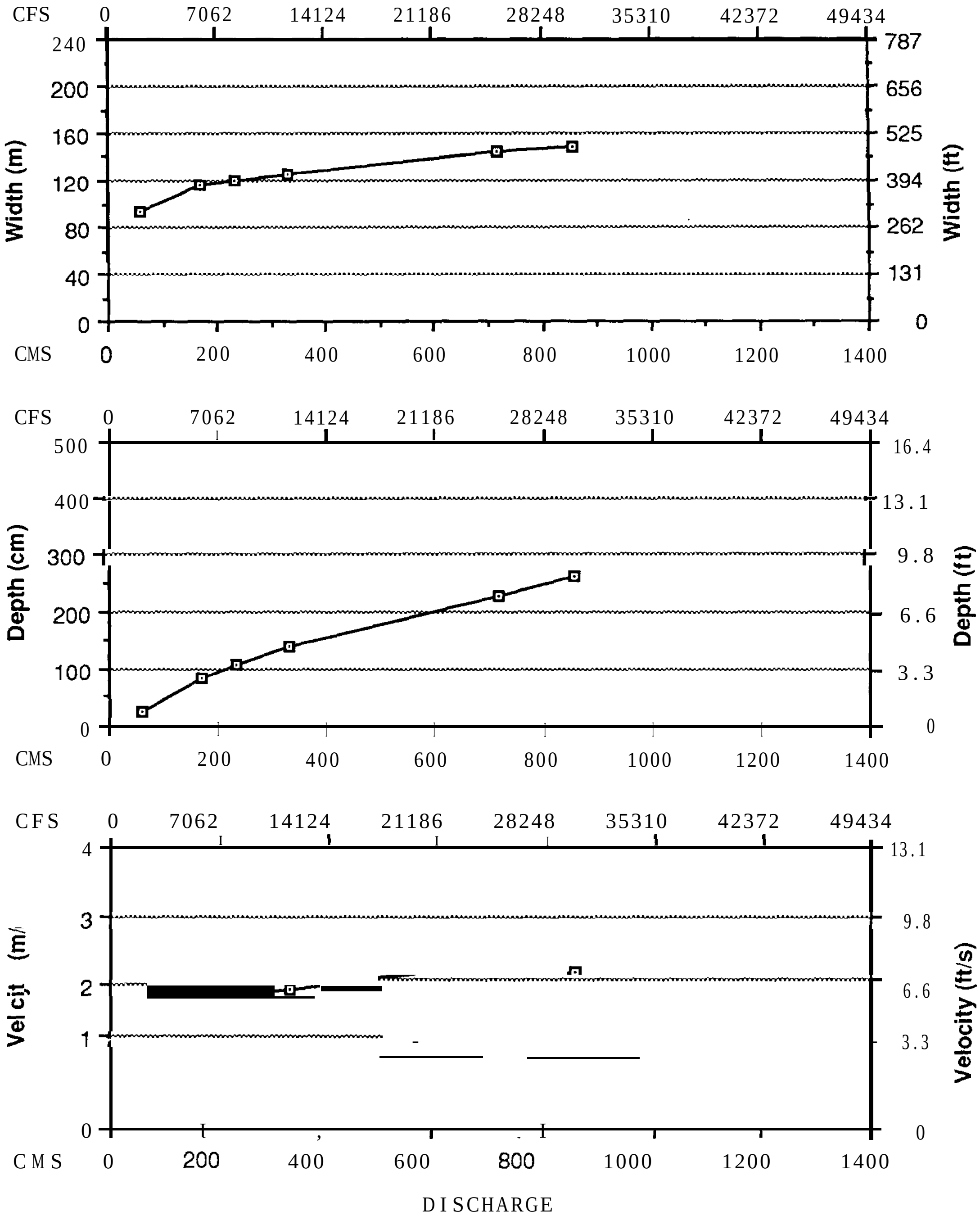

Figure B23. Hydraulicgeometry for BedrockTransect6.

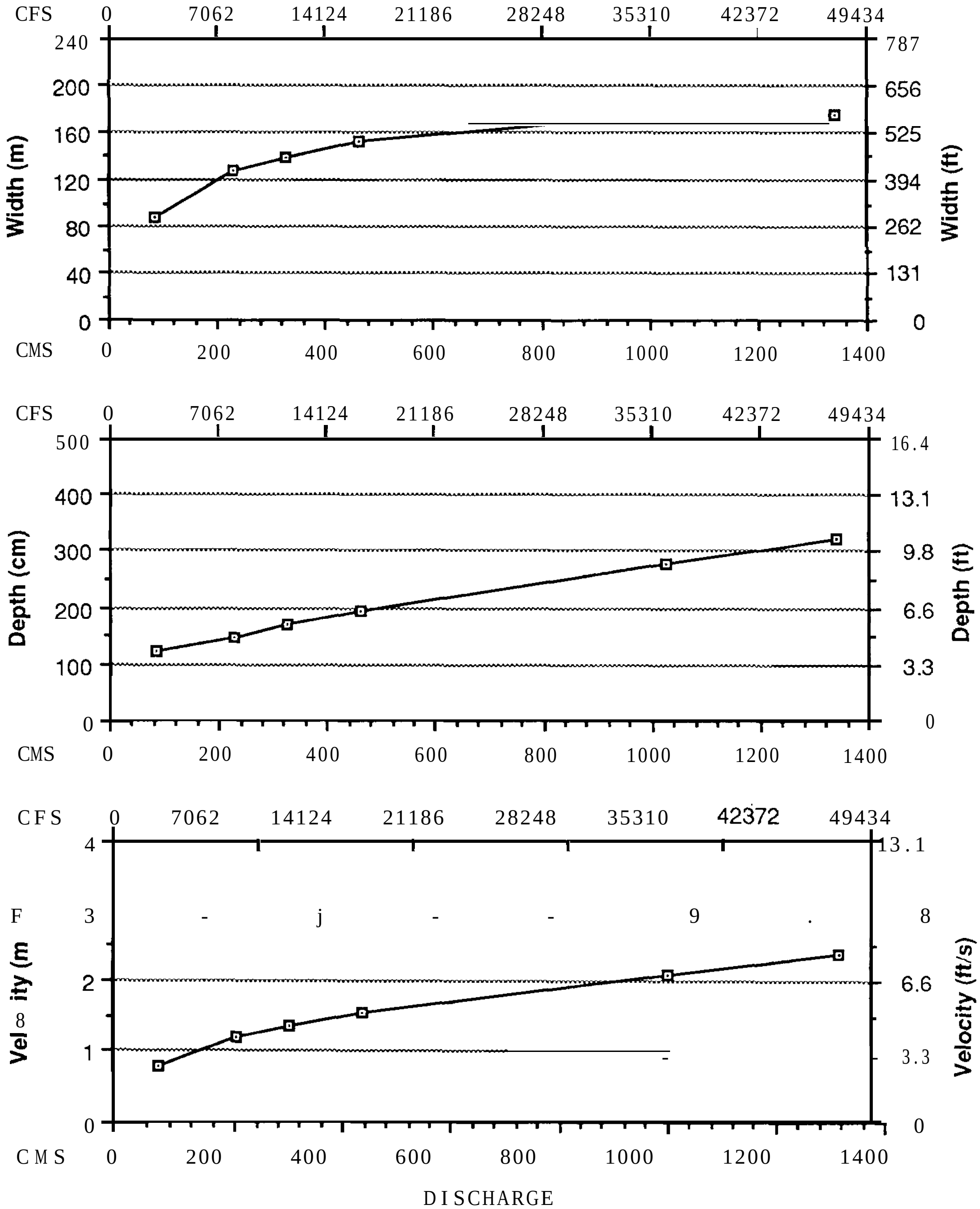

Figure B24. Hydraulicgeometry for Bedrock Transect 7.

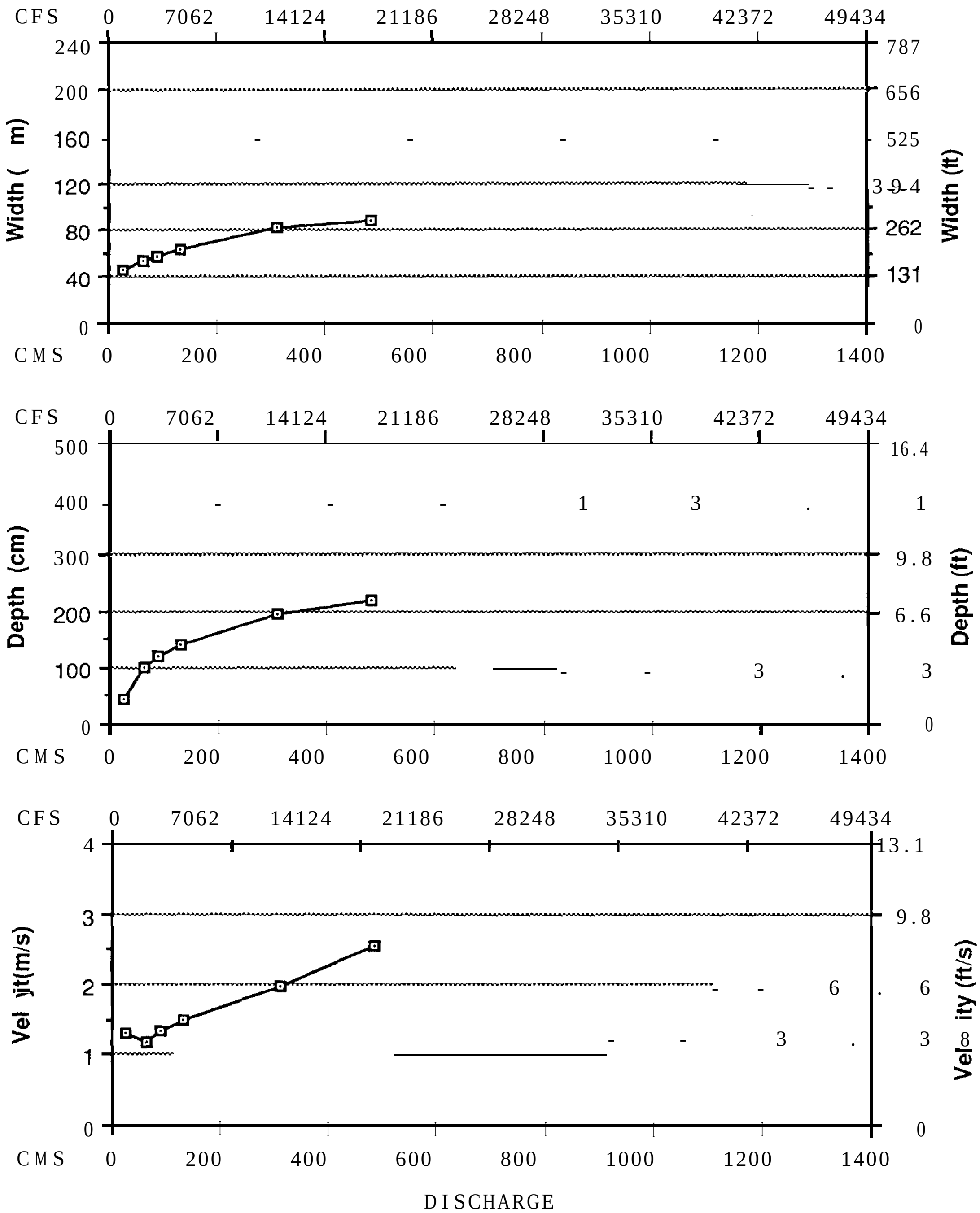

Figure 825. Hydraulic geometry for Bedrock Transect 8.

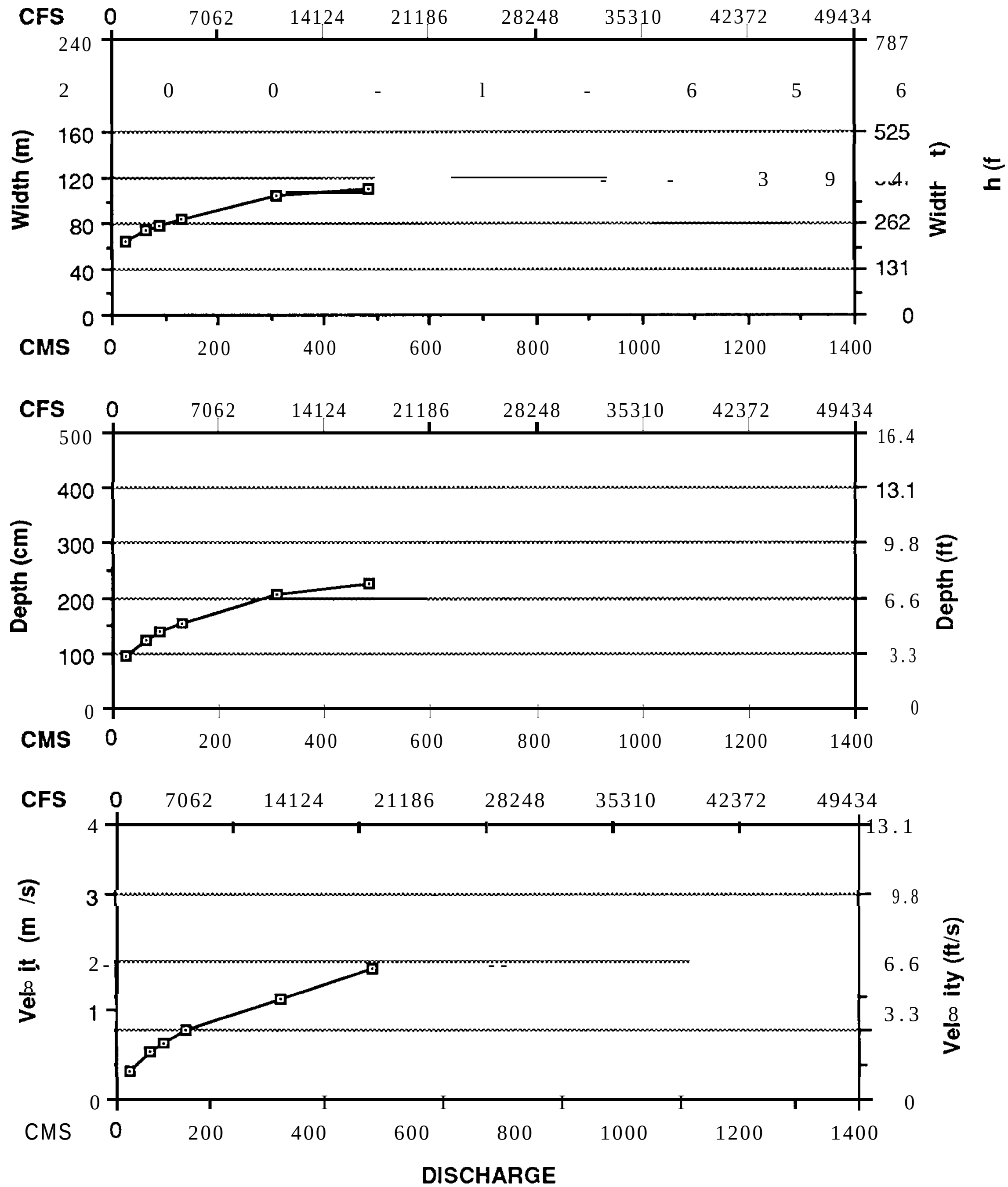

Figure B26. Hydraulicgeometry for Bedrock Transect 9.

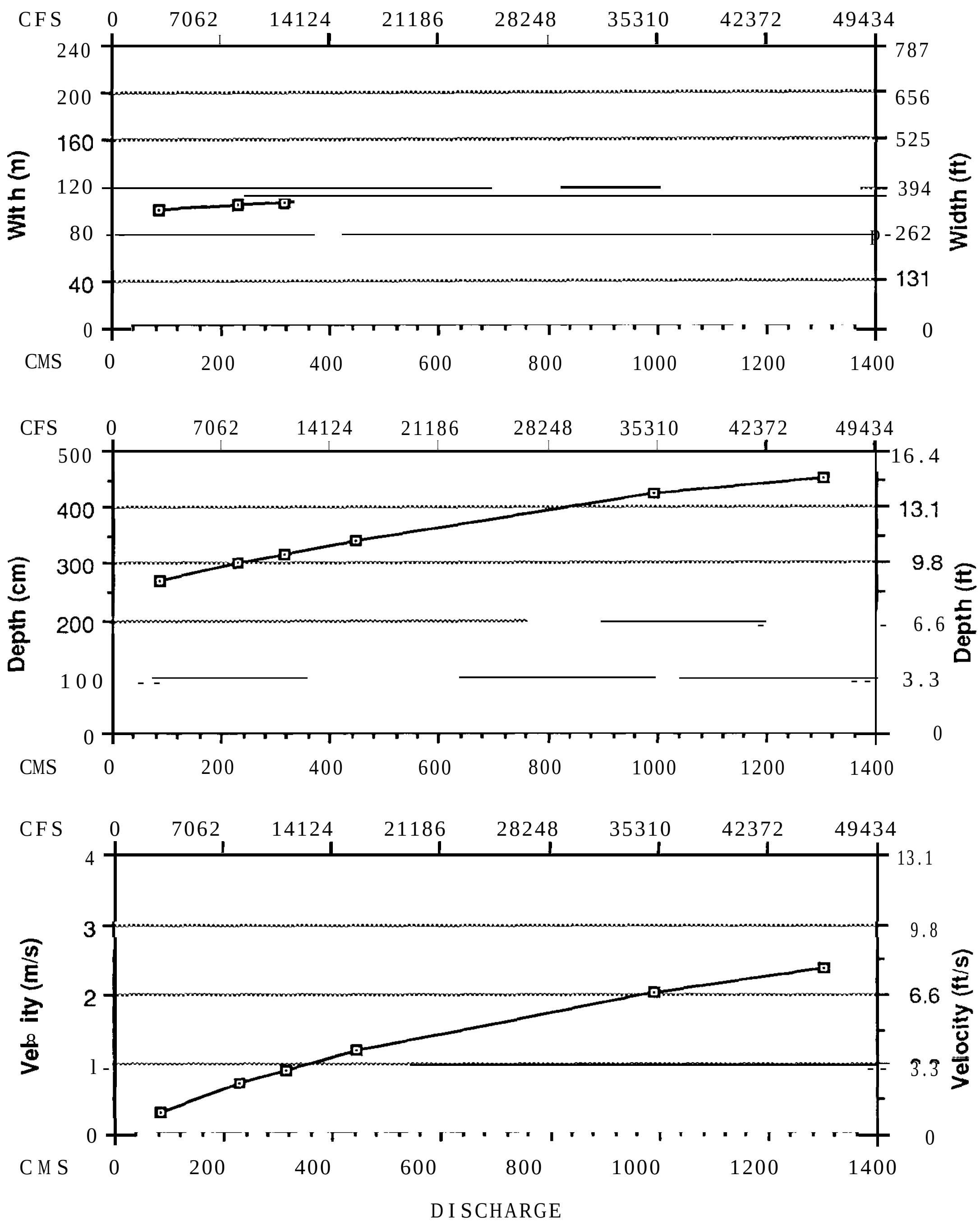

Figure B27. Hydraulic geometry for Big Canyon Transect 1.

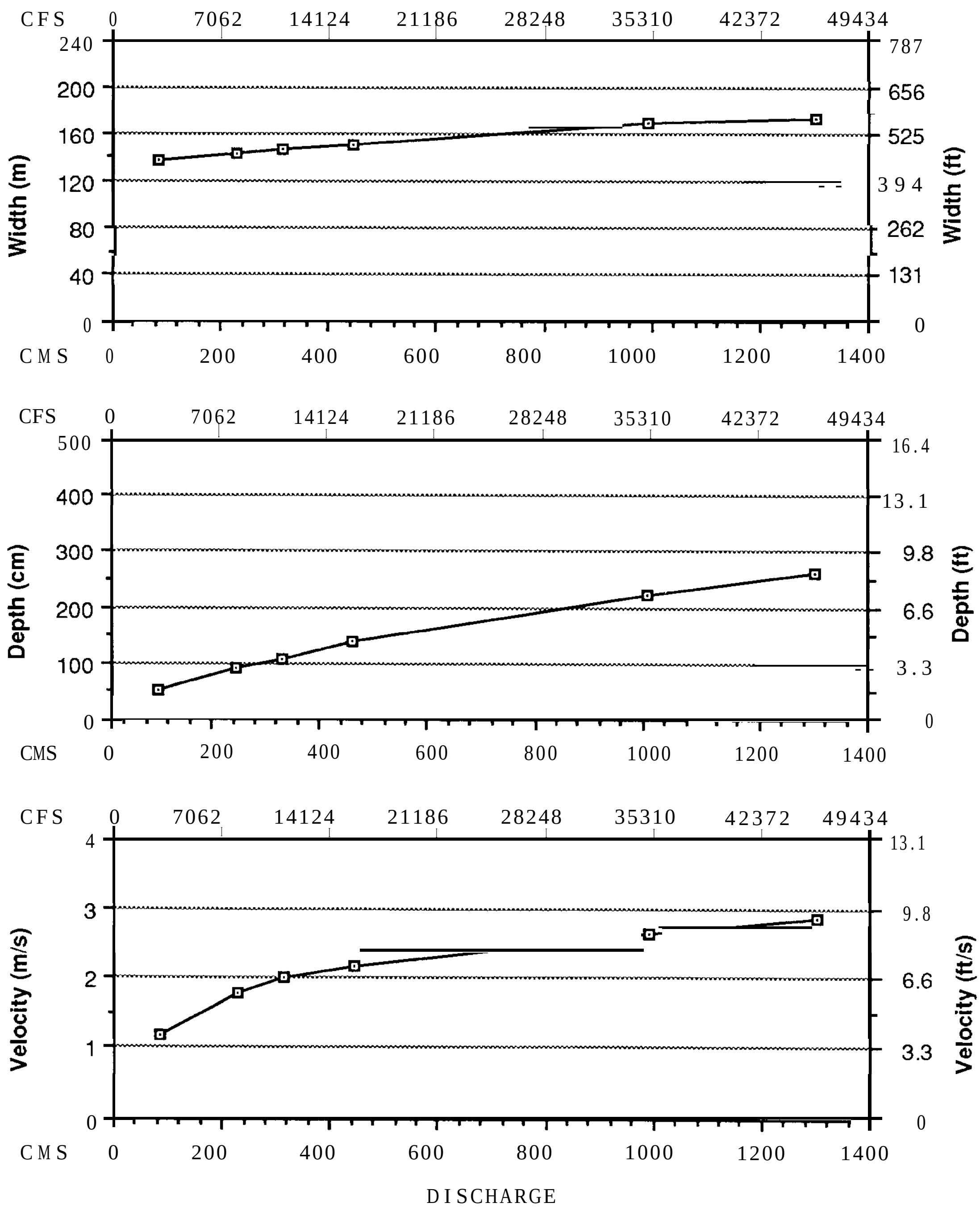

Figure B28. Hydraulicgeometry for Big Canyon Transect 2.

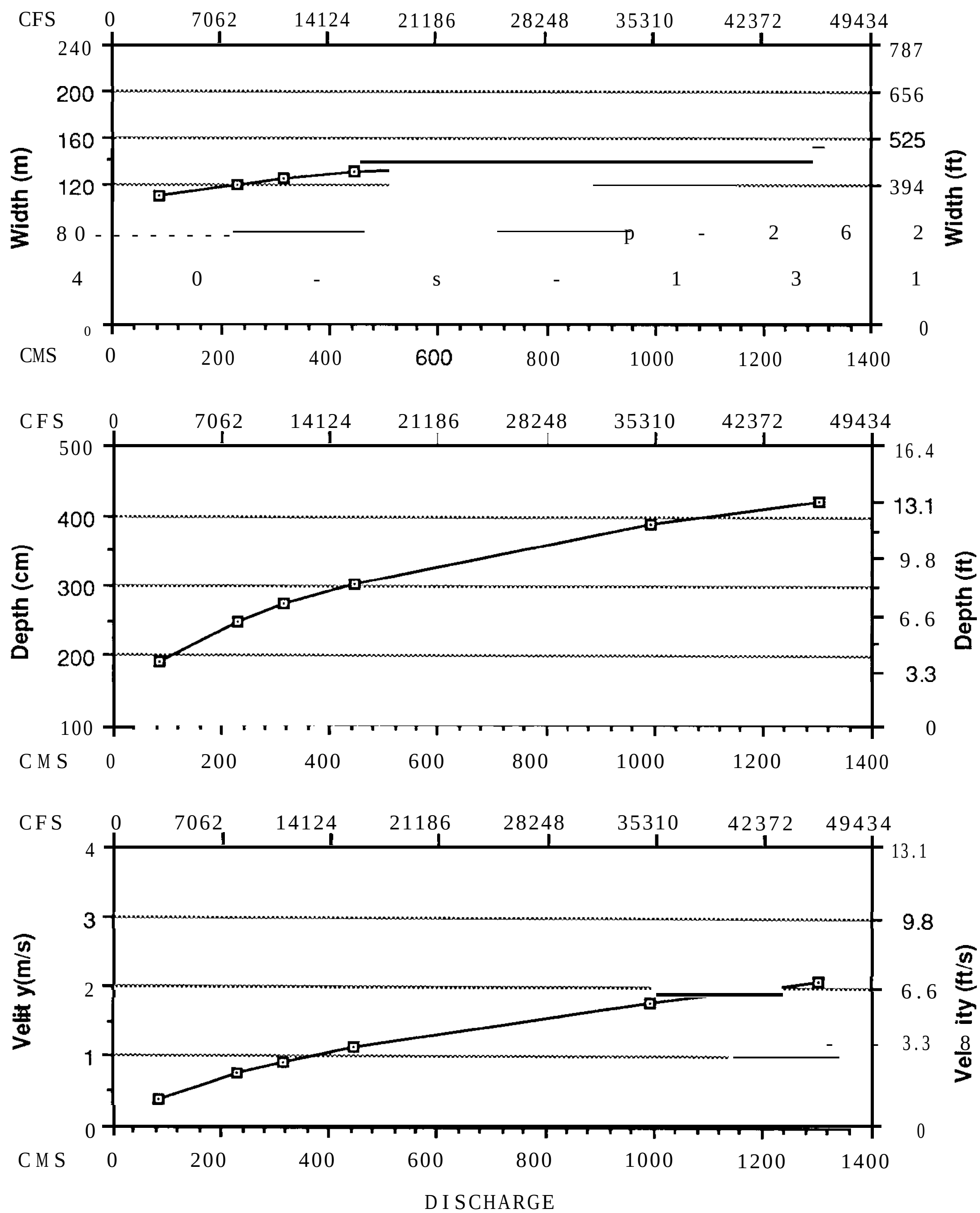

Figure 829. Hydraulicgeometry for Big Canyon Transect 3.

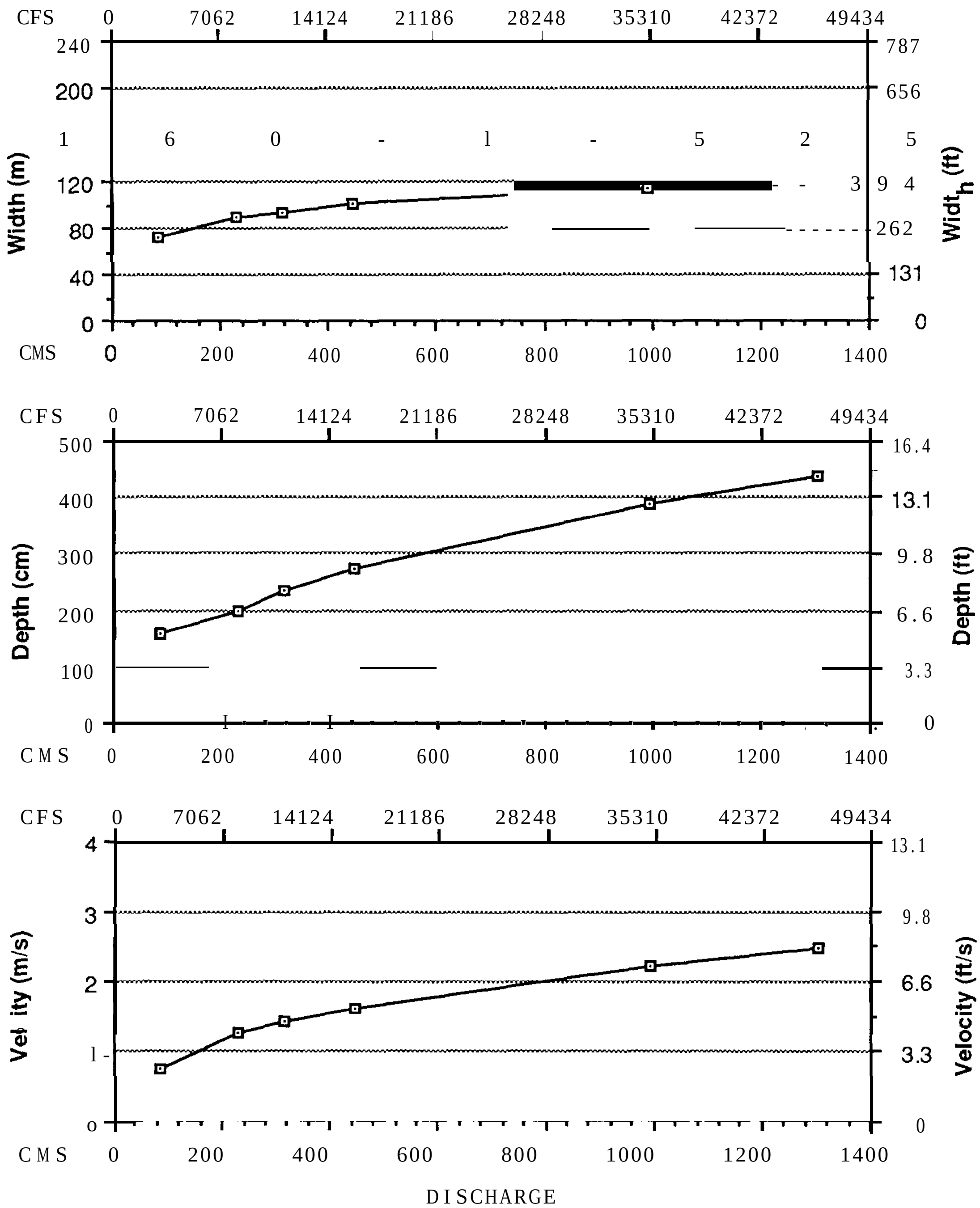

Figure 830. Hydraulic geometry for North Fork Transect 2.

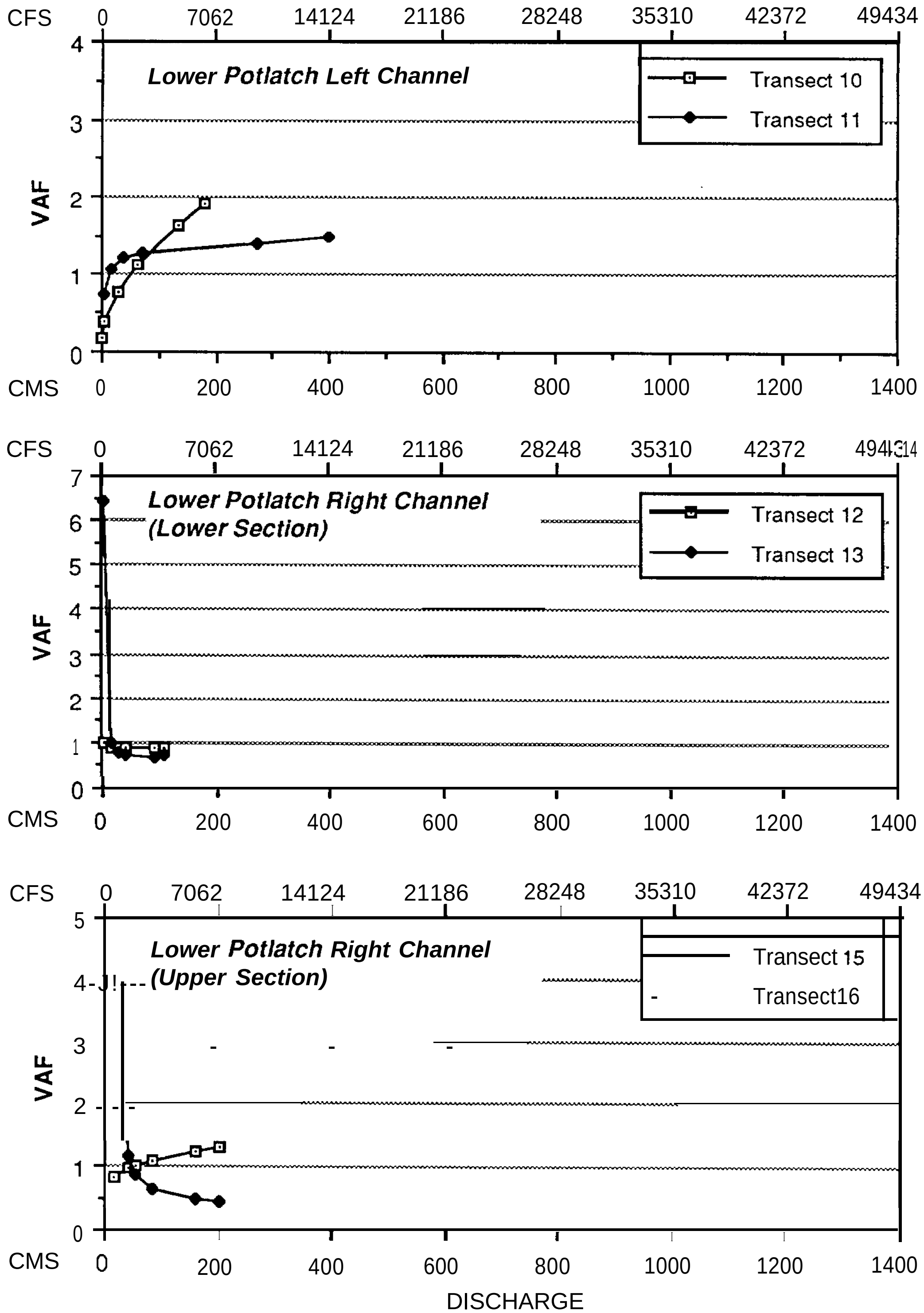

Figure B31. Velocity Adjustment Factor plots by discharge for Lower Potlatch Transects.

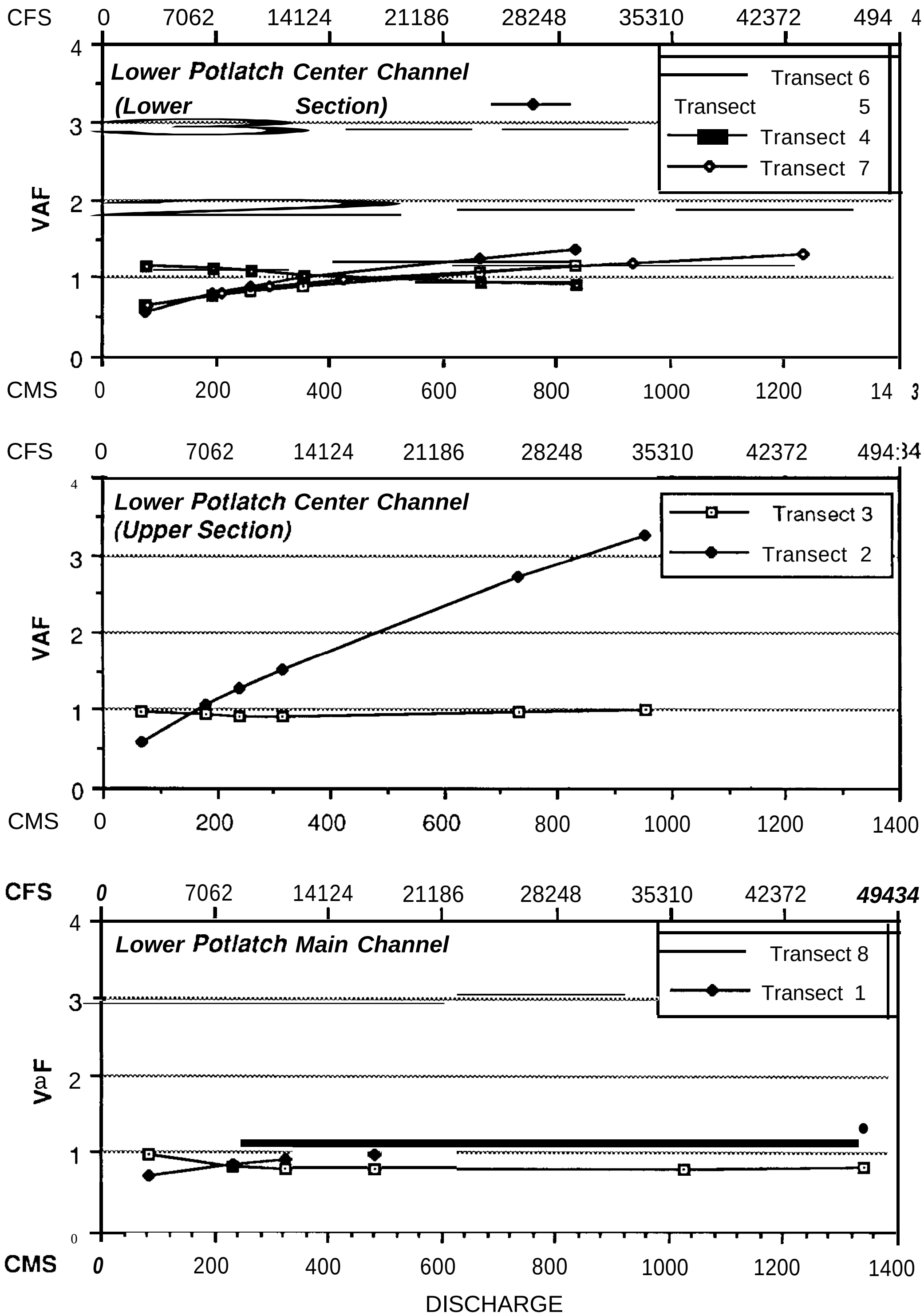

Figure B31 (cont). Velocity Adjustment Factor plots by discharge for Lower Potlatch Transects.

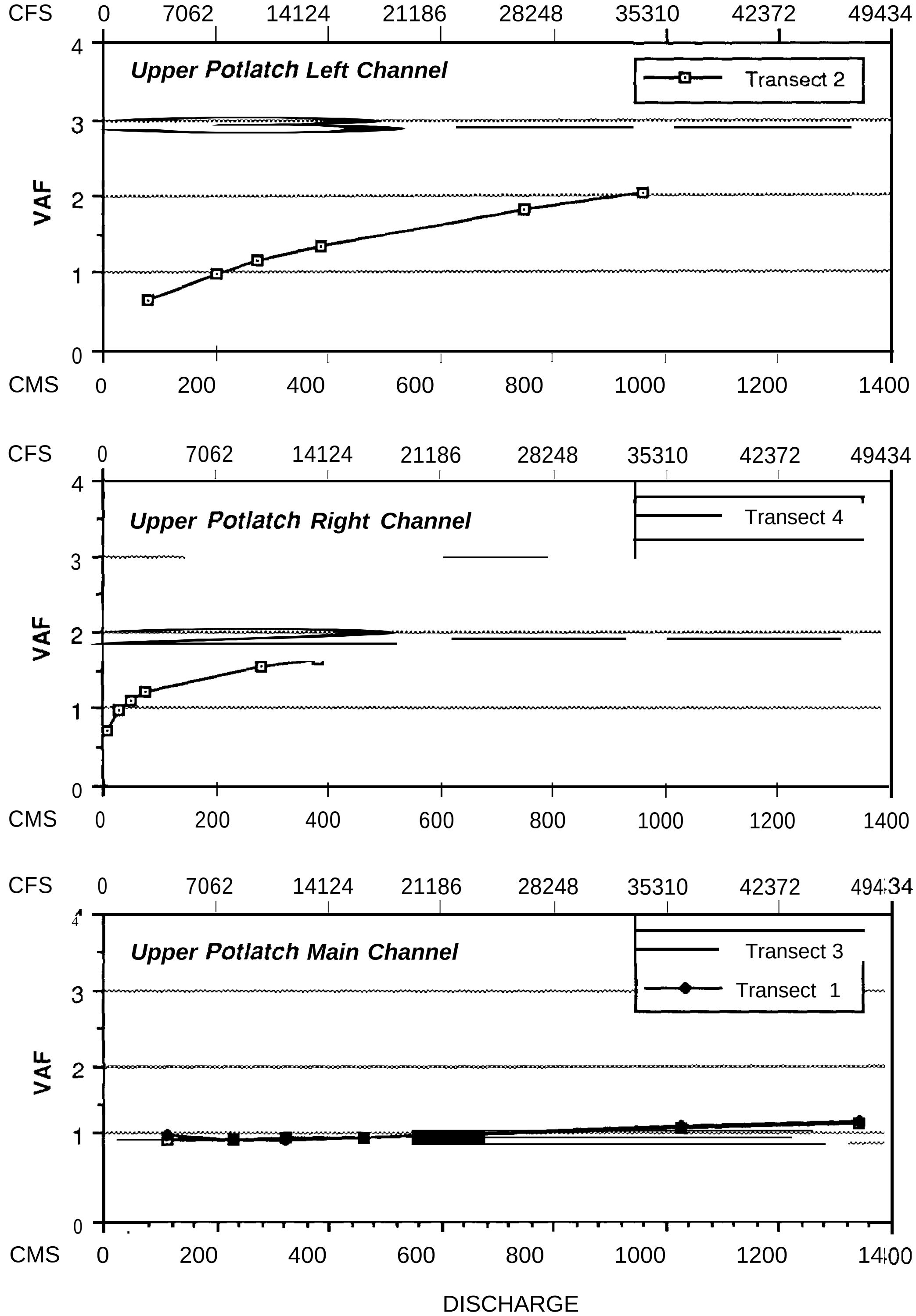

Figure B32. Velocity Adjustment Factor plots by discharge for Upper Potlatch Transects.

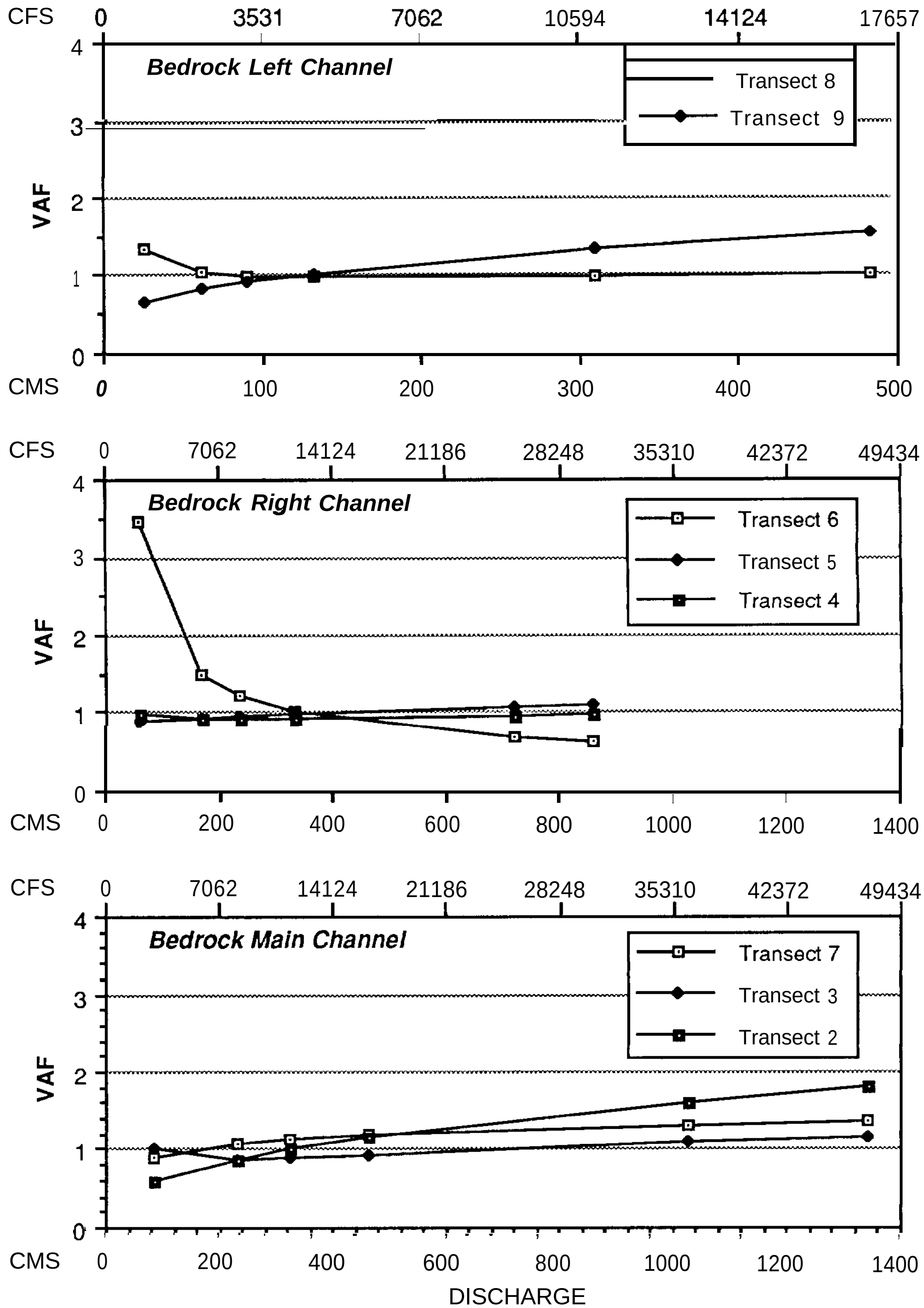

Figure B33. Velocity Adjustment Factor plots by discharge for Bedrock Transects.

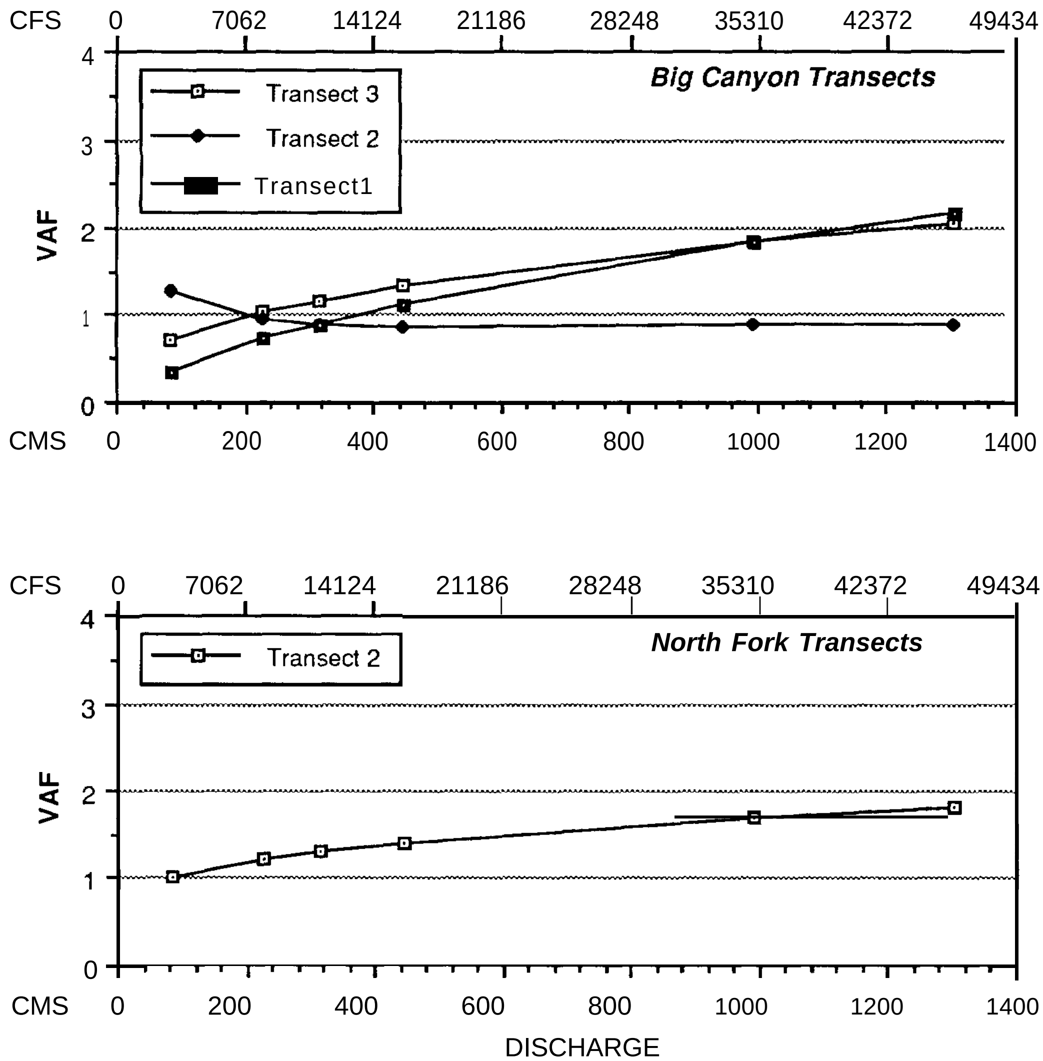

Figure B34. Velocity Adjustment Factor plots by discharge for Big Canyon and North Fork Transects.

APPENDIX C
Direct Observation

Originally, we had planned to sample 366 m (400 yds) of main channel run at the Potlatch River study site (Table C2). However, prior to refining our observation skills we were unable to effectively sample this distance. We used our best field judgement and reduced the lane length to 183 m. Secondly, we found that the channel of a randomly chosen location for an observation lane in a run was in disequilibrium. Again we made a decision in the field to move the lane downriver and across the channel into considerably more representative run habitat (Figure C5). Also, when re-measuring a vandalized lane in the Bedrock Creek study site we misread our field notes. Subsequently, inside bend habitat was overrepresented by 55 m (60 yds) at the Bedrock Creek study site (Table C2 and Figure C6). The same problem occurred at the Big Canyon Creek study site where during re-measurement we under represented rapid riffle habitat by 72 m (79 yds)(Table C2 and Figure C7).

During data analysis we also found an inconsistency in sampling effort distribution between sites. Often in population analysis all subunits of a system are sampled equally regardless of their contribution to area of the system. This misrepresentation is then corrected prior to any statistical analysis of the data by weighting the observations using multiplicative correction factors. We had hoped to avoid this data weighting procedure by weighting our effort between habitat types according to area by varying observation lane lengths so that the most abundant habitat types received the most sampling effort. We also provided for the option to pool data between sites without weighting by calculating all lane lengths at each site in proportion to the length of the lane representing the most abundant habitat type of all sites (Tables Cl and C2). In review, the single most abundant habitat of measured at all the sites was represented with an arbitrarily established distance of 366 m (1200 ft). The remaining lane lengths at all sites were determined by dividing the area of the habitat to be represented by the area of this single most abundant habitat. We then multiplied 366 m by this fraction. This technique would have been successful if study site area was indeed proportional to segment area. However, as described earlier we relocated a transect within the Bedrock Creek study site to consolidate hydraulic transects. We then measured site area from the uppermost hydraulic transect to the lower most transect. Consequently, the largest segment was represented by the smallest site which received the least amount of sampling effort (Tables Cl and C2). These sampling errors will be remedied in 1990 by re-measuring direct observation lanes and applying multiplicative correction factors to 1989 data.

Table Cl. Habitat type area for study sites within the Potlatch, Bedrock Creek, and North Fork segments.

Site[a]	Habitat type	Area (HA)	Site area (HA)
PL	Run	49.8	91.0
PL	Side channel	17.4	
PL	Deep run	16.4	
PL	Intermittent side channel	7.4	
BDR	Run	20.8	48.8
BDR	Side channel	7.7	
BDR	Rapid run	5.8	
BDR	Inside bend run	5.1	
BDR	Outside bend run	3.5	
BDR	Rapid riffle	3.2	
BDR	Intermittent side channel	2.7	
BGC	Rapid riffle	23.0	60.2
BGC	Inside bend pool	14.2	
BGC	Pool	13.4	
BGC	Outside bend pool	9.6	
NF	Rapid riffle	14.6	27.7
NF	Pool	10.9	
NF	Rapid run	2.2	

[a] Habitat area calculated by combining upper and lower Potlatch River site area.

Table C2. Lane assignments, length, and total combined lengths by site and habitat type.

Site	Habitat type	Percent of habitat composition at the site	Lane length (m)	Total combined length (m)
PL	Run	55	366	667
PL	Deep run	18	120	
PL	Side channel	19	127	
PL	Intermittent side channel	8	54	
BDR	Run	43	152	288
BDR	Side channel	15	57	
BDR	Rapid run	12	42	
BDR	Inside bend run	10	37	
BDR	Outside bend run	7		
BDR	Rapid riffle	7		
BDR	Intermittent side channel	6		
BGC	Rapid riffle	38	168	440
BGC	Inside bend pool	24	104	
BGC	Pool	22	98	
BGC	Outside bend pool	16	70	
NF	Rapid riffle	52	106	186
NF	Pool	39	80	
NF	Rapid run	8	—	

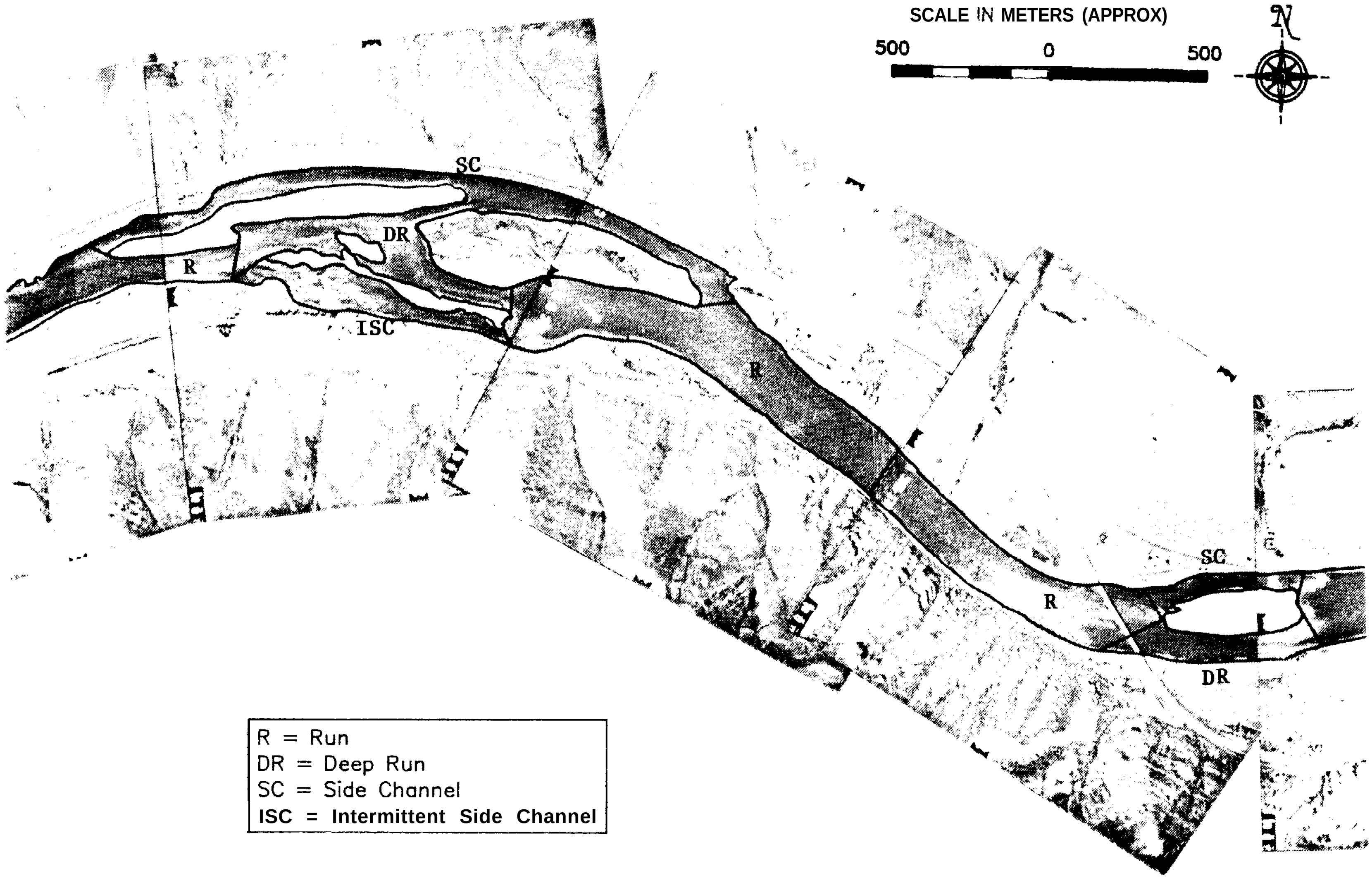

Figure C 1. Mapping strategy used to identify habitat types in the Potlatch River Site for hydraulic cross-section and direct observation lane assignment, lower mainstem Clearwater River (LMCR) project area.

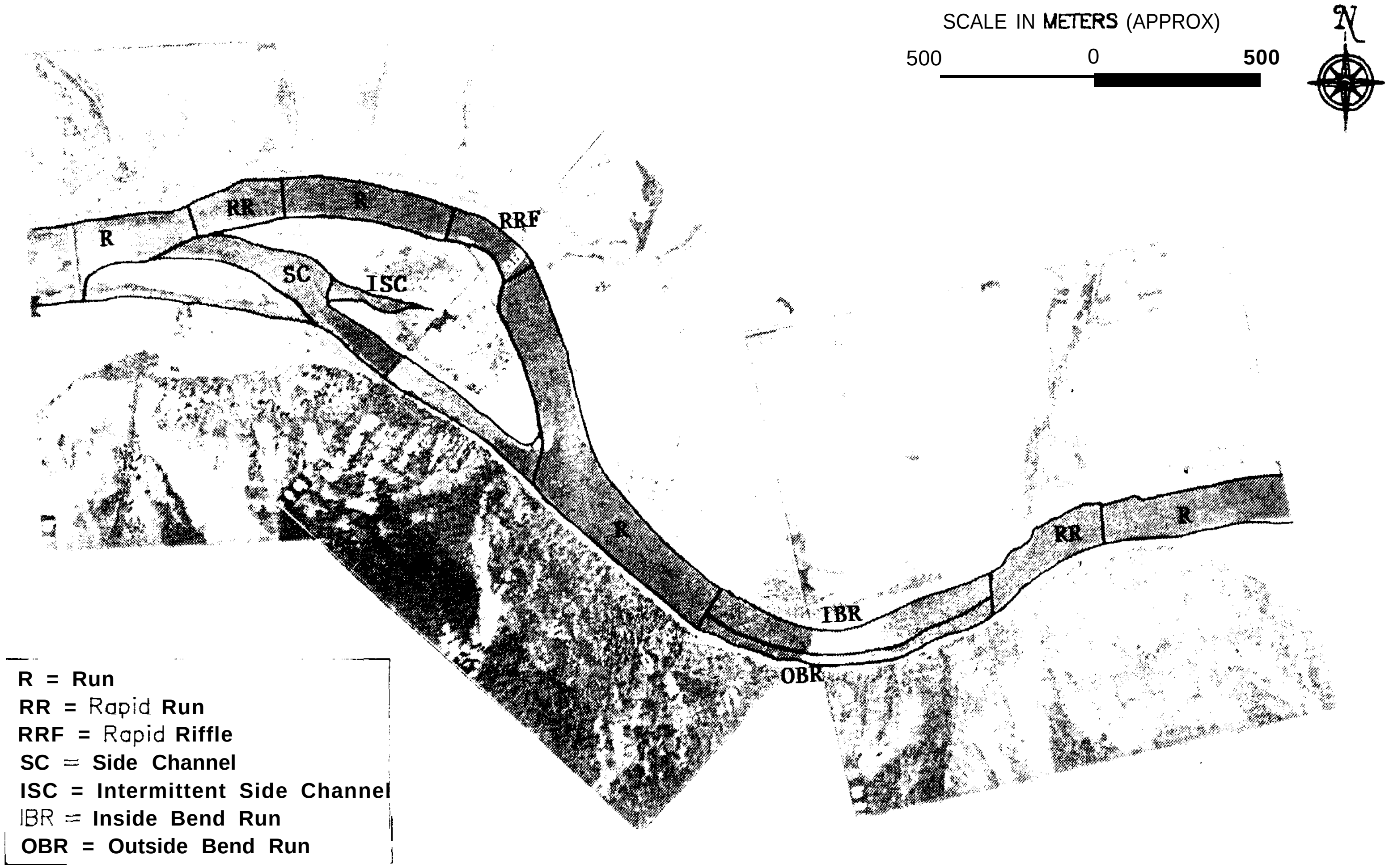

Figure C2. **Mapping strategy used to identify habitat types in the Bedrock Creek Site for hydraulic cross-section and direct observation lane assignment, lower mainstem Clearwater River (LMCR) project area.**

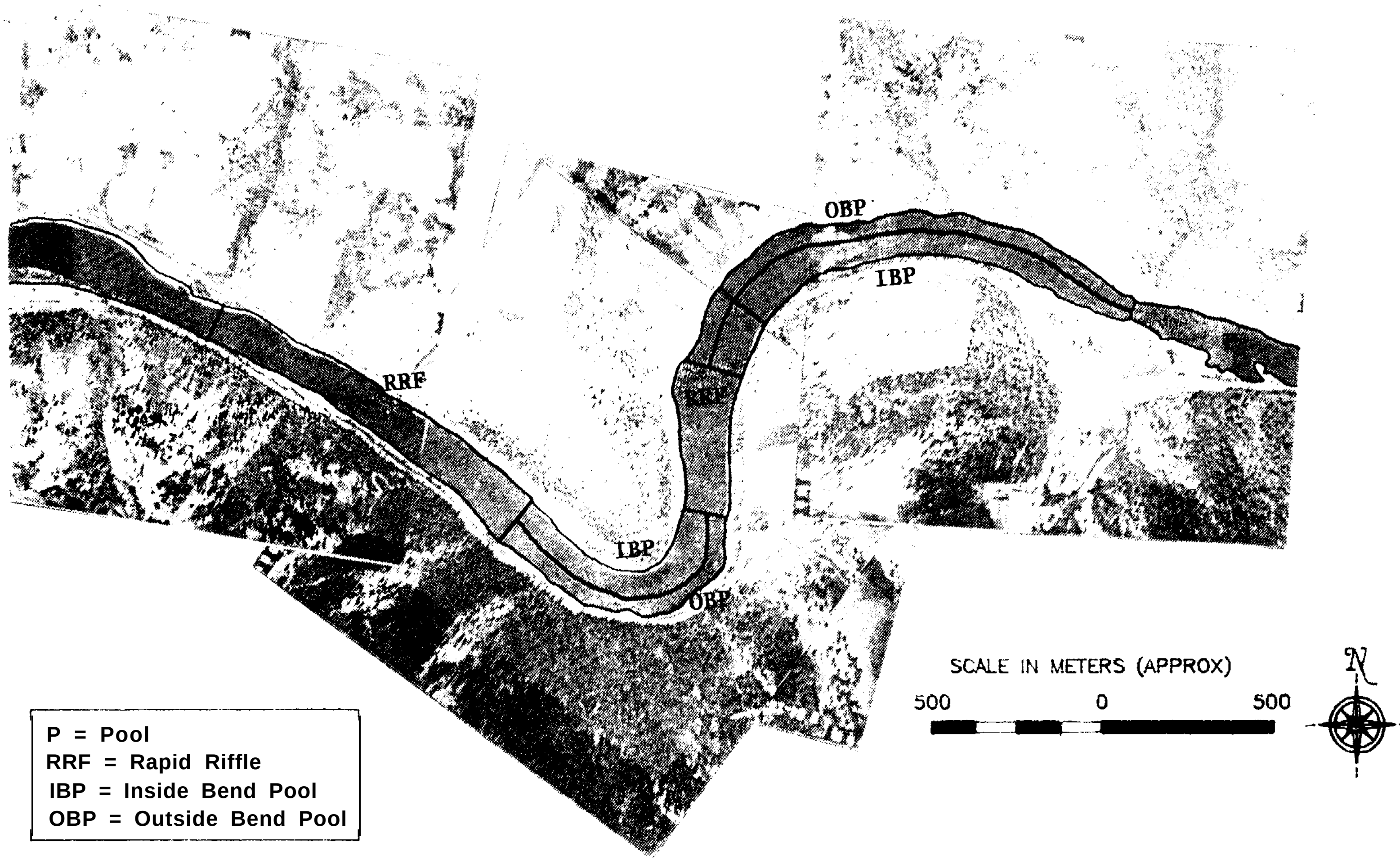

Figure C3. Mapping strategy used to identify habitat types in the Big Canyon Creek Site of the North Fork Segment for hydraulic cross-section and direct observation lane assignment, lower mainstem Clearwater River (LMCR) project area.

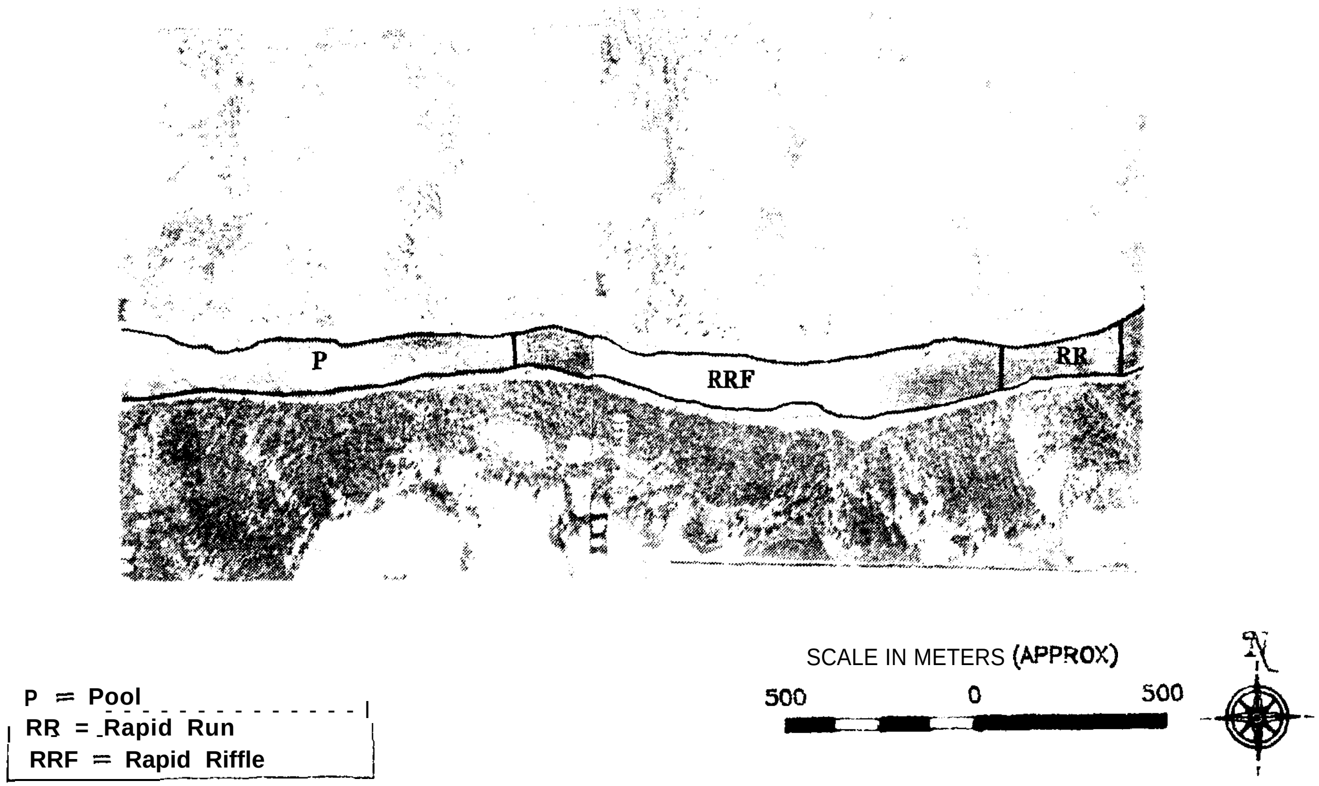

Figure C4. Mapping strategy used to identify habitat types in the North Fork Site of the North Fork Segment for hydraulic cross-section and direct observation lane assignment, lower mainstem Clearwater River (LMCR) project area.

Figure C5. Assignment of direct observation lanes (■) in relation to hydraulic cross-sections (PL#) within the Potlatch River Site of the Potlatch River Segment, lower mainstem Cleat-water River (LMCR) project area.

Figure C6. Assignment of direct observation lanes (■) in relation to hydraulic cross-sections (BDR#) within the Bedrock Creek Site of the Bedrock Creek Segment, lower mainstem Clearwater River (LMCR) project area.

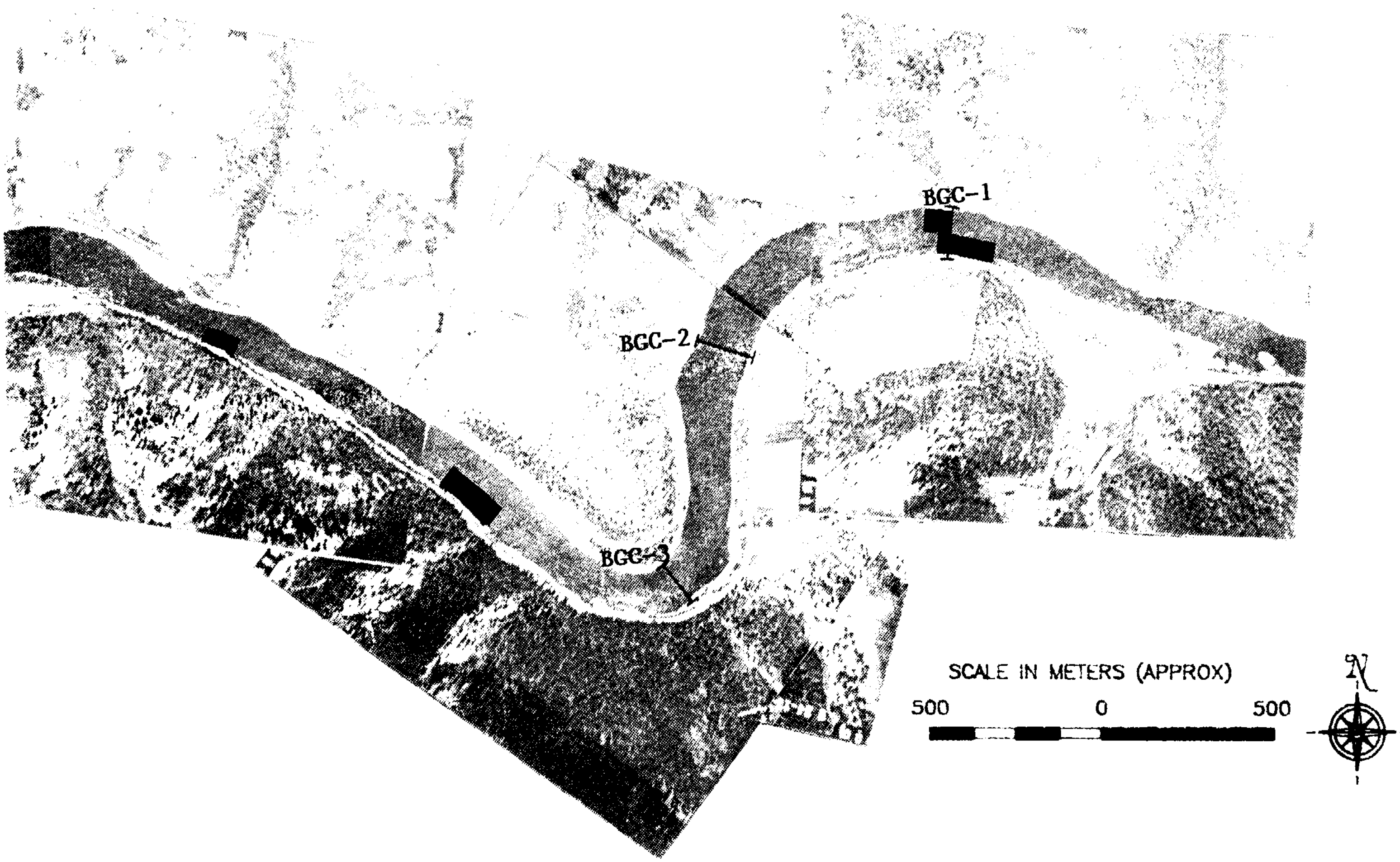

‘igure C7. Assignment of direct observation lanes (▬) in relation to hydraulic cross-sections (BGC#) within the Big Canyon Creek Site of the North Fork Segment, lower mainstem Clearwater River (LMCR) project area.

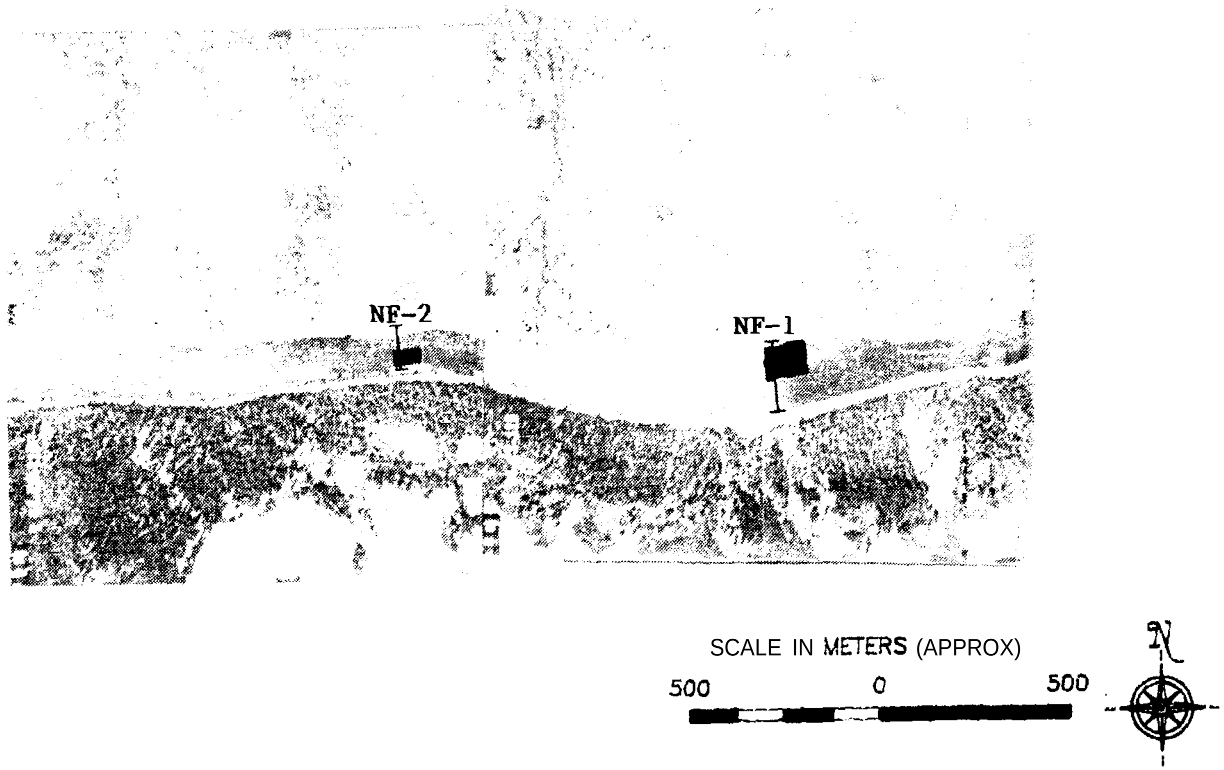

Figure C8. Assignment of direct observation lanes (▬) in relation to hydraulic cross sections (NF#) within the North Fork Site of the North Fork Segment, lower mainstem Clearwater River (LMCR) project area.

Mainstem Rearing of Wild Rainbow\Steelhead Parr Produced in the Tributaries of the LMCR:

Total lengths of age I+ and II + wild parr varied from 124 to 187 mm and 163 to 191 mm, respectively (Table C3). Total lengths of age I+ and II+ hatchery smolts ranged 115 to 200 mm and 58 to 207 mm, respectively (Table C3). No age III+ were sampled. A few young-of-the-year wild rainbow/steelhead trout were sampled throughout our study section but due to our objective of panjet marking only age I+ fish these fish were only sampled for a positive identification.

Most parr and smolts were 110 to 210 mm long (Figure C9). Seventy percent of the smolts were age I+ and 30 percent were age II+. Eighty-one percent of the parr were age I+ and 19 percent were age II+ (Figure C10).

Notably, five juvenile chinook salmon were sampled in a pool just above the mouth of Bedrock Creek but only 2 representative fish (60 and 63 mm) were collected for identification.

In summary we collected and measured a total of 93 parr and 49 smolts from Bedrock Creek. We never observed these marked fish in the LMCR during direct observation work because of this inadequate sample size. However, as mentioned we used this data to subdivide wild rainbow steelhead into age 0+ and I+ categories based on fish size. Age 0+ were those fish less than 127 mm (5 in) and Age I+ were those greater than 127 mm but less than 200 mm (8 in).

Table C3. Length versus number of annuli for wild rainbow/steelhead parr and hatchery steelhead smolts sampled in Bedrock Creek, June 1989.

Parr		Smolts	
length (mm)	number of annuli	length (mm)	number of annuli
63	0	115	1
123	1	123	1
124	1	123	1
128	1	128	1
133	1	132	1
134	1	135	1
136	1	138	1
143	1	140	1
146	1	143	1
154	1	146	1
156	1	148	1
160	1	156	1
162	1	158	2
163	2	164	1
163	1	167	2
164	1	170	2
165	2	171	2
167	1	172	2
168	1	185	1
175	1	186	1
177	1	195	2
185	2	207	2
187	1	209	1
191	2		

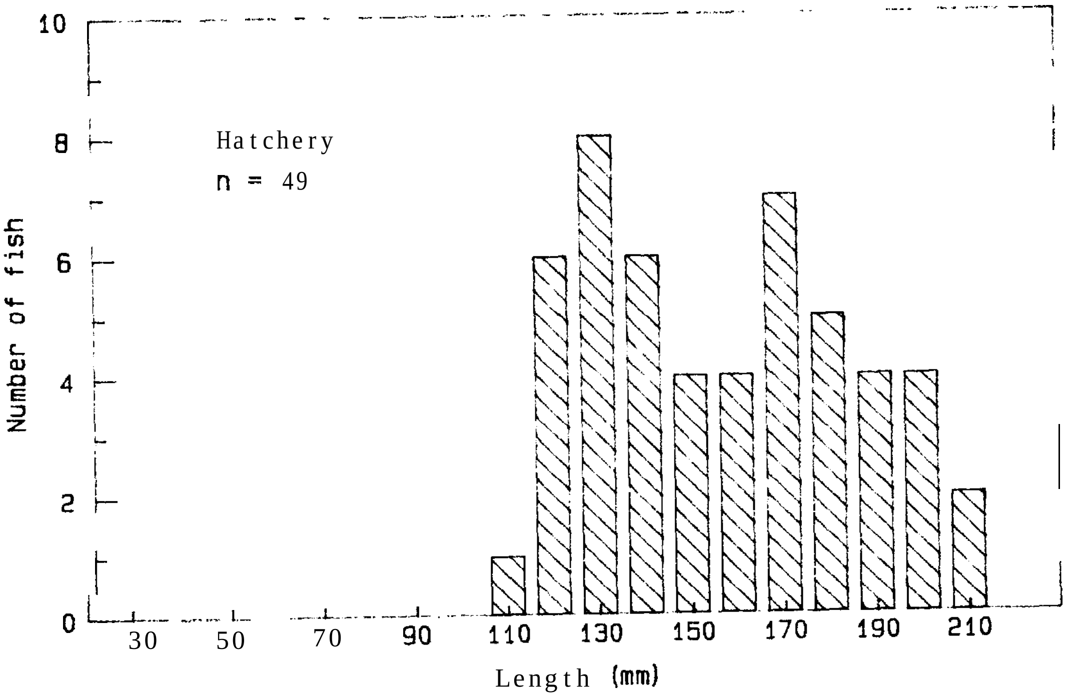

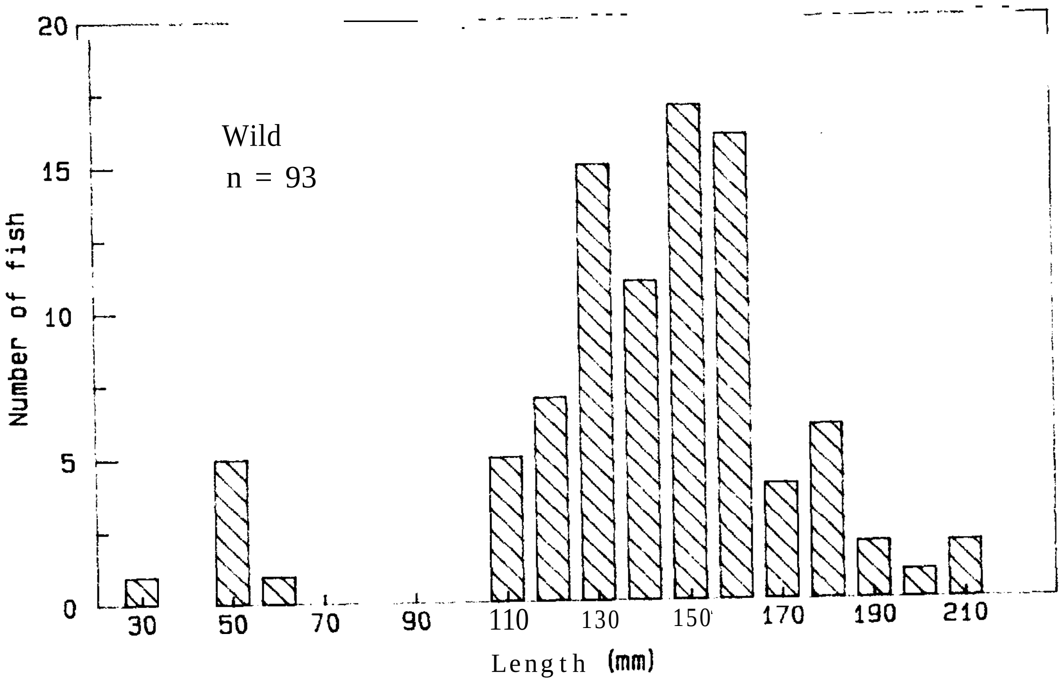

Figure C9. Length frequency distribution of hatchery and wild rainbow/ steelhead trout sampled from Bedrock Creek Idaho during June, 1989.

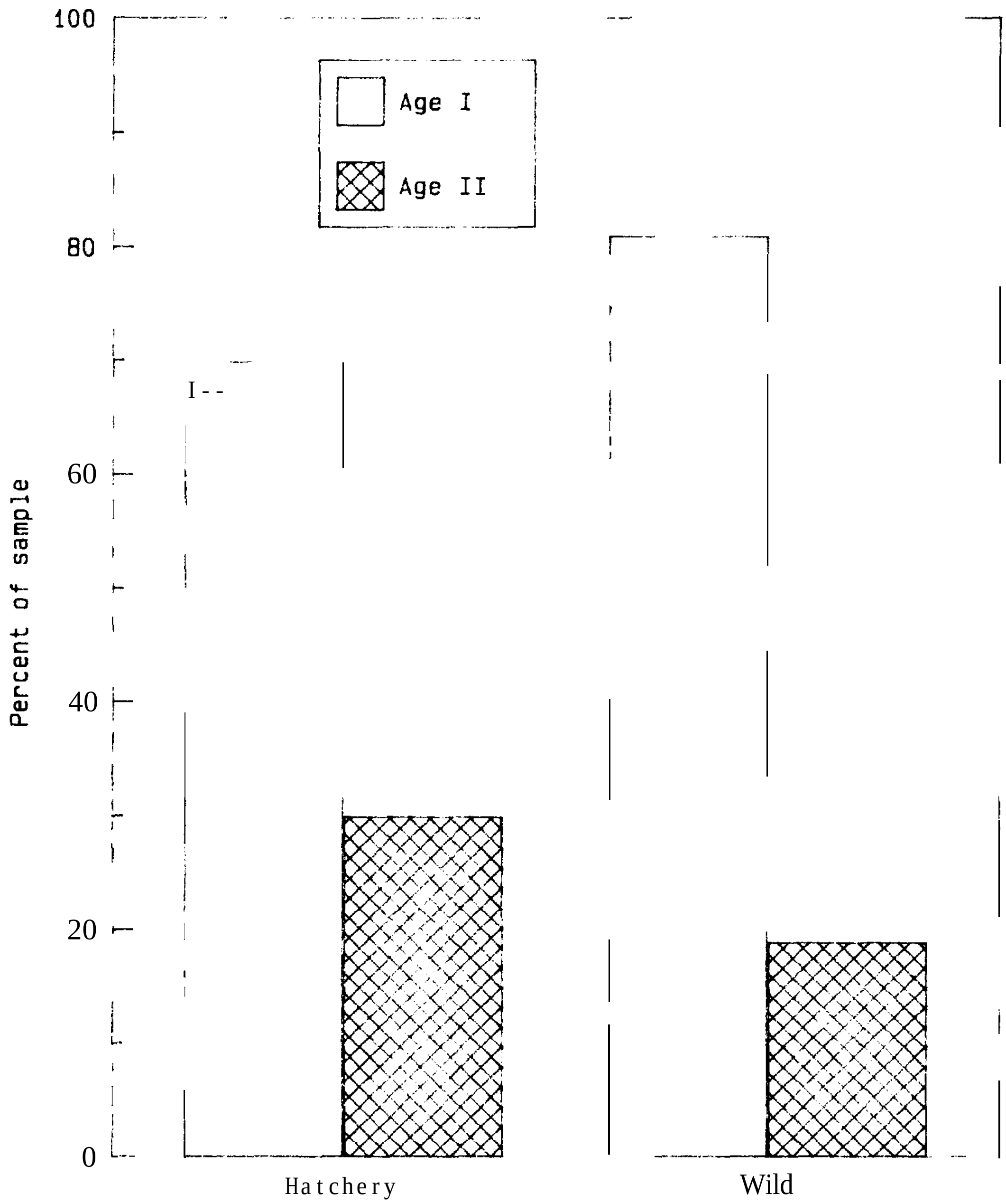

Figure C10. Age class distribution of hatchery (n=22) and wild (n=24) rainbow/steelhead trout sampled in Bedrock Creek, Idaho during June, 1989.